



**Feasibility Analysis of a Battery Energy Storage System
combined with a Utility-Scale Solar PV Power Plant in the
Atacama Desert**

Federico Baldasso

Thesis to obtain the Master of Science Degree in

Energy Engineering and Management

Supervisor: Prof. Rui Manuel Gameiro de Castro

Examination Committee

Chairperson: Prof. Luís Filipe Moreira Mendes

Supervisor: Prof. Rui Manuel Gameiro de Castro

Member of the Committee: Prof. Cristina Inês Camus

October 2021

Abstract

Nowadays the trends are indicating that the world will face different problems related to the CO₂ emissions if the use of conventional energy sources is kept as it was in the past years. Therefore, there is a global need for incorporating renewable energy sources into the grid.

The aim of this project thesis is to study the feasibility of a battery energy storage system combined with the photovoltaic power plant Campos del Sol in Chile, located in the Atacama Desert.

In order to study the economic feasibility, different configurations of battery energy storage systems have been analyzed with the software Matlab. The power of the BESS taken in consideration are 50MW, 100MW, 150MW, 200MW and for each power a capacity of 1, 2, 3, 4 hours has been studied.

A sensitivity analysis has been done by changing the Energy Prices (creating 3 different price scenarios where each scenario multiplies the real value of the energy price by a multiplicative coefficient that depends on the production of photovoltaic energy) and the Initial BESS cost (considering a decrease of 30% of the actual BESS cost).

With the actual battery costs and energy prices, the proposed solution is still not economically feasible (the configuration with the best results has a final NPV of -17.982.354 €).

The best results are reached with the configuration 200 MW 800 MWh Energy Prices scenario 3 (that is the scenario with the highest multiplicative coefficient) and the final NPV is of the order of +59 M€.

Keywords: Photovoltaic System, Energy Storage, Chile, Matlab, NPV

Resumo

Atualmente, as tendências indicam que o mundo enfrentará diversos problemas relacionados com as emissões de CO₂ e mudanças climáticas, se o uso de fontes convencionais de energia for mantido como nos últimos anos. Portanto, há uma necessidade global de incorporação de fontes de energia renováveis na rede.

O objetivo deste projeto é estudar a viabilidade de um sistema de armazenamento de energia com baterias (BESS) combinado com o parque fotovoltaico de Campos del Sol no Chile, no Deserto do Atacama.

Para estudar a viabilidade económica, diferentes configurações de sistemas de armazenamento de energia foram analisadas com o software Matlab. As potências do BESS consideradas são 50MW, 100MW, 150MW, 200MW e para cada potência foi estudada uma capacidade de 1, 2, 3, 4 horas.

Foi efectuada uma análise de sensibilidade, alterando os preços da energia (criando 3 cenários de preços diferentes onde cada cenário multiplica o valor real do preço da energia por um coeficiente multiplicativo que depende da produção de energia fotovoltaica) e o custo inicial do BESS (considerando uma redução de 30% do custo real do BESS).

Com os atuais custos da bateria e preços da energia, a solução proposta ainda não é economicamente viável (a configuração com os melhores resultados tem um Valor Atual Líquido (VAL) de -17,982,354 €).

Os melhores resultados são alcançados com a configuração 200 MW / 800 MWh com preços de energia correspondentes ao cenário 3 (que é o cenário com o maior coeficiente multiplicativo), sendo o VAL da ordem de +59 M €.

Palavras chave: Sistema Fotovoltaico, Armazenamento de energia, Chile, Matlab, NPV

Table of Contents

Chapter 1: Introduction.....	2
1.1 Objectives	2
1.2 Methodology	2
1.3 Outlines	3
Chapter 2: Energy Storage System.....	4
2.1 Battery Energy Storage System Overview	4
2.2 Operation of electrochemical cells.....	5
2.3 Main Parameters of the cell	6
2.4 Different Technologies	11
2.4.1 Lithium-Ion Battery.....	11
2.4.2 Structure of Lithium-Ion Battery.....	12
Chapter 3: BESS and Renewable Energy Sources.....	14
3.1 Integration of BESS with Renewable Energy Power Plant.....	14
3.1.1 Fluctuating Supply.....	15
3.1.2 Uncertainty	16
3.1.3 Balancing Challenge	16
3.2 Storage System Advantages	18
3.2.1 Integration of BESS with intermittent energy Power Plant	18
3.2.2 Ancillary Services	19
3.2.3 Peak Shaving and Load Leveling	22
3.3 Storage System for off-grid power plant	24
Chapter 4: Photovoltaic Energy Production.....	25
4.1 Chilean geographical features and climate conditions.....	26
Chapter 5: Campos del Sol Project.....	30
5.1 Campos del Sol – Case Study Definition	30
5.2 SAM (System Advisor Mode)	32
5.2.1 Location and Resource.....	32
5.2.2 Module.....	33
5.2.3 Inverter	34
5.2.4 System Design.....	34
5.2.5 Shading and Layout.....	35
5.2.6 Losses.....	36
5.2.7 PV Production Results.....	37
Chapter 6: Methods	39
6.1 The System	40
6.2 Photovoltaic Power Plant	42

6.3	Electricity Grid	44
6.4	Battery Energy Storage System	44
6.4.1	Degradation Model	47
6.4.2	Cell Temperature Evaluation Model	48
6.5	Optimization Problem	49
6.5.1	Objective	49
6.5.2	Data	50
6.5.3	Variables	50
6.5.4	Constraints	50
6.5.5	Power flows obtained from the optimization	51
6.6	Economic Analysis	55
6.6.1	Analysis for the evaluation of the initial investment of the BESS	55
6.6.2	Energy Prices	58
6.6.3	Evaluation of effective revenues and economic parameters	61
Chapter 7:	Results	63
7.1	Chosen Configurations	64
7.2	2020 Chilean Energy Price	65
7.3	Initial BESS Cost = 70 % Actual Initial BESS Cost	67
7.4	Energy Prices Scenarios	69
7.4.1	Energy Price = 90% Actual Energy Price	69
7.4.2	Energy Price = 110% Actual Energy Price	71
7.4.3	Scenario 1, Scenario 2	74
7.4.4	Scenario 3	77
Chapter 8:	Conclusions	79
References	80

List of Figures

Figure 1 Schematic diagram describing the design of a Lithium-Ion Battery [3]	5
Figure 2 Equivalent circuit for an electrochemical cell	6
Figure 3 Typical Voltage behavior of the Li-Ion Battery. Different curves for different C-rate [6]	7
Figure 4 Voltage for a Li-Ion cell as a function of the energy for different C-rate [6].....	9
Figure 5 Operation of a typical Li-ion battery [11]	13
Figure 6 Typical cycle life of a Li-ion battery cell [11]	13
Figure 7 Variability in demand and in net load in a challenging week on an area in USA.	15
Figure 8 Power output of a PV plant in Southern California for a partly cloudy day.....	15
Figure 9 Balancing Technologies	17
Figure 10 Basic concept of primary frequency regulation through ESS [23]	19
Figure 11 : Frequency Control Methods and Relevant Time Scales in US [24]	20
Figure 12 Time scale of frequency control (activating times are examples for Germany) [24].....	21
Figure 13 Basic concept of load leveling through BESS [23]	22
Figure 14 Example of energy shifting [25].....	23
Figure 15 Example of peak shaving [25].....	23
Figure 16 Forecast of monthly power generation for Ollagüe’s microgrid [27]	24
Figure 17 Maps of Chilean Global Horizontal Irradiation with the location of Campos del Sol [30]	26
Figure 18 Typical geography of the northern regions of Chile. [31]	27
Figure 19 Maps of Chilean Photovoltaic Power Potential with the location of Campos del Sol [30] ...	27
Figure 20 Irradiation for different longitudes in a) Iquique and b) Copiapó’s latitude. [35]	28
Figure 21 Location of the project Campos del Sol PV Power Plant. Photo from Google Maps.	30
Figure 22 Panoramic view of the area where the PV Plant will be situated (Google Maps)	31
Figure 23 Carrera Pinto Interconnection Substation	31
Figure 24 Irradiance of the area of Campos del Sol PV Plant.....	32
Figure 25 Module data	33
Figure 26 Inverter Data	34
Figure 27 Tracker structure. In each tracker there are 28 modules.	35
Figure 28 Shading analysis of the PV modules and the trackers.....	35
Figure 29 Campos del Sol considered losses.....	36
Figure 30 Campos del Sol computed annual PV Power	37
Figure 31 Campos del Sol generated Power for the first week of the year, computed with SAM	38
Figure 32 Block Diagram of the Considered System	40
Figure 33 Simplified Electric Interconnection Scheme of the considered system.	41
Figure 34 PV power produced for four different days, as example.	42
Figure 35 Energy profile produced by the PV in 25 years, with linear reduction of the power.	43
Figure 36 Simulink Model for the Temperature evaluation.....	48
Figure 37 Optimal Power Flow and SOC profile for a day with variable energy price.....	52
Figure 38 Optimal Power Flow and SOC profile for a day with stable energy price.....	53
Figure 39 Initial BESS Cost in relation to the considered size.	57
Figure 40 Variation of the relative initial cost of the BESS according to the size considered.....	57
Figure 41 Carrera Pinto Substation Energy Prices for different days of year 2020.....	58
Figure 42 Considered Price Scenario.....	59
Figure 43 Prices Profile Scenarios for the first three days of January.....	60
Figure 44 Carrera Pinto 2020 Energy Price. From CEN Website.	65
Figure 45 NPV and Cash Flow for the BESS 50 MW 50 MWh.....	66

Figure 46 NPV and Cash Flow for the BESS 150 MW 300 MWh	68
Figure 47 NPV and Cash Flow for the BESS 200 MW 400 MWh	68
Figure 48 Energy Prices decreased by 10%.	69
Figure 49 NPV and Cash Flow for the BESS 50 MW 50 MWh.....	71
Figure 50 Energy Prices increased by 10%.	71
Figure 51 NPV and Cash Flow for the BESS 50 MW 50 MWh.....	73
Figure 52 NPV and Cash Flow for the BESS 150 MW 300 MWh considering Price Scenario 2.	75
Figure 53 NPV and Cash Flow for the BESS 100 MW 200 MWh considering Price Scenario 2.	75
Figure 54 NPV and Cash Flow for the BESS 200 MW 400 MWh considering Price Scenario 2	76
Figure 55 NPV and Cash Flow for the BESS 200 MW 600 MWh considering Price Scenario 2.	76
Figure 56 NPV and Cash Flow for the BESS 200 MW 600 MWh considering Price Scenario 3.	78
Figure 57 NPV and Cash Flow for the BESS 200 MW 800 MWh considering Price Scenario 3.	78

List of Tables

Table 1 Capacitance values by varying the C-rate from lithium-ion cells evaluated experimentally.	8
Table 2 Characteristics of the electrochemical modules	45
Table 3 Charge and discharge performance of the BESS as function of the C-rate	45
Table 4 Different cost items identified and related values as the BESS size varies [43].....	55
Table 5 Relative cost values calculated as a function of power and energy of the BESS.....	56
Table 6 BESS considered configurations	64
Table 7 NPV and IRR with the actual Carrera Pinto Substation Energy Prices.....	66
Table 8 NPV and IRR considering a 30% decrease in the initial BESS investment	67
Table 9 NPV and IRR considering a general decrease of 10% of the Energy Price.....	70
Table 10 NPV and IRR considering a general increase of 10% of the Energy Price.....	72
Table 11 NPV and IRR considering Price Scenario 1, Scenario 2.	74
Table 12 NPV and IRR considering Price Scenario 3.....	77

List of Abbreviations

AC – Alternate Current
BESS – Battery Energy Storage System
BOS – Balance of System
C-rate – Current rate
CEN – Coordinador Electrico Nacional
DC – Direct Current
DNI – Direct Normal Irradiation
DOD – Depth of Discharge
EPC – Engineering Procurement & Construction
EPS – Electrical Power System
ESS – Energy Storage System
GHI – Global Horizontal Irradiation
HV – High Voltage
IRR – Internal Rate of Return
LV – Low Voltage
MATLAB – Matrix Laboratory
MV – Medium Voltage
NMC – Nickel Cobalt Manganese
NPV – Net Present Value
O&M – Operation and Maintenance
PCHIP – Hermite Polynomial Interpolation
PV – Photovoltaic
RES – Renewable Energy Sources
SAM – System Advisor Model
SOC – State of Charge
SVC – Static Var Compensator
TMY – Typical meteorological year
TSO – Transmission System Operator

Chapter 1: Introduction

The energy request in the world has been increasing rapidly. Nowadays the trends are indicating that the world will face problems if the use of conventional energy sources is kept as it was in the past years. The increasing demand has to be satisfied with sustainably harvested energy. Therefore, there is a global need for incorporating renewable energy sources into the grid. Unfortunately, there are some issues for the incorporating process: the main issues of the renewable energy sources are the unpredictability and the variability of the output. Another issue is related to the fact that at every instant the production of the power systems must match the consumption. Currently this is partly achieved resorting to fossil fuel power plants and their power regulating capabilities. In light of the current decarbonization path, this power regulating function is to be performed by BESS.

In order to fix these issues, it is necessary to schedule the productions of the electricity market during the operational hours of the renewable power system. The increase of the renewable energy power plant grid connected will change the operational and the reliability performance of the grids. An important step to make the renewable power plant more desirable will be the combination with energy storage system, in order to make more constant over time the renewable energy production.

Thanks to the energy storage system, it is possible to control the variability and unpredictability of the renewable energy sources, in particular in this project it has been studied the storage system combined with a photovoltaic power plant.

1.1 Objectives

An increase in the use of renewable energy could be possible with the utilization of a battery energy storage system connected to the renewable energy source.

The main objective of this thesis work is to analyze the economic feasibility of a battery energy storage system connected with the photovoltaic (PV) park Campos del Sol in Chile, located in the Atacama Desert.

In order to study the economic feasibility, different configurations of battery energy storage systems have been analyzed with the software Matlab.

1.2 Methodology

For the development of this work two software have been used in order to compute all the necessary data:

- The software System Advisor Model (SAM) has been used in order to compute the photovoltaic power and energy production of the PV park Campos del Sol. The input data necessary for the software are:
 - Geographical and meteorological data (irradiation), that have been taken from libraries in internet.
 - Data regarding the PV park equipment (modules, inverters, design) have been taken from the company STE Energy during my internship in the company.

- The software MATLAB has been used to study the technical and economic feasibility of a battery energy storage system (BESS) connected to the PV park. . In the software an optimization problem was created in order to maximize the economic revenues from the battery energy storage system.
The optimization problem analyzes the photovoltaic energy production and the energy prices during the day and optimize the Battery Energy Storage System Energy flows, by telling when it is the moment to send the energy from the PV to the BESS, when from the PV to the grid, when from the grid to the BESS and when from the BESS to the grid.

1.3 Outlines

The work has been divided in different stages, that have been studied in the following chapters:

Chapter 1: Introduction of the Thesis work, explaining what the objective of the thesis and the methodology is.

Chapter 2: The Energy Storage System is generally explained, with the focus on Lithium Ion Batteries, that is the main topic of this work. The working principle of this type of battery is presented and then a brief comparison with different technologies is done.

Chapter 3: In this chapter the advantages of combining a storage system with renewable energy park (in this case photovoltaic energy plant) is explained.

Chapter 4: the geographical area of the project and the photovoltaic energy situation in Chile is described.

Chapter 5: The PV Park Campos del Sol and the computations done with the software SAM to compute the PV production are described.

Chapter 6: The work with the software MATLAB is explained in this chapter. The input data and the methodology are explained. The main focus is on the optimization problem.

Chapter 7: The results are presented and discussed.

Chapter 8: The conclusion and future works are explained.

Chapter 2: Energy Storage System

The main part of this project thesis is to study the feasibility of a battery energy storage system (BESS) for the project Campos del Sol. This chapter will give a general description of these storage systems, their working principle and a description of the main parameters that characterize different ones, with a particular focus on the most relevant storage system for this study, that is the Lithium-Ion battery.

Energy storage is the way energy is being conserved in a particular form and then released when needed in the same form or converted to a different form [1].

2.1 Battery Energy Storage System Overview

The main components of the battery energy storage system BEES are the electrochemical cells. The electrochemical cells transform the chemical energy into electric energy. These cells represent a category of the stationary generators of electromotive force called “secondary batteries” which, unlike primary batteries, are rechargeable, so the electric energy can be transformed in chemical energy too. [2] [3]

A single cell is able to generate a variable voltage in the order of some volts, so in order to create a large battery energy storage system, different cells must be connected in series and in parallel to create what are called “modules”, and the modules are then connected in series and in parallel until the requested size of the system is reached.

A BESS is composed also by electronic devices that are needed to control and monitor the system and are used to respect in every moment the constraints for the correct operation and maintenance of the system. These electronic devices are the ventilation system and the air conditioning system that keep under control the temperature of the batteries, an important aspect to keep in mind.

Important characteristics of these energy accumulators are the modularity, since it is possible to have system from few kWh up to dozens of MWh, and the flexibility, because they can be used in different situations, even when it is requested a quick time response.

Another advantage is that the BESS are really easy and fast to be installed and simple to move, while for other storage system this is not even possible. There are different manufacturers of BESS that supply the system partially preassembled and adaptable to different applications with the possibility to move them.

2.2 Operation of electrochemical cells

The operation of an electrochemical cell is based on redox processes that happen during the battery charging and discharging. Generally, they are made up of a species capable of oxidizing by transferring electrons to a species capable of reducing itself by acquiring electrons.

By connecting an electric load through an external circuit, it is possible to exploit the energy deriving from these reactions by channeling the electrons through a conductor in order to obtain the circulation of electric current and a difference of potential on the connected load. By doing this, the cell is discharged: the chemical energy decreases and it is transformed into electrical energy absorbed by the load.

On the other way, by applying an electric field from the outside, it is possible to reverse the direction of the reaction, thus accumulating the electrical energy in the form of chemical energy; in this way the cell is charged.

Together with the redox reactions, during the real process there are also some undesired parasitic reactions that reduce the time and performance of the cells, diminishing the efficiency during charging/discharging and reducing the capacity respect the nominal value [4].

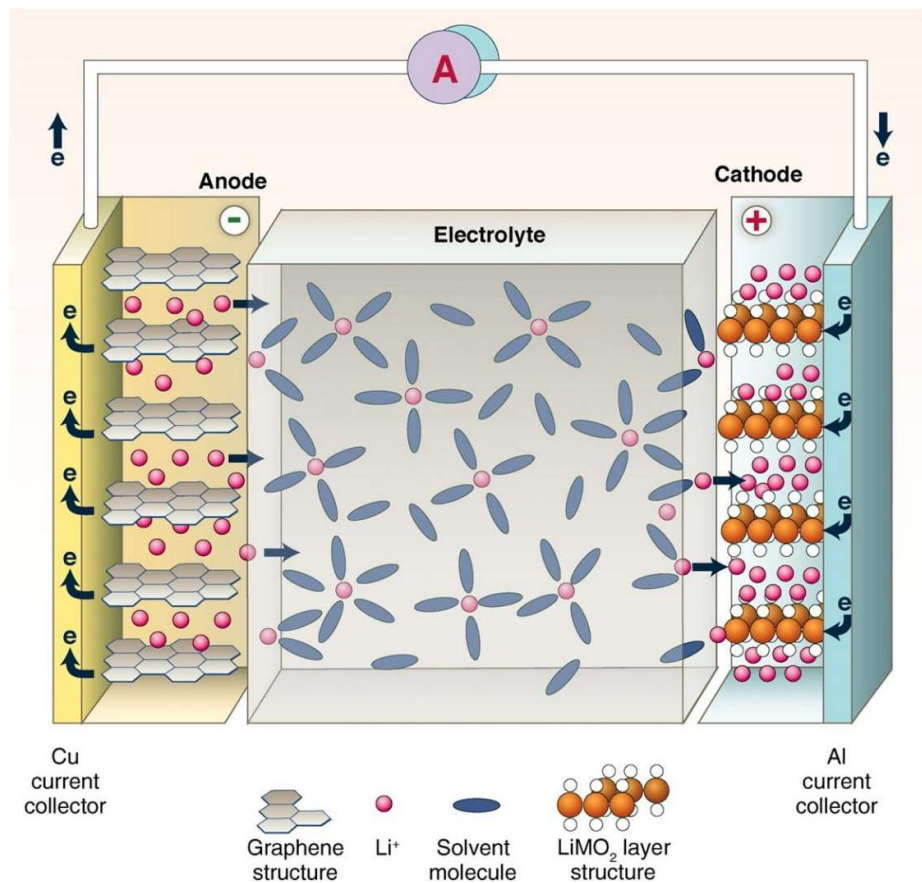


Figure 1 Schematic diagram describing the design of a Lithium-Ion Battery [3]

There are different types of electrochemical cell, but the main structure is always the same: in general, there are two half-cells, each composed by a metallic electrode which is immersed in an electrolytic solution that allows the transition of the ions but prevents direct exchange of electrons.

The two electrodes are called respectively anode and cathode, the anode is the negative electrode, that reduces during the discharge and oxidizes during the charge, while the cathode is the positive, that oxidizes during the discharging process and reduces during the charging process.

The electrolytic solution, or electrolyte, typically contains lithium salts and organic solvents. In the electrolyte the ions are able to flow while the electrons cannot, this prevents the auto-discharge of the battery.

2.3 Main Parameters of the cell

To better understand how an electrochemical cell works, it is important to start from an equivalent circuit, that does not consider the real behavior, but it is an excellent starting point to explain all the rest.

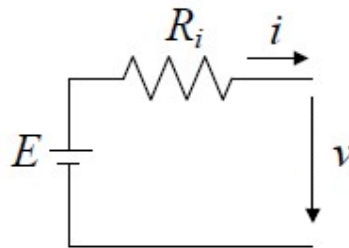


Figure 2 Equivalent circuit for an electrochemical cell

In Figure 2, E represents the electromotive force of the cell, R_i is the internal resistance, v is the available voltage between the terminal and i is the supplied current that depends on the connected charge.

All these factors are connected by the following equation:

$$v = E - R_i i \quad (1)$$

The first parameter considered is the nominal voltage v_n that is strictly linked to the voltage v . The nominal voltage is a conventional quantity (it is expressed in Volt) that represents the average voltage between the two terminals of the cell with a specific discharge process. During the process, the maximum and minimum values of the voltage are analyzed and then the overall average is v_n .

Typical commercial cells have a nominal voltage of 3.7 V. The end of discharge, for example lithium insertion in the cathode (positive electrode), is reached when the anode (negative electrode) is depleted of lithium and the cell voltage drops to about the cut-off voltage of 2.7 V. [5] [3]

In the Figure 3 [6], it is possible to see the typical behavior of the voltage during the discharge process of the Lithium-Ion battery considered for this project, depending on the current and on the connected charge.

It is possible to see that the initial value is around 4.2V and then it decreases while the battery is losing its energy [6].

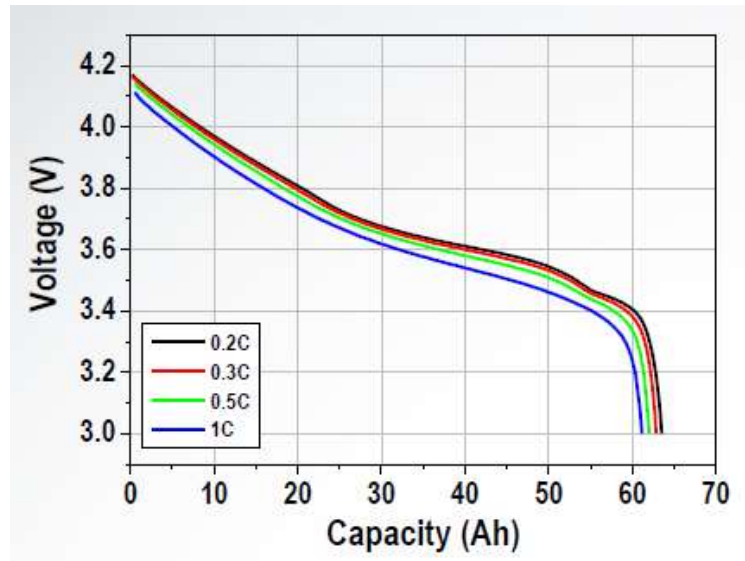


Figure 3 Typical Voltage behavior of the Li-Ion Battery. Different curves for different C-rate [6]

Furthermore, the voltage variation is really important especially in the last part of the curve where the voltage drops to a value around 3.0V. The voltage value in the last part of the curve is called *cut-off voltage* and it indicates the minimum acceptable value for the battery voltage, below this value the battery could be damaged, and the performance could be reduced, so the value never drops lower than this.

Another important parameter is the capacity, measured in Ampere-hour (Ah). It represents the charge that the battery is able to release during the discharging process, it is, of course, dependent on the conditions of the process. It is called effective capacity C_E the capacity supplied during the discharge process starting from the maximum value of charge and finishing to the minimum value of tension. It can be described as the integral of the current in set interval of time:

$$C_E = \int_0^{t_{co}} i(t)dt \quad (2)$$

Where t_{co} represents the time needed to reach the *cut-off voltage*. The capacity depends on different parameters, the most important one is the current at which the discharge process happens, that can often change during the discharging. The nominal capacity of the battery is the effective capacity obtained during a discharge with a standard time and a discharge current that are specified.

An important parameter of the battery is the Current rate (C-rate): it is a measure of the discharge current relative to capacity. The discharge rate of a battery is expressed as C/R, where R is the number of hours required to completely discharge the nominal capacity.

A simple example to better understand the C-rate: consider a cell with a nominal capacity of 5 Ah. This cell is discharged at C/10 rate. This means that the cell will be discharged in 10 h. It can provide a current of 0.5 A. If the discharge rate is only C/5, it takes 5 hours to discharge and the provided current is 1 A. The C-Rate drops as the battery is discharged; anyway, the C-rate is an important parameter to compare and to characterize different

batteries. The amount of energy supplied by a battery (the area under the discharge curve) is dependent upon the C-Rate. [7].

As we can see in the Table 1, as an example from experimental data from [6], the obtainable capacity depends on the C-rate:

Table 1 Capacitance values by varying the C-rate from lithium-ion cells evaluated experimentally.

<i>C</i> -rate (<i>C</i>)	C_E (%)
0.2	100.9
0.3	100
0.5	98.8
1	97.5

In Table 1, C_E is represented as percentage in order to show how the relative values change in relation to the C-rate. Severe discharge regimes could therefore significantly affect the number of charges that can be extracted from the battery. Together with the discharging current, another important factor that affects the extractable capacity from the cell, is the internal temperature during the process. Generally, the capacity is directly proportional to the temperature, so the extractable energy at low temperature could be significantly lower than the nominal value.

Another important parameter is the state of charge *SOC*, that is the remaining capacity (expressed in Ah) of the battery after a partial discharge process from the maximum charged condition. This parameter can be expressed with the formula:

$$SOC(t) = C - \int_{t_{in}}^{t_f} i(t)dt \quad (3)$$

Where C is the maximum capacity deliverable from the cell, t_f is the final moment of the discharge process and t_{in} is the initial moment of the discharge process.

Starting from the definition of the *SOC*, it is possible to introduce the depth of discharge *DOD*, that is the delivered capacity during a partial discharge, usually expressed in relative terms respect the maximum capacity C of the cell:

$$DOD(t) = \frac{C - SOC(t)}{C} 100 \quad (4)$$

The value of *DOD* is very important to be able to evaluate the operative condition of the cell, in fact the *DOD* indicates the depth (in percentage) of charge/discharge of the cycles to which the cell is subjected.

An important parameter that enables to compare different cell technology is the energy that the battery is able to deliver/store, expressed in Wh. The theoretical value of the energy could be conventionally computed as the product of the nominal capacity by the nominal voltage. The real value of the delivered energy, starting from an initial charge until the value of minimum voltage, can be expressed as:

$$E_E = \int_0^{t_{co}} v(t)i(t)dt = \int_0^{t_{co}} p(t)dt \quad (5)$$

Where v and i are time dependent. Therefore, the delivered energy from a cell is variable, depending on the current and on the output power $p(t)$ that has to be reached. In fact, as it can be seen in Figure 4 below, the voltage profiles are represented as a function of the delivered/absorbed energy of a lithium-ion cell with discharge/charge processes characterized by different C-rate values.

As we can see in the Figure 4 for a C-rate equal to 0.2 the extractable energy would be around 230Wh, while for a discharge with a C-rate equal to 1.0 the extractable energy would be only 205Wh, which means around 10% less.

In order to compare different technologies, the energy and the power can be related to the weight of the cell itself, through parameters that are called specific power [W/kg] and specific energy [Wh/kg] or can be related to the volume with the parameters: power density [W/m³] and energy density [Wh/m³]. These parameters are useful to compare different types of storage systems.

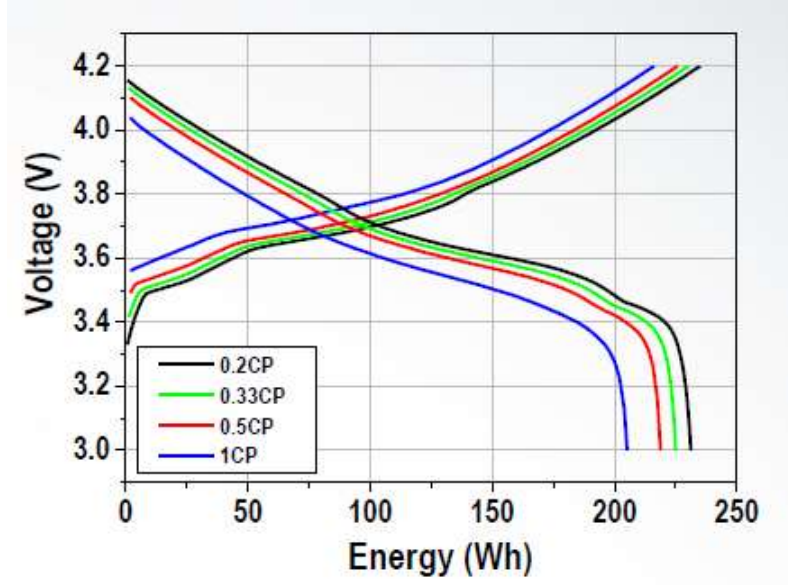


Figure 4 Voltage for a Li-Ion cell as a function of the energy for different C-rate [6].

Another important parameter in order to classify different storage system is the efficiency. The efficiency can be expressed in Coulombian terms or in energy terms. The Coulombian efficiency is the ratio between the supplied charge Q_d and the absorbed charge Q_c during a full cycle from a full charge to a full discharge:

$$\eta_a = \frac{\int_0^{t_d} i_d(t) dt}{\int_0^{t_c} i_c(t) dt} = \frac{Q_d}{Q_c} \quad (6)$$

Where $i_d(t)$ is the discharging current at time t ; $i_c(t)$ is the charging current at time t ; t_d is the considered discharging time; t_c is the considered charging time.

This efficiency decreases when the charging process is done quickly.

η_a is equal to 1 when during the charging process all the absorbed charges take part in the process of formation of the electrodes and then the charges are released during the discharging process, while it is lower than one

when part of the absorbed charges produces substances, through undesirable reactions, which do not participate to the next discharge process.

The energetic efficiency is the ratio between the supplied energy W_d and the absorbed energy W_c during the charge/discharge process:

$$\eta_e = \frac{\int_0^{t_d} v_d(t) i_d(t) dt}{\int_0^{t_c} v_c(t) i_c(t) dt} = \frac{W_d}{W_c} \quad (7)$$

The energetic efficiency is smaller than the Coulombian efficiency because it also considers the internal dissipation of the battery during charging/discharging.

The last parameter that has to be considered is the lifetime of the cell, that indicates the period of time after which the cell is no longer useful. Usually, the battery reaches the end of the lifetime when a capacity around 70-80% of the nominal value is obtained. For this project it has been considered a final capacity equal to 75% of the nominal value.

The lifetime of the cell is influenced by several factors, like the environmental conditions and the temperature. In the factory data of a battery, its life is expressed in terms of number of cycles obtainable, defined by specific charging and discharging conditions.

If the actual operating conditions differ from those used to evaluate the nominal number of cycles, it is possible that the battery reaches the end of its life earlier and that the overall energy exchanged could be significantly lower than expected. [8] [9]

2.4 Different Technologies

There are different types of battery energy storage that differ in the types of the electrochemical pair between which the reaction happens, while the functional characteristics depend on the application purposes. The most common electrochemical accumulators can be divided as following:

- with aqueous electrolyte, that are the lead acid, nickel/cadmium and metal hydride accumulators.
- with electrolyte flow.
- with high temperature, as the sodium/sulfur and sodium/nickel chloride accumulators.
- lithium-ion accumulators.

The most diffused technology is the lead acid, thanks to the low costs and to the easy availability of the raw materials and diffused use. Comparing with other solid-state batteries, the density is low, but this battery can provide a large current that is a great advantage in many applications [10].

The electrolyte flow accumulator is a really interesting option for the future, as in the past years have been under research and development that seems promising. This technology has a separation between the power and the energy of the battery. Indeed, the power depends on the quantity of electrolyte that is used during the reaction, together with the speed of the reaction itself and so with the film area and with the pump speed that moves the electrolyte. The capacity is function of the total quantity of the accumulators and so of the total capacity of the tanks. With these accumulators is possible to gain the accumulator capacity by increasing the dimensions of the tanks, keeping the power constant, or in the other cases, it is possible to increment the power of the accumulator by accelerating the power speed.

The high temperature batteries are characterized by a high specific energy, high energetic performance and a long lifetime. These accumulators work with internal temperatures around 300°C and the operation is independent from the environmental temperature. The used materials have the advantages of low density and costs. It could be a good solution for stationary applications.

Finally, the most promising and researched technology is the lithium-ion battery. These accumulators are characterized by a high energy efficiency and specific power and a long lifetime. Thanks to these properties, this battery can be used for different applications, even as a support for the electric system. This technology is the one considered in this project. [10]

2.4.1 Lithium-Ion Battery

Lithium-ion batteries are the most popular electricity storage technologies for portable appliances and emerging grid applications. Li-ion batteries have a high volumetric energy density, and high charge and discharge current density compared to conventional battery technologies. In addition, Li-ion batteries have longer lifetime and higher efficiency than most other types of battery. In the past the problems connected with the use of this technology were the high cost and the security [11].

There are different types of lithium-ion battery that differ from each other for the electrode and/or electrolytic materials. The only element that is common in these batteries is the ion carrying the electric charge (Lithium ion, Li⁺). [12].

According to the elements that make up the anode, it is possible to divide the different cell technologies:

- Lithium-Cobalt ($LiCoO_2$ - *LCO*): this is the most common type of element used for the construction of the cathode. Cells that contain this type of cathode are still used to make batteries for laptops and cell phones. On the other hand, this technology generally suffers heating problems; in fact, in case of overload, the structure of the material can collapse, releasing a large amount of heat, as well as some instability in the event that the cell box is perforated.
- Lithium - Iron - Phosphate ($LiFePO_4$ - *LFP*): the cathodes made in this element have a superior thermal stability. In fact, lithium phosphate is incombustible and does not decompose even if the cell is short-circuited. It has low ionic conductivity, which leads to a lower flow of lithium ions and therefore internal resistance greater. The ionic conductivity can be increased thanks to various techniques such as doping the oxide, making nano-structured oxides and lining the electrode with carbon atoms. Furthermore, this technology is characterized by a relatively high cyclic life.

The batteries are certainly safer and less expensive, as a consequence of the low electrochemical potential and have no toxicity problems.

- Lithium - Manganese Oxide ($LiMn_2O_4$ - *LMO*): these cells offer high voltage values, good thermal stability, and good performance at high temperatures, with lower energy levels than the other mentioned technologies. The cost is relatively low, and the materials are non-toxic even though manganese has lower cycling.
- Lithium - Nickel - Cobalt - Manganese ($LiNi_xCo_yMn_zO_2$ - *NCM*): these cells represent a good compromise between the various characteristics of the technologies. The combination of nickel and manganese allows to obtain high values of specific energy combined with an excellent crystalline structure to favor the flow of electrons, giving both electrical and structural advantages that make them the most widespread technology for the realization of batteries for electric vehicles and excellent candidates for stationary use. [12]

2.4.2 Structure of Lithium-Ion Battery

Lithium-Ion batteries, in their most common form, consist of a positive electrode (cathode) of lithium oxides, a negative electrode (anode) of graphite and an electrolyte composed of a lithium salt and organic solvent. There are different types of Li-ion battery, that differ in materials. The only element that is common in all these batteries is the ion carrying the electric charge (ion Lithium, Li⁺). A number of different materials can be used as electrodes in Li-ion batteries. The most common combination for portable electronic appliances is lithium cobalt oxide for the cathode and graphite for the anode. Other cathode materials that are used include lithium manganese oxide (used in electric vehicles) and lithium iron phosphate. In general, ether is used as an electrolyte in the Li-ion batteries [13]. As we can see in Figure 5, during the charging process, lithium ions move from cathode to anode, and absorb electrons from an external source of electricity. When the battery is being discharged

lithium, atoms lose electrons at the anode. The electrons drive an external load, and the lithium ions move back toward the cathode.

For a Li-ion battery with lithium cobalt oxide ($LiCoO_2$) as the cathode and with the anode of graphite, the chemical reactions are (charge from left to right; discharge from right to left):

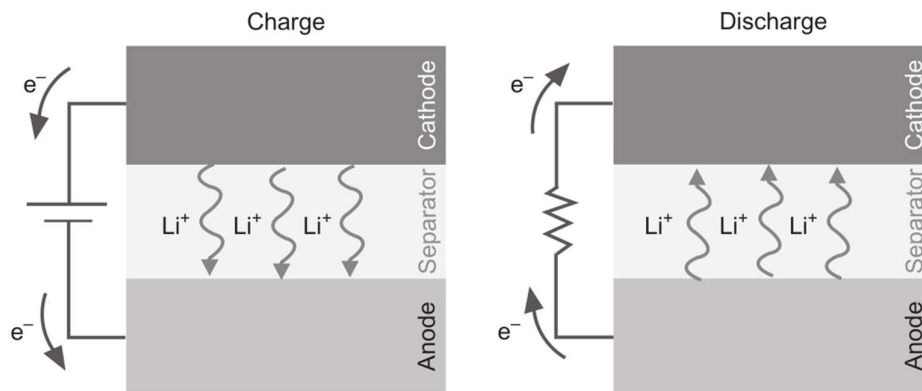
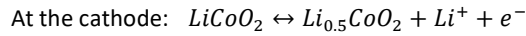


Figure 5 Operation of a typical Li-ion battery [11]

The number of charge and discharge cycles that a battery can complete before losing performance represents the cycle life. The cycle life of Li-ion batteries is affected significantly by the depth of discharge, that is the amount of a battery' storage capacity that is used. For example, a battery that is discharged only by 20% of its full energy capacity has a much greater cycle life than a battery that is discharged more than 80% of its capacity, which means having only 20% of its full energy charge left. Figure 6 shows the cycle life of a typical Li-ion cell.

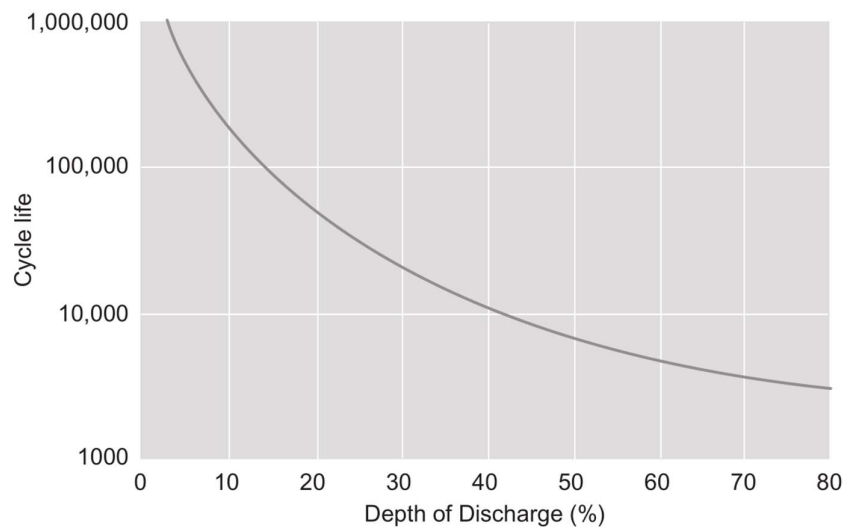


Figure 6 Typical cycle life of a Li-ion battery cell [11]

Chapter 3: BESS and Renewable Energy Sources

The main issues of the renewable energy sources are the unpredictability and the variability.

The increase of the renewable energy power plant grid connected is changing the operational and reliability performance of the grids.

An important step to make the renewable power plant more and more desirable is the combination with energy storage system, in order to make more constant the renewable energy production. [1]

3.1 Integration of BESS with Renewable Energy Power Plant

The energy generation from renewable energy sources (RES) has several advantages and disadvantages. The major advantage of renewable energy is that it can never be depleted, and it requires very little maintenance. Renewable energy sources are environmentally friendly as they do not pollute and do not generate wastes that are a big problem for the ecosystem.

However, the energy produced by the fossil fuel sources is much more reliable than the energy generated from renewable energy sources. The renewable energy sources depend, essentially, on nature which represents the main drawback of this technology: its intermittency. A great way to sustain renewable energy is through storage devices [14].

The intermittency of the Renewable energy sources needs to be improved thanks to storage techniques that have to be integrated into the energy system. In this way it would be possible to provide or to absorb energy during the periods with imbalance between the power demanded and the power supplied.

With the growth of renewable power generation, we will reach a point where the conventional power sources will be definitely overwhelmed, and the electricity will be produced only from wind, solar PV and other renewable energy sources [15].

With the combination of the renewable Power Plants and Storage systems, it is possible to solve two problems at the same time: reducing emission and pollution and controlling demand's valleys and peaks with a better control of the power outages that are a huge problem because they affect many facets of our world.

3.1.1 Fluctuating Supply

One of the problems of renewable energy sources is that they are not constant over time: the energy output fluctuates according to the energy resource availability, that cannot be well predicted but can be controlled using energy storage systems. These fluctuations must be handled in order to maintain a balance between supply and demand and by changing the consumption for a given period rapidly and more frequently than normal operation. In case of large energy penetration in the grid, an exaggerated variability is introduced in frequency and rate of

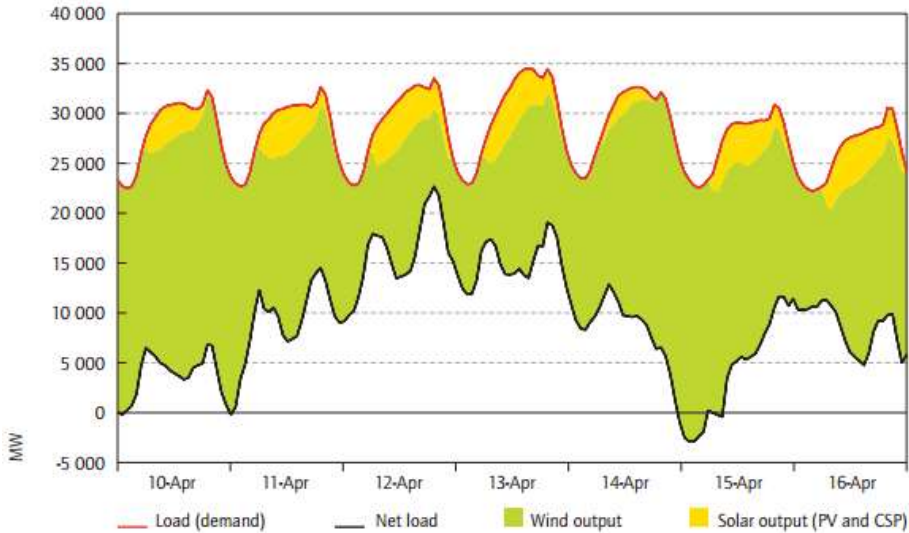


Figure 7 Variability in demand and in net load in a challenging week on an area in USA.

variability. In Figure 7, it is possible to see an example of the modelled effect of large share of RES penetration on an area in United States - with a penetration equal to 30% of wind and 5% of solar energy. From the figure, it can be interpreted that, in some periods the balance of the renewable energy would be a very challenging issue, considering the variability of the RES output that can change very fast from high values to low values. [16]

The movement of the sun is very well understood and supported by gathered data so it can be said that variation in solar energy output can be predicted easily during the day and yearly. However, there is an aspect that is really

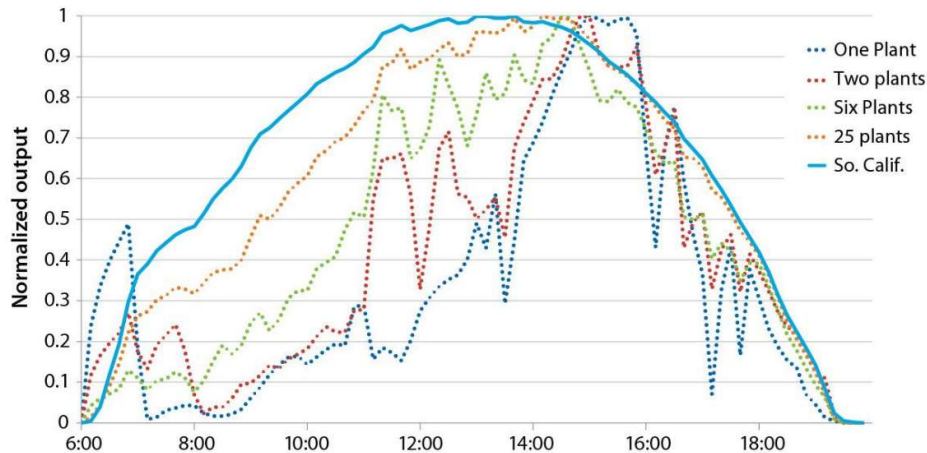


Figure 8 Power output of a PV plant in Southern California for a partly cloudy day

difficult to predict and that it is important for the power production: the shading due to the clouds that pass over the PV plant even for just a short period of time and cause losses for the PV plant production. Shading effect can result in significant and rapid changes in output of PV systems, but the impacts on the power system is very limited considering that PV plants geographically are installed in relatively large areas, and normally, only small parts of the plant are exposed to shading conditions at the same time.

It is important to try to understand how to balance the increasingly variable net load, instead of focusing on how to balance the variable RES output. The variability on the demand side is related to the variability in renewable energy sources output on supply side.

3.1.2 Uncertainty

The second factor to keep in mind is the uncertainty of the renewable challenge which is related to the unpredictability of the power output from Renewable Energy plants.

An example is the wind power output that could vary quickly or slowly, for long or short periods and with almost unnoticeable pattern, due to changes in wind profile. Photovoltaic plants without storage, during the night are not in operation and will not generate electricity, so other generators in the electrical power system can be scheduled accordingly. In addition, the PV output power, even under cloud cover, does not drop to zero as PV systems operate with diffuse radiation as well as direct sunlight, although the power output is reduced. For this reason, power output from a single cell will not fall below around 20% of rated capacity during the day. [17]

3.1.3 Balancing Challenge

To maintain an equilibrium between demand and supply, the balance of the operations shall be performed in a timescale varying from 36 hours down to 15 minutes ahead of the time of use of the electricity.

The 36 hour-period covers the maximum extent of variability in output that the Electrical Power System (EPS) will face. Therefore, one of the main concerns of the balancing challenge is to analyze the tools available to handle balancing needs in this timeframe. When demand for electricity and output from variable power plants are changing simultaneously in opposite directions the balancing challenge will be greater. [16]

In order to achieve the stable performance of the grid, system operators mostly need to access and utilize ancillary services to maintain the supply demand balance. Ancillary services include operating reserves, reactive power support in order to increase voltage when needed and black start capability, ability to restart the power system in case of a black-out as it will be explained in detail in the next paragraphs.

In order to achieve the stable performance of the grid, system operators mostly need to access and utilize ancillary services to maintain the supply demand balance.

The System Operator shall determine proper balancing method considering aspects such as reducing the need for investment in generation and network infrastructure, improving the efficiency of system operation and asset utilization.

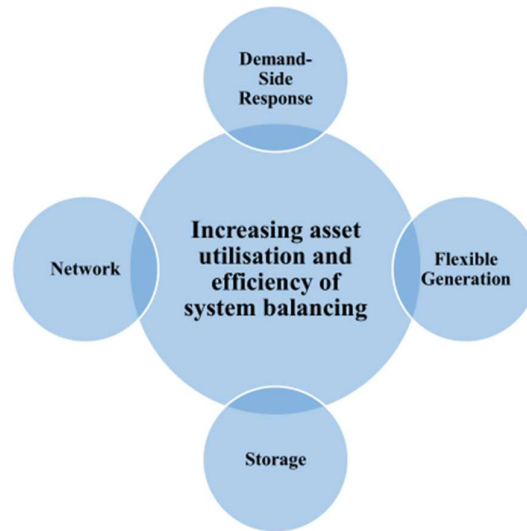


Figure 9 Balancing Technologies

As illustrated on Figure 9, these options are network solutions (such as reinforcements and investments in the grid infrastructure), demand-side response, flexible generation technologies and the application of energy storage systems [18].

3.2 Storage System Advantages

Both energy crisis and environmental degradation promote the blistering advancement of renewable energy sources such as photovoltaic power (PV).

In this context, the number of the industrial customer with PV is increasing rapidly for the higher power supply reliability and lower electricity bill. The battery energy storage system (BESS) helps further reduce the electricity bill of the industrial customer with PV by peak-shaving and load-shifting, as will be explained in this chapter. [19] Thanks to the high specific energy and power, together with a long lifetime and an excellent energetic efficiency (usually more than 90%), Li-ion accumulators satisfy different services. It is possible to divide the services into two main categories:

- services *front-of-the-meter*: aimed for the correct operation of the public network.
- services *behind-the-meter*: aimed to create advantages for the customers.

In this chapter, different fields of application will be studied in order to understand that the BESS can become more and more important for the electric systems worldwide.

3.2.1 Integration of BESS with intermittent energy Power Plant

The energy storage systems can be integrated with all the energy power plants thanks to the significant flexibility, due also to the presence of a large number of technological options [20].

The energy storage systems are particularly interesting when are integrated with renewable power plants, this will be the main focus of this thesis project.

The energy request in the world has been increasing rapidly. Nowadays the trends are indicating that the world would be facing problems if the use conventional energy resources is kept as in the past years. These demands have to be faced in a sustainable way. Therefore, there is a global need for incorporating the renewable energy sources into the grid.

There are various applications for electricity storage systems in the utility power system:

- Ancillary services
- Peak shaving
- Load leveling

3.2.2 Ancillary Services

The Ancillary Services are all the services required by the transmission or distribution system as well as the power quality [21]. In other words, the ancillary services are necessary for the stable operation of the electricity system.

The ancillary services are really important when the renewable energies are taken into consideration.

In order to keep under control the RES, the BESS can deliver the following ancillary services:

- Frequency Control
- Voltage Control
- Standing Reserve
- Black Start Capability

There are other ancillary services that the BESS cannot deliver as “Grid loss compensation”, “Remote generation control” and “Emergency control actions”. However, these services are required for renewable and conventional power generation alike. In other words, renewable generation in combination with storage systems can deliver all services which conventional power generation provide today.

3.2.2.1 Frequency Control

Considering the renewable energy systems, it is important to keep in mind that these are normally low inertial generation units. If they are not utilized together with Energy Storage Systems, the transient changes in the system states may result in uncontrollable oscillations which may force the grid to become unstable.

Thanks to the BESS, this problem can be kept under control and the storage system plays a key role in adjusting the grid frequency during the transients and in increasing the stability of the power plant [22].

The frequency adjustment for the grid depends strongly on injection and withdrawal of real power within short time (of the order of few seconds).

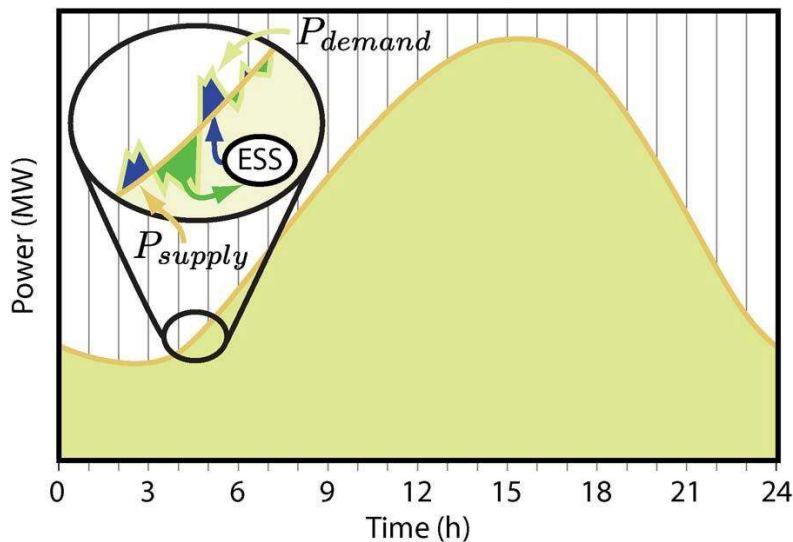


Figure 10 Basic concept of primary frequency regulation through ESS [23]

For these reasons, an energy storage system with rapid charge and discharge durations can be integrated to the renewable power system in order to stabilize the frequency. [23]

For instance, this application may contribute to the frequency stability of isolated utilities.

Different kinds of frequency control approaches are shown on Figure 11.

The Primary Frequency Control is the automatic response to the variations of the frequency that is activated for some seconds when there is a deviation from the 50 Hz frequency. This service has been delivered by conventional power plants up until now. These power plants generally operate at lower power than the maximum output power, in order to be able to ramp up and down in case of necessities.

In the near future, with more and more shares of renewable power plant, primary control might be delivered by energy storage system like BESS. [24]

After some seconds, the primary frequency control is automatically replaced by Secondary Frequency Control. This timeframe is different in different countries. The secondary frequency control can be supplied by BESS too.

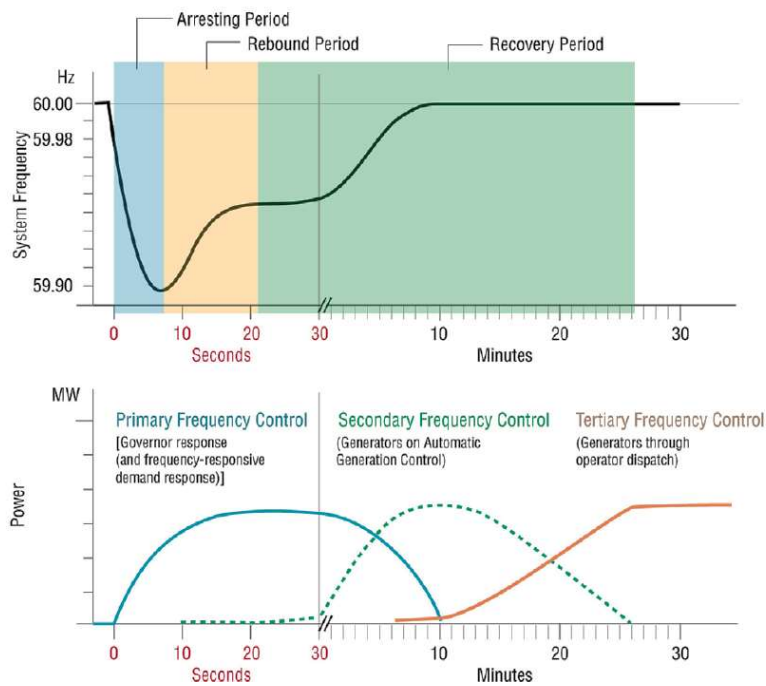


Figure 11 : Frequency Control Methods and Relevant Time Scales in US [24]

After the secondary frequency control, there is the Tertiary Control, also called Minute Reserve. The Transmission System Operators (TSO) must request it from the supplier. For this control, typically hydro pumped storage systems or gas power plants are used, as the delivery time is longer than for primary and secondary frequency control. In Figure 11 and Figure 12 it is possible to see examples for the different step of Frequency control.

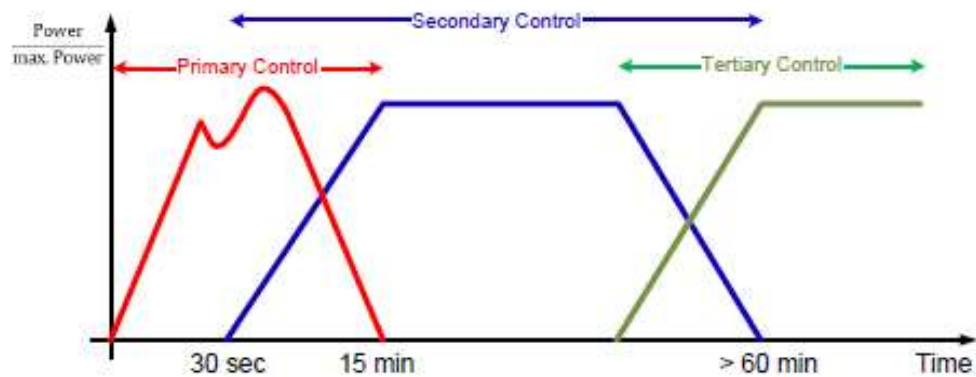


Figure 12 Time scale of frequency control (activating times are examples for Germany) [24]

3.2.2.2 Voltage Control

In the transmission and distribution lines the voltage has to be maintained between certain limits. These limits could be crossed when there are losses, weak networks, times of low consumption and high power injection.

One way to control the voltage is the injection or absorption of reactive power. This can be supplied by systems which are solely installed for this purpose (SVC – Static Var Compensator) and also energy storage systems which can supply reactive power in addition to their primary purpose. [22]

3.2.2.3 Standing Reserve

Standing reserve is the power generation capacity which can be used to increase generation, but which is not synchronously on-line. Standing reserve is a method to provide control power. The same functionality can be provided by storage systems for medium and long term storage or reduction of consumption.

Also renewable generators which are kept offline can act as standing reserve. [24]

3.2.2.4 Black Start Capability

The black start capability provides power and energy after a system failure. Many units of the power system are not able to restart after such an event. Energy storage systems can be used to provide energy to help other units to restart and provide a reference frequency for synchronization of other generation units.

Several studies have considered the use of BESS to restore the service of the plant and the network to which it is connected in case of failure, one of which is reported in [25], in which the operation of a photovoltaic system with a BESS (that can be used for black start) has been optimized from a technical point of view. The critical points are once again related to the uncertainty on photovoltaic production which does not allow to estimate with absolute precision the state of charge of the storage system which must however be able to restart the system at any time. For this reason, an optimization strategy was considered aimed at always satisfying the minimum power requirements necessary for the black start while maintaining the SOC levels within a reasonable range whatever the weather conditions when the failure occurs.

3.2.3 Peak Shaving and Load Leveling

One of the main goals of the BESS integrated with renewable energy power plants is the Energy shifting: that is the possibility to store energy for a long time before delivering it, this way the production would be separated from the utilization of the stored energy.

This service is really useful especially for the power plants that are not programmable, where the energy production depends on the availability of an intermittent energy source, and it is not possible to modulate it. For example, in a photovoltaic power plant the production depends on the solar radiation that reaches the solar panel.

Some of the beneficiaries of this service are the prosumers, that are at the same time consumer and producer of electric energy. Typically, the prosumers are private people or small companies with small power plants (usually photovoltaic) finalized to the production of a part (or all) of the used energy. In these systems, thanks to the energy shifting, it is possible to accumulate the surplus of energy when the production exceeds the consumptions, in this way the surplus can be used in the periods when the production of energy is zero or not enough to satisfy the requests. This situation is typical for the night hours, when for a photovoltaic plant the production is zero, or when the meteorological conditions are adverse. Generally, it is important to maximize the energy production because it reduces the need to buy energy from the grid, because most of the energy is consumed during the daylight hours. Indeed, it is always disadvantageous from the economic point of view to sell the energy to the electric grid and then buy the energy from it when there is the need, because the price for selling and buying the energy are always different [26].

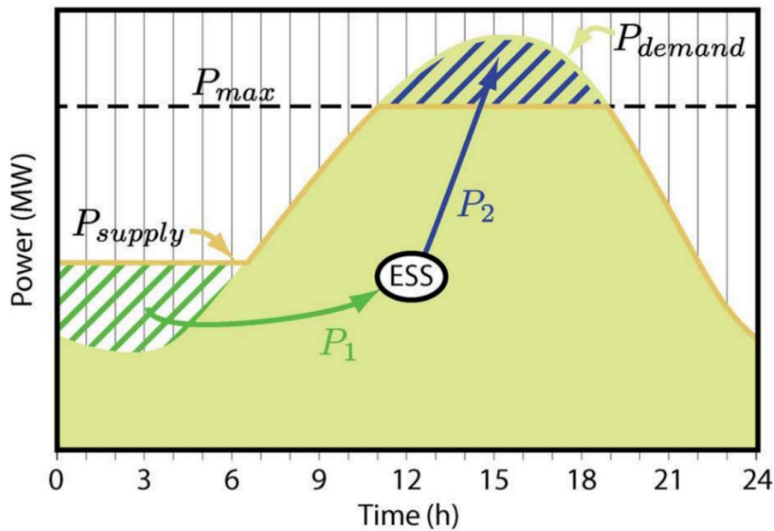


Figure 13 Basic concept of load leveling through BESS [23]

Other people that can take advantage from the energy shifting are the owners of renewable power plants that supply the electric grid. The *energy shifting* allows to maximize the revenues from the sale of the produced energy. The remunerability of the produced energy depends on its value that, in the electrical market, changes continuously, every hour of the day, and it is connected to the “difficulty” to produce the electric energy in that

precise moment. The price is really low when there is a lot of production, as it is during the day with a lot of renewable energy power plants working. Thanks to the energy shifting it is possible to focus the energy selling in the periods where the price is at its highest. [25]

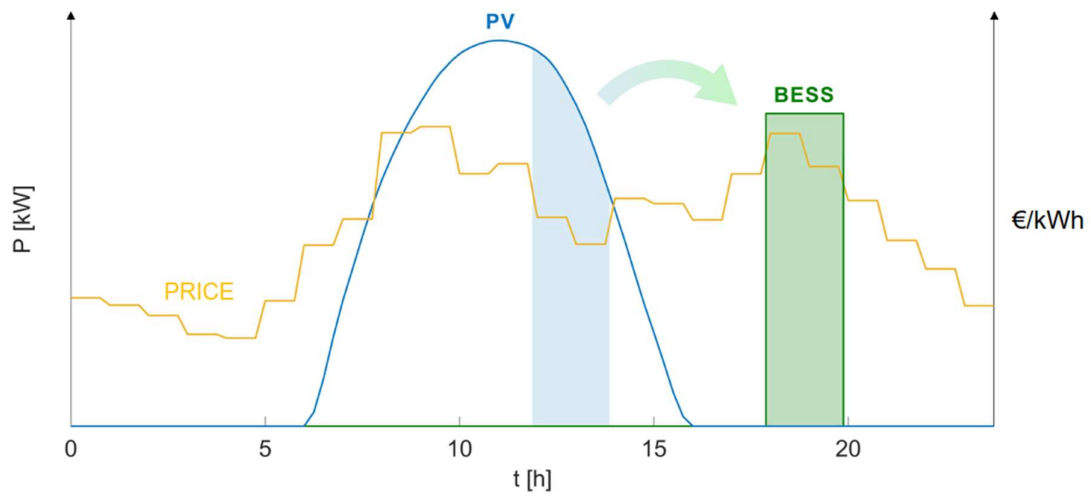


Figure 14 Example of energy shifting [25]

Another fundamental function that is possible with the utilization of BESS is called the peak shaving. It consists of the possibility to accumulate part of the produced energy in the peak-production hours in order to level the

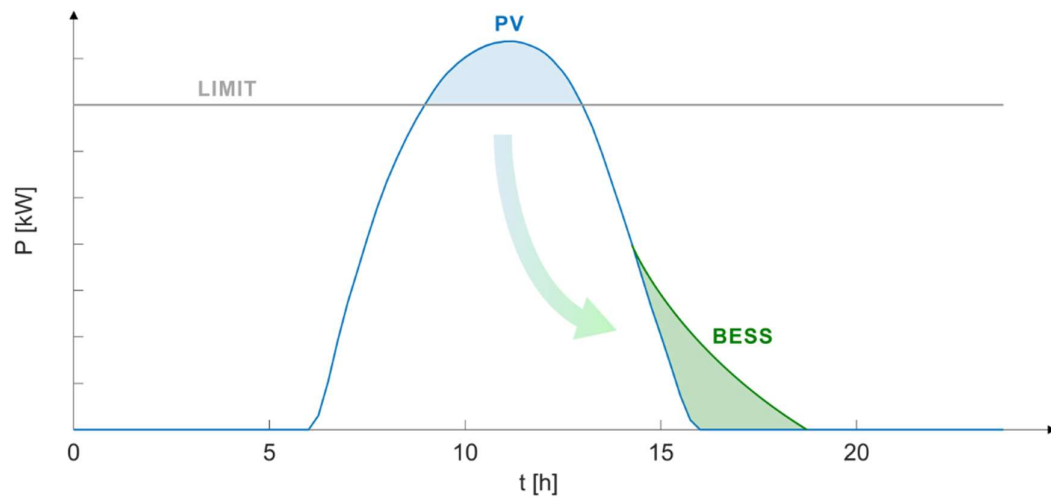


Figure 15 Example of peak shaving [25]

production profile by deleting the energy peaks. This service allows to have an energy production curve more similar to the consumption curve and it allows to respect the power limit of the energy grid if any. As we can see in Figure 15 the energy production is respecting the limit and thanks to the BESS the power plant can satisfy more energy requests during the day. Generally, the peak shaving operation is executed within a time period of 1 to 10 hours. [26]

3.3 Storage System for off-grid power plant

Another possible application for the electrochemical accumulators integrated with renewable power plant is the realization of off-grid power plant. These power plants are not connected to the national electric grid and generally are built to satisfy the local utilities in places that are difficult to connect to the grid, as for example mountain areas or isolated places.

Traditionally in these places the energy is produced by diesel generators, that were easy to adapt to the energy needs and were a very used technology, but this technology is very bad for the emissions, so also for isolated places is preferred to find a green way to supply energy.

Due to the variability of the renewable energy sources, the storage system is fundamental for this application that are really influenced by the variation of energy production.

In this way, the renewable energy system with overrated peak power can store the excess energy for later thanks to the BESS.

As an example, it can be considered one of the first off-grid systems built by Enel Green Power integrated with a BESS in the village of Ollagüe, a small village in Chile at an altitude of 3700 m and with a population of around 300 people [27].

Before the installation of a photovoltaic power plant (205 kW_p), a small wind turbine (30kW_p) and an electrochemical storage system (752 kWh), that today covers almost all the energy request, the energy supplier was only a diesel generator of 250 kW, that today is used only as a backup generator.

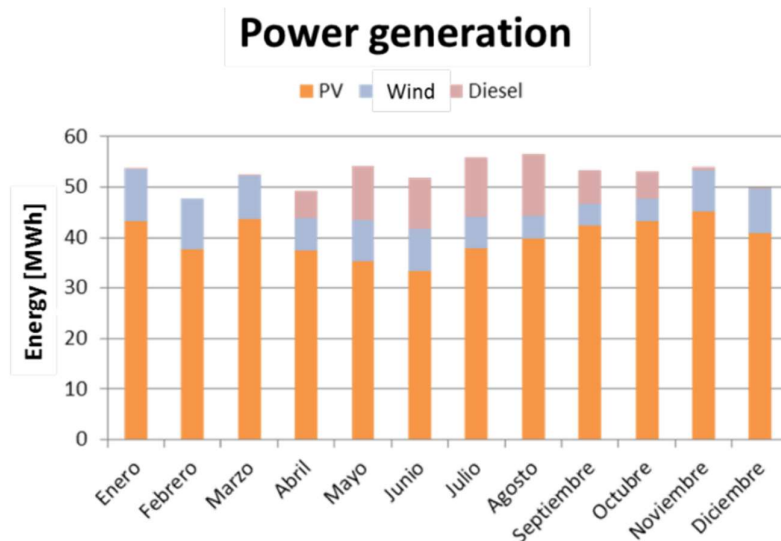


Figure 16 Forecast of monthly power generation for Ollagüe's microgrid [27]

This system was able to supply the energy only 16 hours a day, while from 1am to 8am the village had to live without electricity. Now, thanks to the renewable power plant and the storage system as we can see in Figure 16, it is noticeable the high share of renewable energy production of the project. In fact, it is expected for the overall share of renewable energy (PV and wind power) to be around 100% for 5 months, from November until March. Moreover, by taking the year round, the renewable energy share is approximately 85%. [27].

Chapter 4: Photovoltaic Energy Production

In this chapter it will be analyzed the method and the analysis done in order to compute the energy production of the PV park Campos del Sol.

First of all, a brief description of the geographical and meteorological condition of the location will be done since it was chosen for its particularly fitted conditions.

The PV Park Campos del Sol is located in the Atacama Desert, the region with the highest radiation in the world.

Second of all, the used data and the calculations done with the software SAM (System Advisor Model) will be described.

Finally, the results obtained from the software will be shown.

4.1 Chilean geographical features and climate conditions

The Chilean geography can be considered unique. The country is 4337 km long in a latitude range between 17°35'S (from the Altiplano highs) and 56°S (to Tierra del Fuego) [28] which contributes to different climates. The hot desertic climates change to lower temperatures as the country extends to the south with a progressive rise of elevation from west to east, in fact in the east side of the country there is the Chain of the Andes. Due to the particular geographical and climate conditions, the solar radiation reaches higher values in Chile compared to the rest of the world. Considering these natural properties, it is possible to consider three different zones: the extreme north, the central zone, and the extreme south.

In the northern region the climate is extremely dry, and it is possible to identify two different zones, known in Chile as the Norte Grande and Norte Chico. Arica and Parinacota, Tarapacá and Antofagasta regions integrate the Norte Grande (the largest northern zone of the country) while the Atacama and Coquimbo regions form the Norte Chico. In these regions the aridity is extremely high because precipitations are almost non-existent, and temperatures of these areas have really important variations between day and night conditions [29]. These extreme conditions explain why in the north of Chile the level of solar irradiation is one of the highest in the world (probably the highest) with an average yearly total between 2400 and 2800 kWh/m² of Global Horizontal Irradiation (GHI), as can be seen in Figure 17. Just to have a comparison, in Portugal the maximum yearly values of GHI are around 1900 kWh/m² in the South of Portugal (Algarve) [30].



Figure 17 Maps of Chilean Global Horizontal Irradiation with the location of Campos del Sol [30]

In the Northern Chile, it is located the Atacama Desert, known because it is one of the driest places on Earth placed from the Norte Grande to the north of Coquimbo [32]. In the Atacama Desert, the combination of high-altitude zones and extremely high aridity, endow this desert as the place on earth with the highest solar radiation.

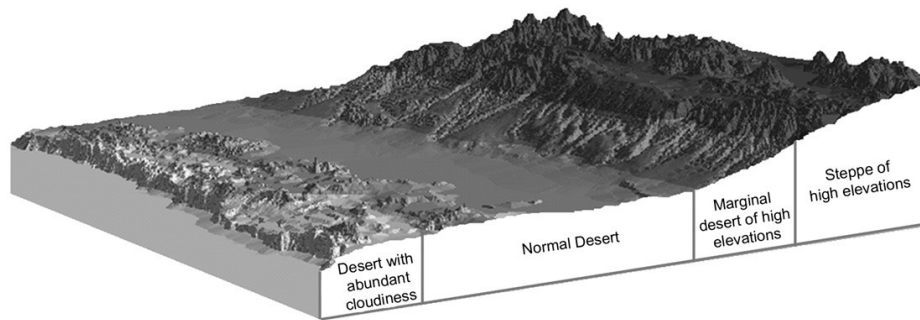


Figure 18 Typical geography of the northern regions of Chile. [31]

The subtropical position of this desert is one of the reasons of the hyper-aridity condition of this area, where the precipitations in the zone are reduced by the pressure and the air circulation; another cause of the Atacama condition is the fact that the Andes mountains stop the moisture advection from the east and in the coast the water is cold because of the Humboldt Current from the Pacific Ocean. [33]

Because of the proximity to the Ocean, in the coastal area of the North Chile there is abundant cloudiness and foggy conditions exhibiting marked oceanic influence. An example of this condition is the “foggy desert” that is



Figure 19 Maps of Chilean Photovoltaic Power Potential with the location of Campos del Sol [30]

possible to see especially in the morning, when there is the phenomenon called “Camanchaca” which produces abundant and heavy fog and high humidity with no rains due to the density of the fog near the mountains [31]. This phenomenon is only present near the coastal area, in fact, after the Coastal range, the influence from the Pacific Ocean disappears and extreme aridity and clear skies domain. Therefore, a relationship between the longitude and the solar resource has been found as a result of the geography variation from the coast to the eastern limit of the country. In Figure 20 it is possible to see the yearly totals of Global Horizontal Irradiation (GHI) and Direct Normal Irradiation (DNI) varying the longitude in the same latitude. In the Figure 20 are shown two locations: Iquique (-20.22°S , -70.17°W), a coastal city located in the Tarapacá region with a typical climate of coastal desert; and Copiapó (-27.37°S , -70.32°W), which is located at 390 m above the sea level and approximately 60 km from the coast in the longitudinal intermediate depression of the Atacama Region. [34] Copiapó is around 60km near the project Campos del Sol.

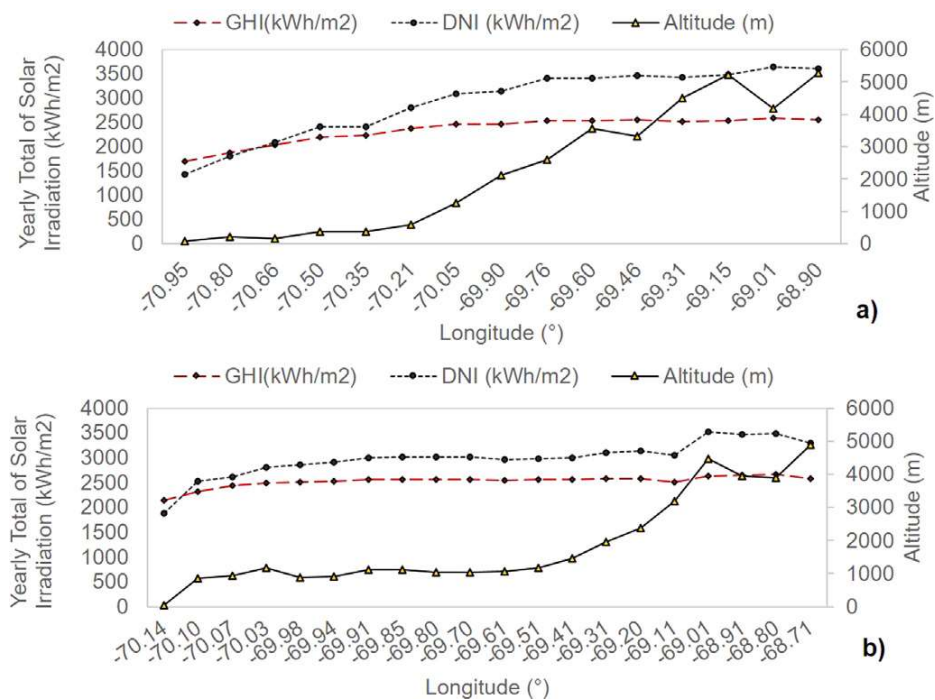


Figure 20 Irradiation for different longitudes in a) Iquique and b) Copiapó's latitude. [35]

The altitude profile shows the variation in the transversal topography of the northern region of Chile. The yearly totals of GHI and DNI can be seen changing in the same way: it is possible to say that they tend to increase when the distance from the coast is growing, and when the altitude is increasing. However, this tendency has a higher impact in the DNI than in the GHI. In the Copiapó's latitude the elevation remains steadier than in Iquique latitude, so the variation in the irradiation is lower in this case. For these reasons, latitude and longitude are serious regulators of the solar irradiation in Chile.

The proximity to the ocean and the decrease of altitude influence the tendency of GHI to decrease with the longitude. The higher air mass together with a higher load of atmospheric gases and particles, and a higher presence of clouds created from the sea convection are associated to the GHI's tendency. These parameters are always relevant, in fact, after the clouds, the aerosols load is one of the most important modifiers of the solar

irradiance: the more the aerosols the less the irradiance [35]. One of the properties that makes the irradiation increase is the altitude, in fact at higher altitude the irradiation is higher due to the reduction of the atmosphere thickness and the predominance of clear sky situation.

Some studies have determined that the best natural conditions for solar PV application are in the north Chile, 5-20 kilometers from the coast and at altitudes higher than 1000 meters above the sea level [35], with these conditions a very low number of cloudy days has been found and high sky clearness indexes [36].

The project Campos del Sol meets all the best criteria:

- it is in the North of Chile (near the city of Copiapó).
- it is around 80 km away from the coast.
- it is situated at an altitude of about 1700 meters.

Looking the project's properties, it is possible to say that the project is located in one of the best location possible, where the irradiation is favored by the geographical characteristics.

The studies stress the fact that the Atacama Desert is one of the best areas for potential solar applications, due to its natural characteristics and the high amount of irradiation received. In this desert in fact, the environmental conditions attract investor that want to make this area one the most exploited in the world for the production of photovoltaic solar energy. These are the causes of the rapid growth in the last year of the development and deployment of big solar power plant in the Atacama Desert. [37]

Chapter 5: Campos del Sol Project

In the next paragraphs the energy production of the Campos del Sol photovoltaic Power Plant will be computed, in order to analyze the hourly behavior of the PV Plant and compute the best BESS solution for this power plant.

It has been possible to find all the photovoltaic data thanks to the company STE Energy, where I did my internship last year.

STE Energy is a contractor for Campos del Sol project, and it developed the engineering, procurement and construction (EPC) of the substations, while other companies supplied the modules and the other equipment for the solar plant.

During the internship it was possible to find all the data regarding the PV modules, the inverters and the design of the PV park.

5.1 Campos del Sol – Case Study Definition

The 385 MWp Campos del Sol PV plant will generate around 920 GWh per year when fully up and running, savings more than 9000.000 tons of CO₂ emissions.

The project is located 60 km northeast of Copiapó, in the Atacama Desert.

As already previously discussed the combination of high-altitude zones and extremely high aridity, endow this desert as the place on earth with the highest solar radiation values: the average yearly total radiation is between 2400 and 2800 kWh/m² of Global Horizontal Irradiation (GHI).

This PV Power Plant is the largest solar plant currently under construction in Chile and it is facing north, and the tracking system is monoaxial (east to west). The modules are bifacial modules, a technology that maximizes energy generation by capturing solar radiation from both sides of the panel, generating on average 12% more electricity than conventional modules. [38]



Figure 21 Location of the project Campos del Sol PV Power Plant. Photo from Google Maps.

With these properties, this PV power plant will be one of the biggest PV installations of the world (the biggest in the South America by now).



Figure 22 Panoramic view of the area where the PV Plant will be situated (Google Maps)

In the area where the Campos del Sol project will be situated, there are already two other PV Power plants, the 141MW PV Plant Luz del Norte and the 97MW Carrera Pinto PV Plant, as we can see in Figure 22.

In the Campos del Sol PV plant, around 970 thousand of bifacial solar panel will be installed, which shows how the Chilean energy sector is going towards a renewable energy future.

The project Campos del Sol will be connected to the substation Carrera Pinto after a resizing of the substation, to allow the engagement of the energy coming from Campos del Sol PV Plant.

From the Carrera Pinto substation, the electricity will be injected into the grid.



Figure 23 Carrera Pinto Interconnection Substation

5.2 SAM (System Advisor Mode)

The software SAM has been used to compute the energy production of the PV park Campos del Sol.

In the software SAM, the input data are:

- Location and Resource
- Module
- Inverter
- System Design
- Shading and Layout
- Losses

In the next paragraphs, the process that has been used in order to compute all the parameters and all the required data is going to be described.

5.2.1 Location and Resource

The data regarding the meteorological condition of the year 2020 have been found in the SAM website Weather Page [39].

In the Figure 24 it is possible to see the annual irradiance for the considered area of the Atacama Desert. [36]

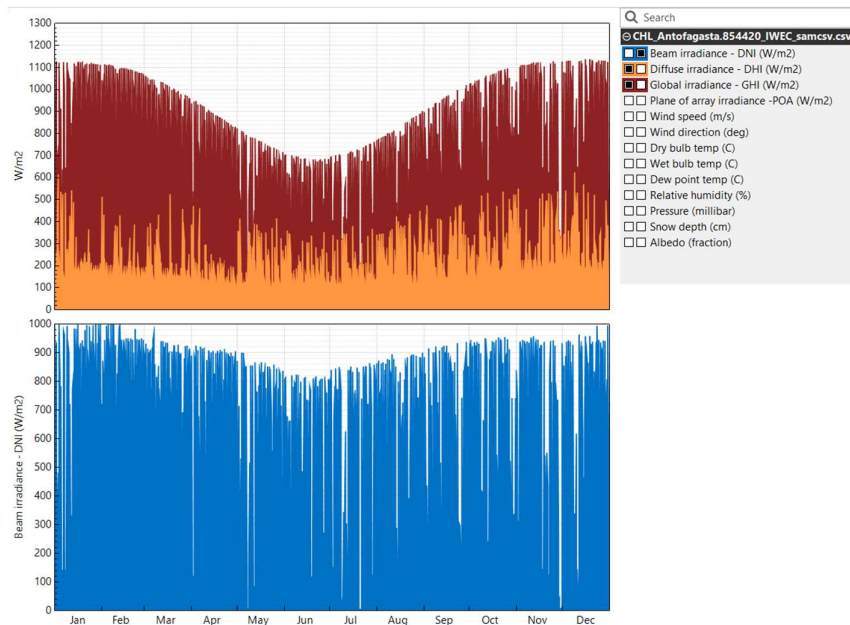


Figure 24 Irradiance of the area of Campos del Sol PV Plant

The data used are of the type “tmy (typical meteorological year)”, so the values are the most accurate possible to compute the real radiation of the next 25 years (typical lifetime of a photovoltaic module).

A tmy file takes the average from the last 30 years and then selects the month that has the irradiance values closer to the calculated average. This way, the most precise month is selected from a 30 year span, and it is taken as reference for the irradiance data.

5.2.2 Module

The information regarding the photovoltaic module have been taken during the internship in STE Energy.

As we can see in Figure 25 the modules have a P_{max} of 385.92 W.

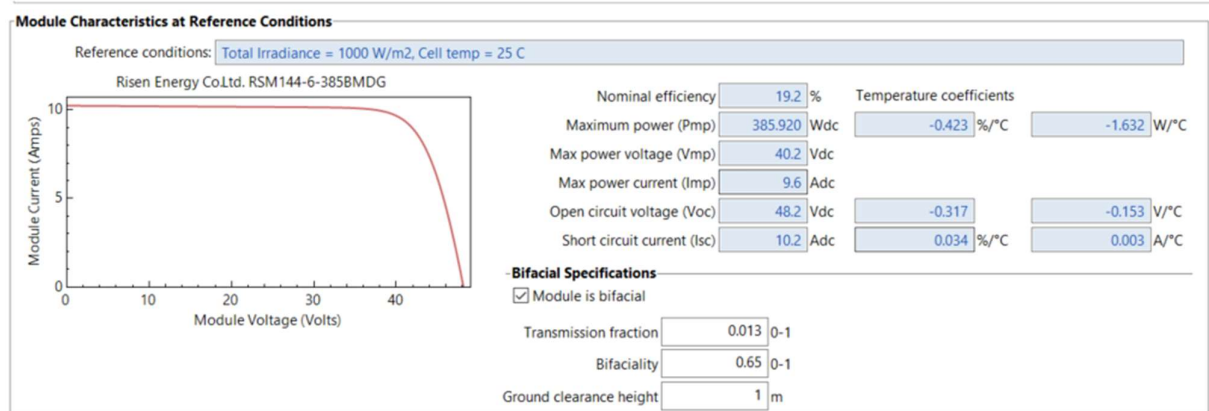


Figure 25 Module data

As previously described, the modules are bifacial, and this characteristic increases the efficiency of the module.

The bifaciality of the solar panels used is particularly exploited in the Atacama Desert because of the vast spaces available. In fact, in order to maximize the light reflected from the ground and minimize the shadowing, the PV panels have to be placed in rows distanced from one another.

5.2.3 Inverter

The PV Park Campos del Sol is divided into subfields, in each subfield are installed two inverters that are then connected to a transformer and to the Medium Voltage/High Voltage Substation. The characteristic of the inverter can be seen in Figure 26.

Each inverter receives the DC Power from the modules and transforms it into AC power.

Power Ratings	
Maximum AC output power	3.593e+06 Wac
<input checked="" type="radio"/> Weighted efficiency	99
<input type="radio"/> Manufacturer efficiency	98.7
Maximum DC input power	3.62929e+06 Wdc

You can specify either a weighted or nominal efficiency. The weighted efficiency can be either CEC or European. The manufacturer efficiency can be either peak or nominal. See Help for details.

Operating Ranges			
Nominal AC voltage	35000 Vac	Minimum MPPT DC voltage	875 Vdc
Maximum DC voltage	1500 Vdc	Nominal DC voltage	1500 Vdc
Maximum DC current	4178 Adc	Maximum MPPT DC voltage	1300 Vdc
		Number of MPPT inputs	1

Figure 26 Inverter Data

5.2.4 System Design

The Campos del Sol PV Park is divided into 63 subfields.

Each subfield has:

- 15.456 modules that are installed into
- 552 trackers (each tracker has 28 modules)
- 2 inverters (each inverter is connected to 276 trackers approx.)
- 1 transformer, connected to the two inverters. From the transformer the MV Power flows until the MV/HV substation that is then connected to the grid.

It means that in total in the PV park Campos del Sol there are:

- 1.000.000 of modules (approx.)
- 35.000 trackers (approx.)
- 126 Inverters
- 63 Transformers LV/MV

with a total installed capacity of 385 MW_p.

5.2.5 Shading and Layout

On each tracker are installed 28 modules (2 rows of 14 modules) as can be seen in Figure 27.

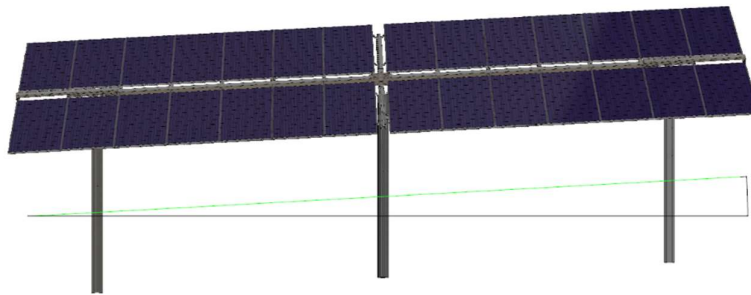


Figure 27 Tracker structure. In each tracker there are 28 modules.

It is really important to study the shading of the PV park in order to take in consideration the losses due to shadowing. In fact, the shadowing coming from the inclination (up to 55°) of each row of trackers has to be considered to define the distancing between the panels.

In order to compute the losses it has been taken into consideration the distance of the rows of the tracker, the layout of the trackers and the total occupied area of Campos del Sol Park.

The shading of the system has been estimated in the software SAM as can be seen in Figure 28.

Array Dimensions for Self Shading, Snow Losses, and Bifacial Modules

The product of number of modules along side and bottom and number of rows should be equal to the number of modules in subarray.

Module orientation	Portrait	Portrait	Portrait	Portrait
Number of modules along side of row	2	2	2	2
Number of modules along bottom of row	560	9	9	9

-Calculated System Layout

Number of rows	894.959	0	0	0
Modules in subarray from System Design page	1,002,354	0	0	0
Length of side (m)	3.69703	3.69703	3.69703	3.69703
GCR from System Design page	0.171323	0.3	0.3	0.3
Row spacing estimate (m)	21.5793	12.3234	12.3234	12.3234

Module aspect ratio	1.7
Module length	1.84851 m
Module width	1.08736 m
Module area	2.01 m ²

row spacing = length of side + GCR

module orientation (portrait)

number of modules along bottom

Figure 28 Shading analysis of the PV modules and the trackers

5.2.6 Losses

For the project the losses for each component have been considered and, for the components for which the data were not available, the default losses suggested in the software SAM were used.

In the Figure 29 the considered losses can be seen.

Irradiance Losses
Soiling losses apply to the total solar irradiance incident on each subarray. SAM applies these losses in addition to any losses on the Shading and Snow page.

	Subarray 1	Subarray 2	Subarray 3	Subarray 4
Monthly soiling loss	<input type="text" value="Edit values..."/>			
Average annual soiling loss	<input type="text" value="3"/>	<input type="text" value="5"/>	<input type="text" value="5"/>	<input type="text" value="5"/>

Bifacial modules only
Average annual rear irradiance loss due to soiling, mismatch, or external shading (%)

	<input type="text" value="0"/>	<input type="text" value="0"/>	<input type="text" value="0"/>	<input type="text" value="0"/>
--	--------------------------------	--------------------------------	--------------------------------	--------------------------------

DC Losses
DC losses apply to the electrical output of each subarray and account for losses not calculated by the module performance model.

Module mismatch (%)	<input type="text" value="2"/>	<input type="text" value="2"/>	<input type="text" value="2"/>	<input type="text" value="2"/>
Diodes and connections (%)	<input type="text" value="0.5"/>	<input type="text" value="0.5"/>	<input type="text" value="0.5"/>	<input type="text" value="0.5"/>
DC wiring (%)	<input type="text" value="2"/>	<input type="text" value="2"/>	<input type="text" value="2"/>	<input type="text" value="2"/>
Tracking error (%)	<input type="text" value="1"/>	<input type="text" value="0"/>	<input type="text" value="0"/>	<input type="text" value="0"/>
Nameplate (%)	<input type="text" value="0"/>	<input type="text" value="0"/>	<input type="text" value="0"/>	<input type="text" value="0"/>
DC power optimizer loss (%)	<input type="text" value="0"/> All four subarrays are subject to the same DC power optimizer loss.			
Total DC power loss (%)	<input type="text" value="5.396"/>	<input type="text" value="4.440"/>	<input type="text" value="4.440"/>	<input type="text" value="4.440"/>

Total DC power loss = 100% * [1 - the product of (1 - loss/100%)]

Default DC Losses
Apply default losses to replace DC losses for all subarrays with default values.

Apply default losses for: Central inverters Microinverters DC optimizers

AC Losses
AC losses apply to the electrical output of the inverter and account for losses not calculated by the inverter performance model.

AC wiring %

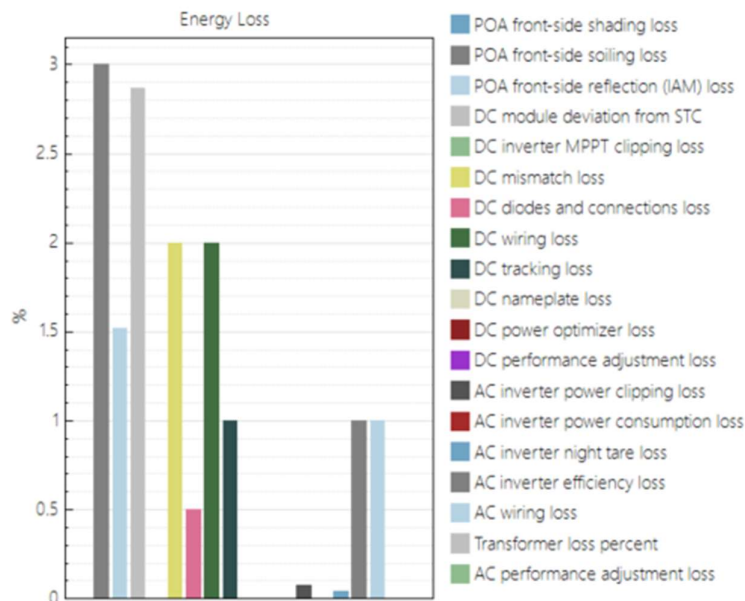


Figure 29 Campos del Sol considered losses.

5.2.7 PV Production Results

The results from the software SAM show the annual energy production of the PV park Campos del Sol for the first year of production.

The production has the highest values (November to January) during the summer and the lowest values (May to July) during the winter.

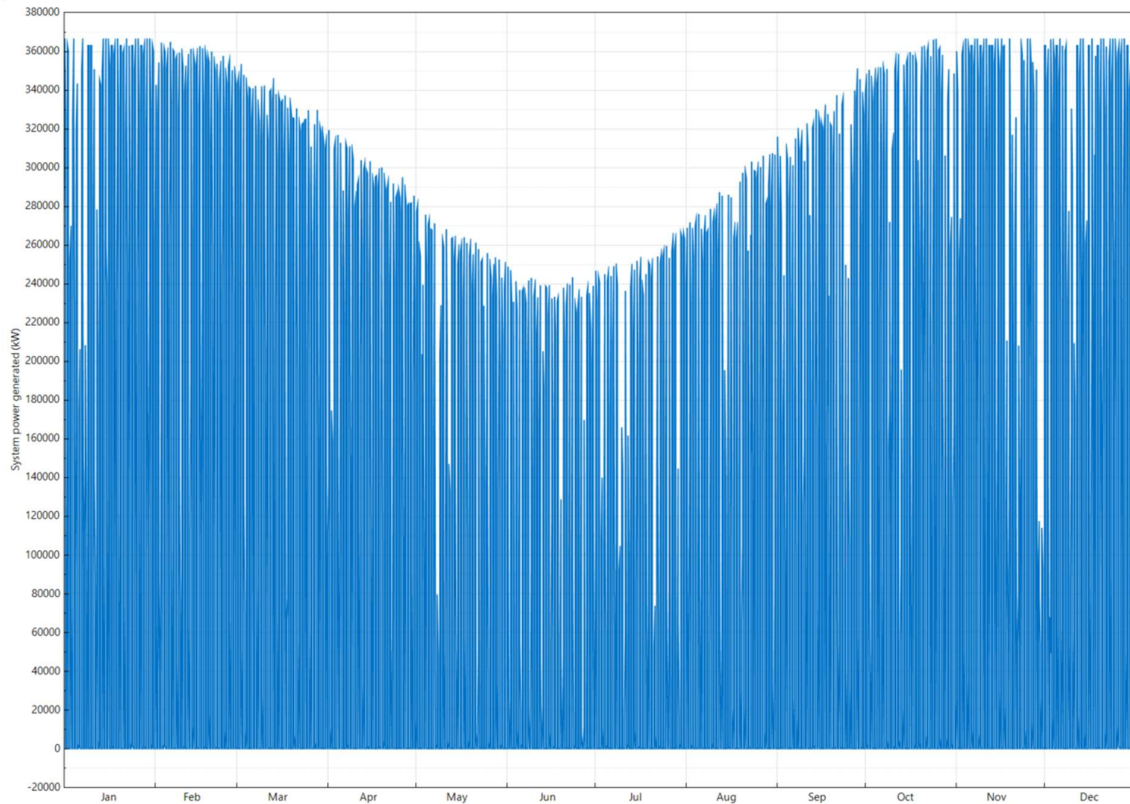


Figure 30 Campos del Sol computed annual PV Power

As we can see in Figure 30, the production has a regular curve during the year, there are just some intermittencies probably due to cloudy days. The overall yearly production of the PV park is of the order of 920 GWh, as per the SAM results.

In the second part of the project, when the BESS feasibility will be analyzed, the whole lifetime of the PV park (25 years) will be studied, considering a degradation factor of 0.5% for each year.

In the Figure 31 it can be seen the power generated from the PV park for the first week of the first year.

It can be seen that the production reaches the maximum value of 360 MW during the first week.

Once the PV production is computed, the results have been used for the main scope of the thesis: the BESS feasibility analysis.

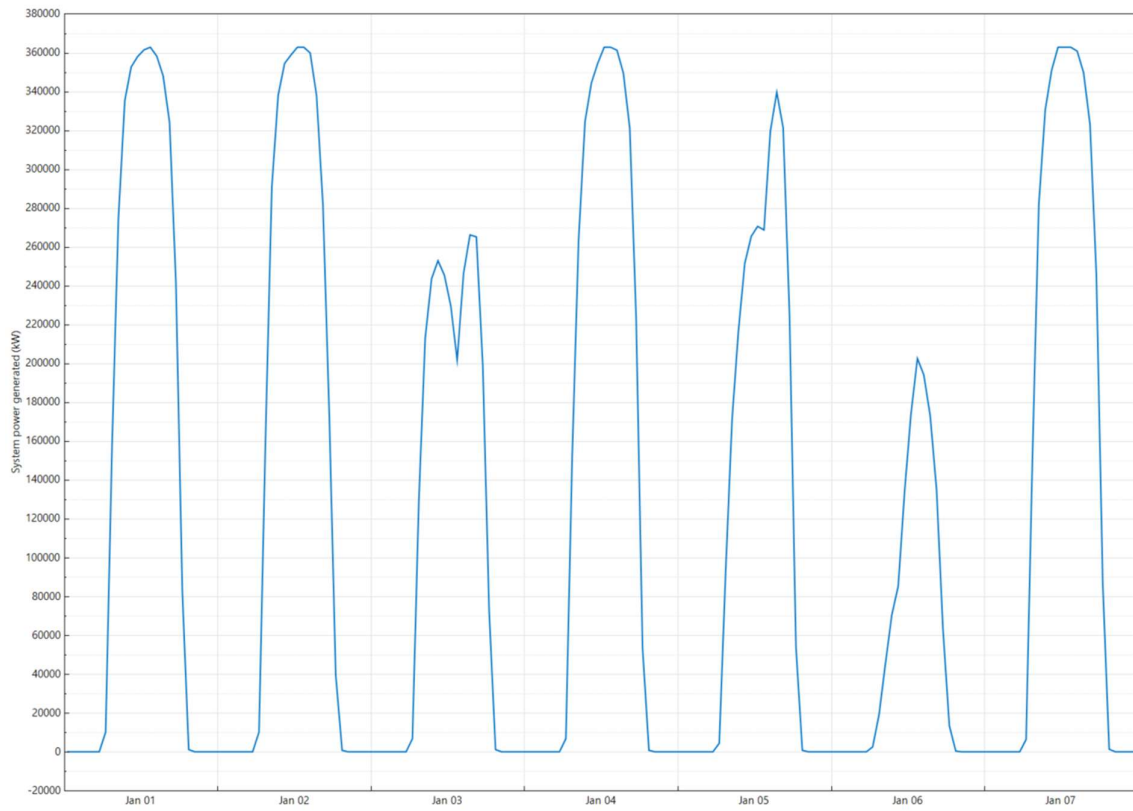


Figure 31 Campos del Sol generated Power for the first week of the year, computed with SAM

Chapter 6: Methods

The main part of this thesis project is the study of the feasibility of a battery energy storage system for the 385 MW_p photovoltaic project Campos del Sol.

Due to the fact that the solar energy is not a predictable nor constant energy source throughout the day, the coupling with a battery system is the solution to have constant energy production during the day.

With the use of a battery system, it could be possible to proceed with “energy shifting” saving energy during the day in order to deliver it to the grid in the late afternoon hours and evening hours when the energy price is higher.

6.1 The System

The system taken into consideration is composed by three main components interconnected between them:

1. Photovoltaic Power Plant Campos del Sol (PV)
2. National Electric Grid
3. Battery Energy Storage System (BESS)

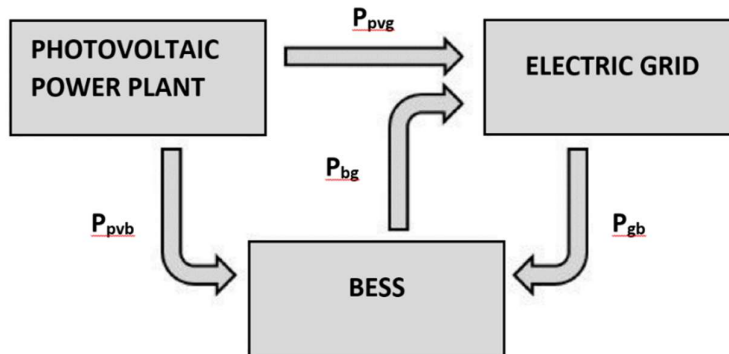


Figure 32 Block Diagram of the Considered System

The block diagram of the system is shown in Figure 32, in which it can be seen that there is no connected local load in the considered system. It was considered that the production plant is built exclusively to produce energy to be fed into the grid in order to generate revenue for the system's owner. Nevertheless, the tool created is particularly adaptable and allows to easily introduce, if needed, a constraint for the satisfaction of a generic load profile directly connected to the photovoltaic system and to the storage system.

The power flows exchanged between one component and another of the system have been considered separately with the direction shown.

Specifically, all the power flows considered are:

- P_{pvb} : power generated from the photovoltaic park that is injected directly into the grid.
- P_{pvb} : power generated from the photovoltaic park that is used to charge the battery system.
- P_{bg} : power delivered from the battery system to the grid.
- P_{gb} : power delivered from the grid to the battery system.

Of course, observing the connection scheme between the considered system, represented in Figure 33, it can be understood that the interconnections between the components are not ideal and consequently they introduce power losses. In particular, the use of a bidirectional inverter is considered for the conversion of the power produced by the PV, connected with the storage system and a transformer for coupling with the electricity grid was used.

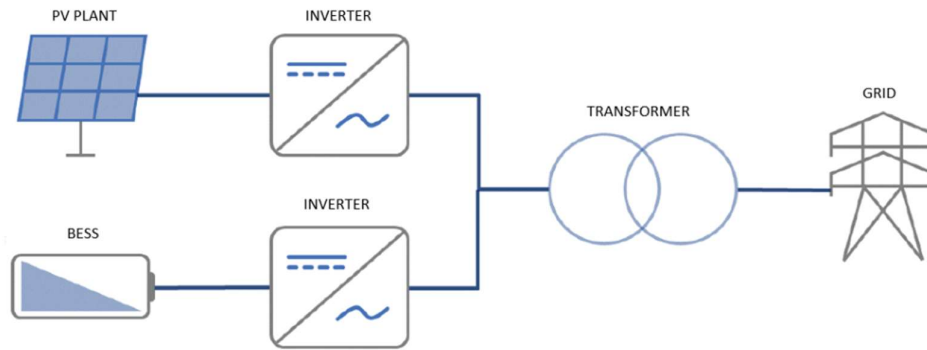


Figure 33 Simplified Electric Interconnection Scheme of the considered system.

The efficiency values used for the inverter and the modules have been described in the previous chapter, while the efficiencies attributed to all the losses due to the use of transformers and connections for feeding energy into the grid, have been assumed, to simplify constant as the transferred power varies. Hence, the used efficiencies for power exchange between each system can be divided as:

- The power exchange efficiencies between the PV and the electricity grid ($\eta_{pv,g}$), between the BESS and the electricity grid ($\eta_{b,g}$), and vice versa between the electricity grid and the BESS ($\eta_{g,b}$), are assumed to be 0.980. This value considers the efficiency of the inverters for the transformation from direct current to alternating current and vice versa and the power transformation performance connected to the electricity grid.
- The efficiency value attributed to the connection between the PV and the BESS ($\eta_{pv,b}$) is equal to 0.97. It considers the efficiencies of the inverters connected to the photovoltaic system and to the storage system for the conversion from direct current to alternating and vice versa from alternating to direct current. [40]

6.2 Photovoltaic Power Plant

The photovoltaic Power Plant has been described in Chapter 5.

The PV Plant Campos del Sol production has been computed with the software SAM (System Advisor Model). The data timeseries obtained, containing the value of power produced by the PV for each hour, was subsequently processed with the software MATLAB in order to increase the sensitivity of the results that can be obtained. In fact, increasing the number of annual data by means of Hermite polynomial interpolation (PCHIP), a photovoltaic production profile consisting of four values of power for each hour was obtained.

The PCHIP interpolation takes the hourly values of the PV power and creates 4 values for each hour by making the average between the value of one hours and the values of the following hours. It means that for each day there are 96 values (24 hours x 4 values/hour).

As an example, Figure 34 shows some daily production profiles obtained, referred to different periods of the year.

The software SAM gives as output the hourly PV power production for each day of the year, in Figure 34 the four

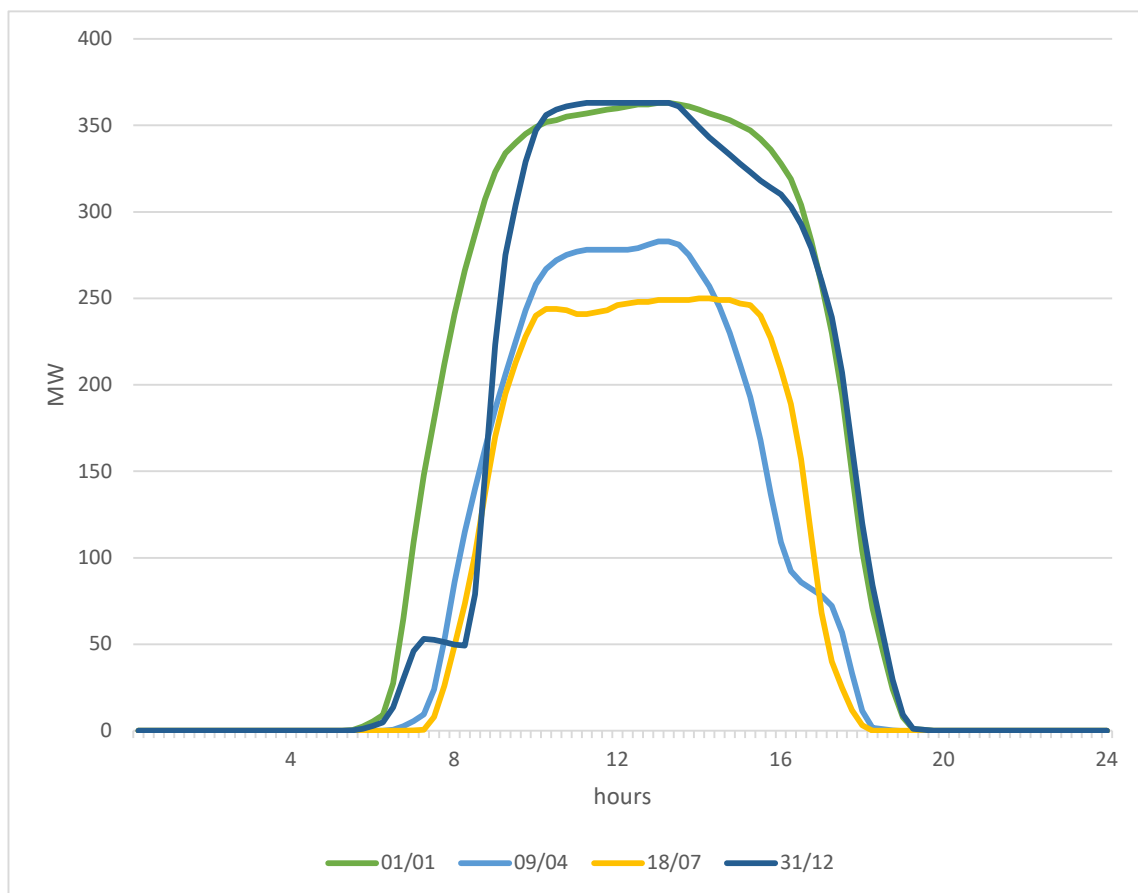


Figure 34 PV power produced for four different days, as example.

profiles show the PV Power Production of four days of the year (1st January, 9th April, 18th July and 31st December), as example.

Finally, since the period of time considered in the simulations is generally greater than one year and because the estimated life of the photovoltaic system has been assumed to be equal to 25 years, the overall production profile was found by repeating the annual profile obtained assuming a reduction of the power produced linearly with time.

In particular, a 0.5% decrease in the power produced at the end of each year was assumed. Figure 35 shows the profile obtained over a period of 25 years.

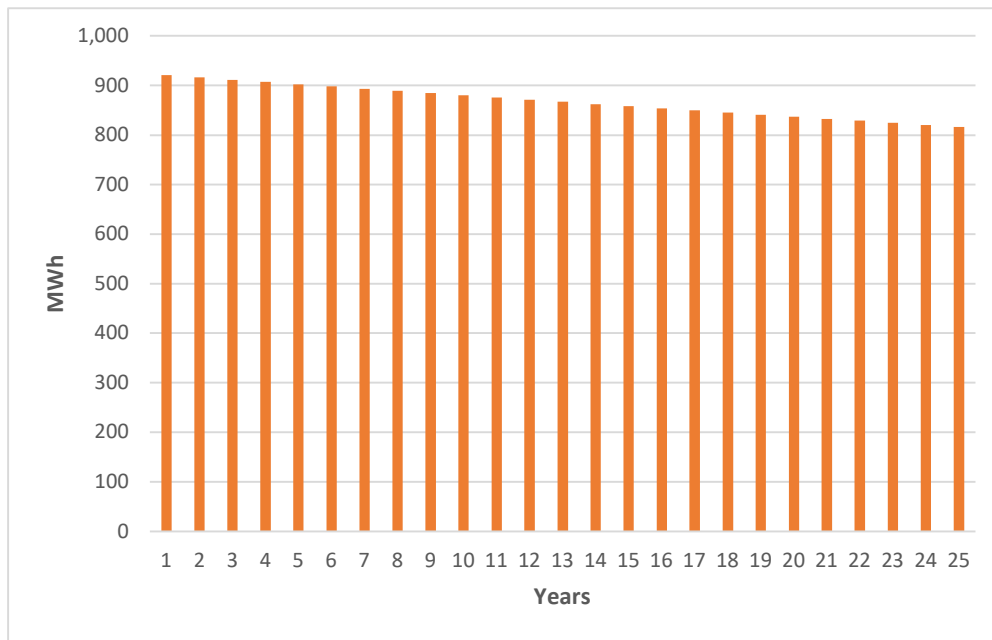


Figure 35 Energy profile produced by the PV in 25 years, with linear reduction of the power.

6.3 Electricity Grid

The electrical grid in the model created is considered as a component capable of absorbing or delivering power at any time with the only constraint of compliance with the maximum power limits supposed to be equal, both in input and output, to the photovoltaic peak power (385 MW).

This means that, at any given instant, the sum of the power fed directly into the grid by the PV P_{pv} and the power discharged from the P_{bg} battery cannot exceed this maximum value.

The flexibility of the tool allows to vary the maximum power that can be fed by extending the field of applicability even to scenarios in which the photovoltaic system is oversized compared to the power accepted as input from the grid, where therefore the storage system can be used to provide peak service shaving to enhance the energy profit.

6.4 Battery Energy Storage System

The component of the system studied in detail is the electrochemical storage system.

It is able to absorb power both from the PV and from the electricity grid during the charging process and to deliver power to the grid during the discharging process, respecting the limits on the state of charge. Specifically, the BESS can accumulate energy as long as its state of charge does not reach the maximum fixed value, while it can discharge the accumulated energy until the minimum fixed state of charge value is reached. This way, the storage system allows to delay the hours in which the energy is produced by the photovoltaic park from its injection into the grid and, if convenient, to implement the sale of energy in order to maximize revenues based on the price trend.

It has been assumed that each BESS considered is constituted by the connection of identical electrochemical modules, characterized by the same characteristics which have been obtained from the LG Chem documentation [6]. In detail, Table 2 shows the specifications of the modules taken into consideration.

As can be seen, the technology of the cells used is with a Lithium-Nickel-Cobalt-Manganese (NMC) cathode, with a negative electrode (anode) made of graphite.

It has been analyzed in the second chapter that the use of this technology has advantages both from an electrical and a structural point of view and the interest in its use in stationary applications is growing after it has become commonly used in the automotive sector. [12]

For these reasons and due to the availability of numerous data in this regard, this type of modules was considered the best candidate for the development of this project.

Table 2 Characteristics of the electrochemical modules

Item	Unit	JH3
Nominal Capacity	Ah	63.0
Nominal Energy	Wh	233
Nominal Voltage	V	3.70
Energy Density	Wh/L	410
Specific Energy	Wh/kg	197
Voltage Range	V	3.0 ~ 4.2
Storage Temperature (for shipping state)	°C	-30 ~ 60
Weight	g	1,180
Volume	mL	569
Dimension (W/L/T)	mm	100.2 / 352.5 / 16.1
Chemistry	(+)	NCM
	(-)	Graphite

For the modeling of the functioning of the modules some simplifications have been introduced with respect to the real behavior. In fact, it has been assumed that the energy that can be stored / discharged from the system is proportional to the capacity that can be stored / discharged, assuming that the cell voltage remains constant as the state of charge varies.

Table 3 Charge and discharge performance of the BESS as function of the C-rate

C-rate	η_c/η_d
0.20	0.985
0.25	0.983
0.33	0.979
0.5	0.984
1.00	0.977
2.00	0.962

Furthermore, the absorbable / deliverable capacity was assumed to be constant as the input / output power of the modules varies, although, as already described, it is a function of the specific C-rate performed. In any case, this last simplification introduces in the model only errors by default on the total quantity of accumulated and discharged energy since the charge and discharge efficiencies of the system, which determine the shares of energy dissipated inside the cell during the two phases, are fixed for each size considered according to the maximum C-rate at which this BESS can work. Therefore, in the event that the storage system does not work at

the maximum allowed power in some instants, the associated efficiency will in fact be underestimated. Specifically, the different values of charge efficiency η_c and discharge efficiency η_d , assuming to use two different modules according to the required performances of the same technological family, are shown in Table 3.

The discharged energy E_d and the accumulated energy E_c during a time interval between the instant t_i and the instant t_f can, in general, be expressed respectively as:

$$E_d = \frac{1}{\eta_d} \int_{t_i}^{t_f} pb_d(t) dt \quad (8)$$

$$E_c = \frac{1}{\eta_c} \int_{t_i}^{t_f} pb_c(t) dt \quad (9)$$

Where pb_d and pb_c are respectively the discharging and charging power exchanged between the accumulator and the system. Starting from these equations, in the tool created in MATLAB, where the power values within a time interval are limited or the evaluations are necessarily conducted on a discrete model, the shares of overall energy discharged and loaded have been calculated as:

$$E_d = \frac{1}{\eta_d} \sum_{i=1}^N Pb_d(i) \Delta t \quad (10)$$

$$E_c = \frac{1}{\eta_c} \sum_{i=1}^N Pb_c(i) \Delta t \quad (11)$$

Where N represents the number of instants contained in the considered time interval, $Pb_d(i)$ is the i -th outgoing power value from the storage system, $Pb_c(i)$ is the i -th incoming power value and Δt is the time period that separates one value and the next which in our case is equal to 0.25 h, since, as already mentioned, there are four power values for each hour. Since the power outgoing from the BESS is delivered only to the grid, it can be concluded that the power outgoing from the BESS at any moment is equal to the power delivered to the grid:

$$Pb_d(i) = P_{bg}(i) \quad (12)$$

While the incoming power into the BESS in every instant is given by sum of the share of power produced by the PV used to load the BESS and the power absorbed by the grid, reduced by the shares of power lost due to the interconnection efficiencies between the systems:

$$Pb_c(i) = \eta_{pvb} P_{pvb}(i) + \eta_{gb} P_{gb}(i) \quad (13)$$

Where the efficiencies η_{pvb} and η_{gb} have already been described in this chapter.

Finally, starting from the shares of energy charged and discharged in each i -th time interval $E_c(i)$ and $E_d(i)$, the state of charge at each instant considered $SOC(i)$ was calculated thanks to the following equation:

$$SOC(i) = SOC(i-1) + \frac{E_c(i) - E_d(i)}{E_{TOT}} 100 \quad (14)$$

Where E_{TOT} is the maximum energy that can be accumulated/discharged from the storage system, proportional to the capacity value on the day considered. In fact, the E_{TOT} value, during the simulations, is updated every day

as a function of the decrease in degradation capacity assessed on the previous day, as will be explained in the next paragraph.

6.4.1 Degradation Model

In order to make the model as close as possible to reality, a specific function was created in Matlab, dedicated to the evaluation of the degradation of BESS considering every day . In fact, the storage system can reach the end of life more or less quickly depending on the operating conditions. In the tool created, given that the power profiles are evaluated by solving an optimization problem that will be detailed in the next paragraphs, the operating conditions vary day by day according to the trend of the PV production profile and the daily price profile and moreover, they are different according to the capacity and power of the BESS being analyzed. For this reason, for an accurate estimation of the life of the system it is necessary to evaluate every day the degradation rate for the evaluation of the lost capacity, studying the SOC profile that derives from the daily optimization itself. The rate of degradation and, therefore, the share of daily capacity lost are calculated starting from the evaluation of the stress parameters, using the semi-empirical equations already introduced, referring to the study conducted by Bolun Xu et al., [41] which have been implemented in the Matlab model. In order to apply these equations, a preliminary study of the profile of daily SOC is necessary to identify the number of cycles performed and their characteristics.

Furthermore, it is necessary to know the internal temperature profile of the cells, for this reason a specific Simulink model has been created that simulates the heat exchange between the modules and the external environment, as described in the next paragraph.

6.4.2 Cell Temperature Evaluation Model

To simulate the thermodynamic behavior of the electrochemical cells that make up the BESS to derive the trend of the internal temperature, useful for estimating the degradation rate, a Simulink model was created whose general scheme is shown in Figure 36.

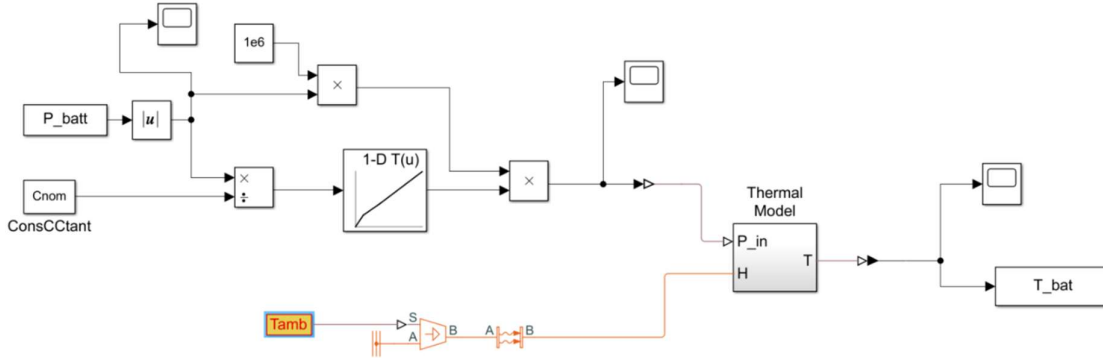


Figure 36 Simulink Model for the Temperature evaluation

This model reproduces the behavior of the cells by evaluating the amount of heat that is not dissipated through the convective exchange with the external environment, from which it processes the temperature trend. The heat generated in each instant is strictly correlated to the C-rate performed.

The model therefore considers that all the dissipated energy is transformed into heat inside the cell which causes an increase in the internal temperature, neglecting the effects of the enthalpy variation of the cells. However, this simplification has a limited impact, in fact the variation of enthalpy is a reversible phenomenon, which has an opposite effect on the temperature trend in the charging phase compared to the discharge, [42] negligible in average terms.

Therefore, according to the profile of power supplied/absorbed by the BESS and the value of energy that can be accumulated on the specific day considered, the model first evaluates the trend of the C-rate, from which it calculates the heat produced moment by moment. After this, it simulates the heat exchange processes, supposed to be exclusively convective, between the module and the environment, thus obtaining the temperature trend.

In addition to the power profile [MW] and the accumulable energy value [MWh] for the calculation of the C-rate, the following parameters are provided to the model as input data.

- The ambient temperature outside the modules, considered constant and equal to 22°C, assuming the use of suitable ventilation systems.
- The useful heat exchange surface. Evaluated starting from the geometry and dimensions of the modules used. The total surface was obtained by multiplying the useful exchange surface of each module (lateral surface) by the number of modules necessary to compose the BESS.
- The total weight of the storage system. This is also obtained by multiplying the weight of each module obtained from the plate data by the number of modules needed to compose the BESS.

- The heat transfer coefficient. Fixed at 30 W/m²K, assuming that the heat exchange is due to forced convection due to the use of ventilation systems.
- The specific heat at constant pressure of the cells. Assumed equal to 1100 J/kg/K.

With these data the model gives back the temperature profile which is supposed to be the same for all the cells that make up the BESS, from which the average daily temperature and the average temperature of each cycle identified by the Rainflow algorithm are subsequently calculated.

After identifying the number of daily cycles and the temperature profile of the cells that make up the BESS, it is possible to calculate the stress factors and the amount of capacity lost during the day.

6.5 Optimization Problem

In the next paragraphs it will be described the optimization problem that has been develop with the software Matlab in order to maximize the revenues of the BESS.

6.5.1 Objective

The objective of this project is to maximize the daily revenues for the owner of the system.

The objective function is expressed as the sum of all the components of earnings and costs (these last ones are expressed with a negative sign), that characterize the trade of the daily energy production.

In the system the only expense is linked to the power that is bought (when the energy prices are low) to charge the BESS, while the energy delivered from the PV system to the BESS does not count as a cost. This element can be expressed as:

$$C_{gb} = \sum_{i=1}^N P_{gb}(i) \Delta t Price(i) \quad (15)$$

Where N is the number of intervals that are considered during the day.

On the other side, the revenues come from selling the energy to the grid, both the energy from the PV system and the energy from the BESS. These revenues, supposing that there are not price variations between the purchase price and the selling price at the same considered time, can be expressed as:

$$R_{pvg} = \sum_{i=1}^N P_{pvg}(i) \eta_{pvg} \Delta t Price(i) \quad (16)$$

$$R_{bg} = \sum_{i=1}^N P_{bg}(i) \eta_{bg} \Delta t Price(i) \quad (17)$$

So, the function to be maximized is composed by the sum of the revenues without the sum of the costs:

$$f = R_{pvg} + R_{bg} - C_{gb} \quad (18)$$

The solution of this problem gives as a result the time profiles of the exchanged power between the systems that maximize the daily revenues and the SOC profile associated.

The objective function is:

$$f = MAX(R_{pvb} + R_{bg} - C_{gb}) \quad (19)$$

These results are then used to see if it makes sense to incorporate the BESS with the PV system or not from an economic point of view.

6.5.2 Data

The useful data for the optimization algorithm are the arrays containing the values of the power produced by the PV, called $P_{pv}(i)$, and the energy price values, called $Price(i)$, at every i -instant of the day considered for optimization. All the efficiency values must also be provided in order to consider the power dissipated in the transfer between one system to another and the share of energy lost within the storage system during the charging and discharging processes. In the latter case, the yield associated with these processes was considered varying according to the C-rate used. Finally, the values of energy that can be stored in the initial conditions E_b and power P_b must be entered which define the nominal size of the BESS studied and the values within which the state of charge SOC_{max} and SOC_{min} must be maintained.

6.5.3 Variables

The variables of the problem are all the values of the power exchanged between the systems and the value of SOC at every i -instant of the day.

The variables can be divided as:

1. $P_{pvb}(i)$, that represents the power produced by the PV system that is used to charge the BESS.
2. $P_{pvg}(i)$, that represents the power produced by the PV system that is directly delivered to the grid.
3. $P_{bg}(i)$, that represents the power delivered from the BESS to the grid.
4. $P_{gb}(i)$, that represents the power absorbed from the grid by the BESS during the charge.
5. $SOC(i)$, that represents the state of charge of the battery system. It is function of the input and output power of the BESS.

So, the variables related to the systems are actually only four, because the $SOC(i)$ is considered only to avoid situations of over charge or over discharge of the BESS.

6.5.4 Constraints

The constraints of the variables essentially concern the limit of the *power flow* of the system (first law of Kirchhoff) and the limits regarding the maximum accumulated/delivered energy of the BESS in function of the size of the system. Specifically, analyzing in a separate way the constraints of each component of the system, it is possible to identify three different constraints regarding the output power of the photovoltaic system:

$$1. \quad P_{pvb}(i) \geq 0 \quad (20)$$

$$2. \quad P_{pvg}(i) \geq 0 \quad (21)$$

$$3. \quad P_{pvb}(i) + P_{pvg}(i) = P_{pv}(i) \quad (22)$$

The first and the second constraint impose that the produced power from the PV system charges the BESS and the part of the power that is directly delivered to the grid has to be positive, because the PV system can only deliver power, not absorb it. The third constraint defines that the amount of the powers delivered from the system must be the same of the absorbed power in each instant.

Subsequently, considering the BESS, it is possible to consider four constraints:

$$1. \quad 0 \leq P_{bg}(i) \leq P_b \quad (23)$$

$$2. \quad P_{pvb}(i)\eta_{pvb} + P_{gb}(i)\eta_{gb} \leq P_b \quad (24)$$

$$3. \quad SOC(i+1) = SOC(i) + \frac{[(P_{pvb}(i)\eta_{pvb} + P_{gb}(i)\eta_{gb})\eta_c - P_{bg}(i)\eta_d]\Delta t}{Eb} 100 \quad (25)$$

$$4. \quad SOC_{min} \leq SOC(i) \leq SOC_{MAX} \quad (26)$$

The first and the second constraints are necessary in order to control the power from/to the battery in every moment at the maximum nominal power given as an initial value.

The third constraint is needed to discriminate the state of charge of the BESS that has to be maintained between the maximum and minimum values imposed by the constraint 4.

Finally, taking into consideration the electric grid, it is important to introduce other 2 constraints.

One of these constraints is about the power flux needed to charge the BESS that can be considered only positive, while the second constraint is about the power limit P_{max} that can be injected in the grid:

$$\bullet \quad P_{gb}(i) \geq 0 \quad (27)$$

$$\bullet \quad P_{pvb}(i)\eta_{pvb} + P_{gb}(i)\eta_{gb} \leq P_{g,max} \quad (28)$$

It has been considered that at any moment the photovoltaic system does not dissipate part of the produced energy, so this constraint is necessary in order to respect the limit value that the grid can support.

Of course, it must be reminded that it is not possible that the values of $P_{pvb}(i)$ and $P_{gb}(i)$ are both positive at the same time (in fact, in this project the idea is to prefer the charge of the BESS when it is possible to absorb energy from the photovoltaic system).

6.5.5 Power flows obtained from the optimization

Thanks to the resolution of the optimization problem with the software Matlab all the power profiles described are identified. In general, it can be said that, in order to maximize revenues, the recharge of the BESS takes place during the hours in which the price of the energy is lower through the absorption of power produced by the photovoltaic and/or the electricity grid, while the discharge takes place in the hours when the price is higher or in which feeding energy into the grid is more profitable. As example, Figure 37 and Figure 38 show the daily trends of the powers as a function of the price trend evaluated by the algorithm in different days and the associated SOC trend, assuming the use of an accumulation system of power equal to 50 MW and accumulable energy equal to 50 MWh associated with the photovoltaic plant with a nominal peak power of 385 MW.

From Figure 37 and Figure 38 it is possible to draw some general evaluations that find correspondence in every optimization done in the algorithm. For the first day taken into consideration it is possible to see that the grid is charging the battery in the first hours of the day (from 04:00 to 05:00) when the energy price is low and then the battery is discharging energy into the grid from 07:00 to 08:00 when the price is higher. The battery is completely discharged, in fact the SOC value is zero at 08:00. The battery is then 100% charged from the PV park from 10:00

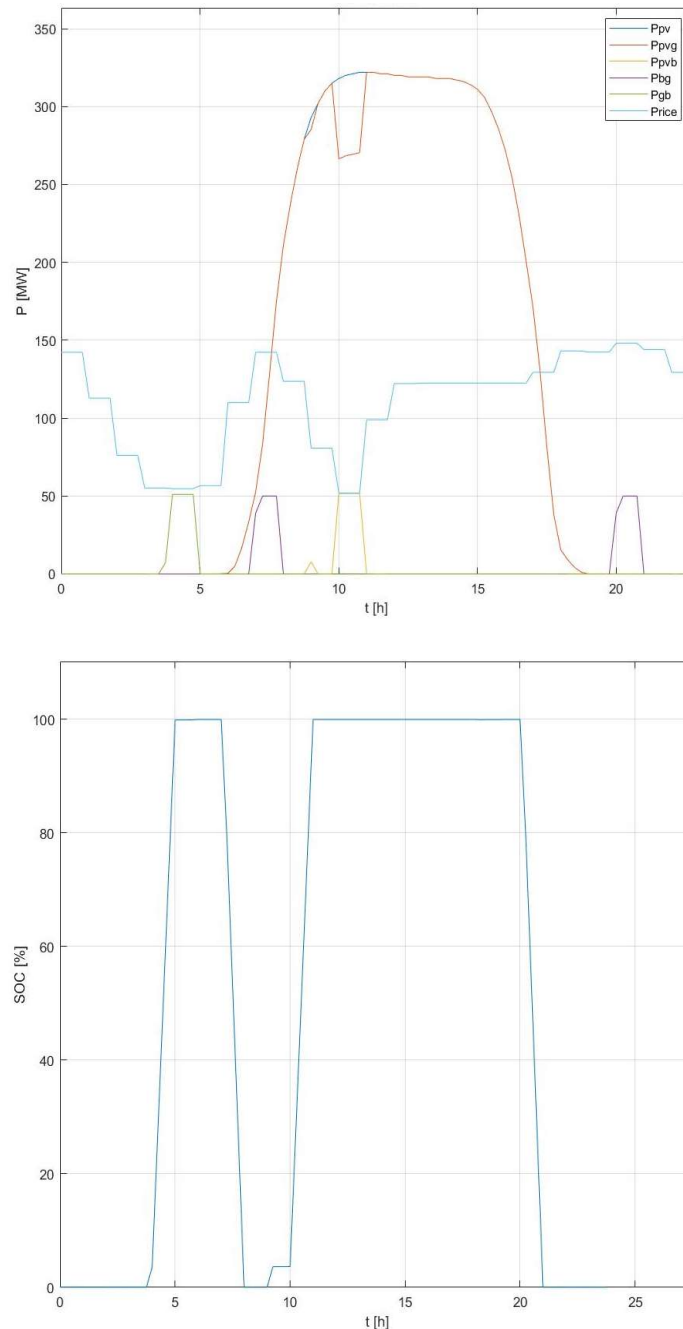


Figure 37 Optimal Power Flow and SOC profile for a day with variable energy price

to 11:00 when the price is low and the next BESS discharge into the grid is in the night hours (from 20:00 to 21:00) when the price is at the highest value of the day, so the SOC reach again the value of zero. We can see that the PV park power that is not used to charge the battery is always flowing into the grid.

For a day where there is not much energy price variations (Figure 38), the battery is charging only from the PV Park. As we can see in Figure 38 the BESS is charging from 10:00 to 11:00 from the PV park, when the energy price is low and then the batteries are feeding the grid in the night hours (from 21:00 to 22:00) when the price is at the highest value of the day.

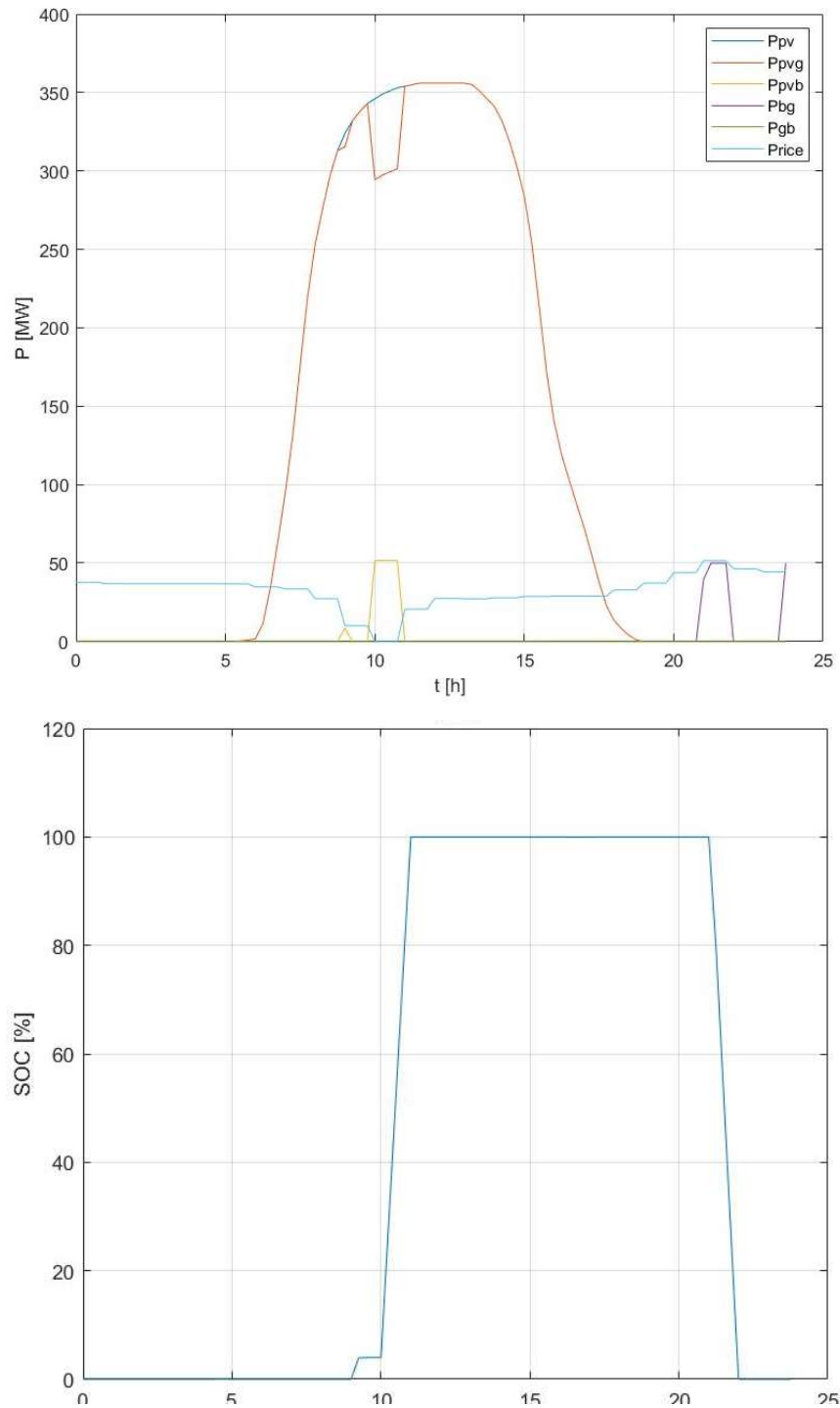


Figure 38 Optimal Power Flow and SOC profile for a day with stable energy price

In the next paragraphs it will be described in detail the economic aspects considered for this analysis.

It is fundamental to see that the difference of the energy prices during the day is significant for both days taken into consideration.

In details, for the first day taken into consideration (Figure 37) the energy price at 00:00 is around 150€/MWh while at 05:00 is around 50 €/MWh, this means that there is a price difference of 100 €/MWh already in the first hours of the considered day and this aspect is considered in the algorithm.

The energy prices have been taken from the *Coordinador Electrico Nacional* (CEN) website for the year 2020, as it will be analyzed more in details in the next paragraphs.

In conclusion, it is possible to say that the optimal solution, as predictable, involves the accumulation of energy in the BESS during the hours in which the price is lower, giving priority to the power consumption produced by the photovoltaic park or using the power consumption from the network if necessary.

Instead, the supply of the BESS energy takes place during the hours characterized by the maximum price. However, it must be kept in mind that, in order for the valuation to be true in net terms, the price spread between charging and discharging must be sufficiently high to compensate for the lost revenues due to the share of energy that is lost due to the efficiencies involved, which are considered within the optimization problem.

6.6 Economic Analysis

In this paragraph the economic aspects taken into consideration within the generated model will be analyzed. In particular, the following points will be explained:

- Analysis for the evaluation of the initial investment of the BESS.
- Study for the creation of different prices scenarios for the sensitivity analysis.
- Procedure used to evaluate the net revenues resulting from the introduction of the BESS into the system and the parameters used to assess whether the insertion brings benefits from an economic point of view.

6.6.1 Analysis for the evaluation of the initial investment of the BESS

In order to attribute an initial cost to the storage system considered in each simulation, a dedicated function has been developed in the Matlab calculation environment. In literature, there is usually a tendency to neglect the price variation as a function of the size in power, expressing all the relative costs as if they were exclusively linked to the accumulated energy (€/kWh), neglecting that increasing the power with the same capacity can increase the size of the investment.

However, in the context of this thesis project, in order to be able to discriminate the optimal size also in terms of power, an appropriate division of costs is necessary, for this reason the need arose to divide the contributions related to capacity from those related to power.

Initially, in order to evaluate which are the cost components that have to be considered to subsequently make an appropriate subdivision, various data presented in the literature were analyzed.

All the items identified and some of their values as the BESS size considered obtained are shown in Table 4.

Table 4 Different cost items identified and related values as the BESS size varies [43]

Costs Type	240 MWh	120 MWh	60 MWh	30 MWh
	60 MW	60 MW	60 MW	60MW
Battery Costs (BS)	50.160 M€	25.080 M€	12.540 M€	6.270 M€
Inverter Costs (IC)	4.200 M€	4.200 M€	4.200 M€	4.200 M€
Structural BOS Costs (SC)	3.121 M€	1.813 M€	1.160 M€	0.833 M€
Electrical BOS Costs (EC)	8.602 M€	6.119 M€	4.877 M€	4.256 M€
Installation labor & equipment (ILC)	5.479 M€	4.322 M€	3.744 M€	3.455 M€

The value of this table have been taken as a reference since it is possible to see the costs for different configuration with the same battery power. In fact, the configuration have always a battery power of 60 MW and the capacity changes from 30 MWh to 240 MWh.

The cost related to the capacity of the BESS for each item considered was obtained from the ratio between the total cost variation and the accumulated energy variation. After that, the share of the cost related to the power

was obtained by taking the total cost minus the cost attributed to the accumulated energy (previously assessed) for the power value considered.

In doing so, the values relating to both the accumulable energy (€/ MWh), and the BESS power (€/ MW) were calculated for each item considered, shown in Table 5.

Table 5 Relative cost values calculated as a function of power and energy of the BESS.

Costs Type	€/MWh	€/MW
Battery Costs (BS)	209000	0
Inverter Costs (IC)	0	70000
Structural BOS Costs (SC)	10897.333	8429.533
Electrical BOS Costs (EC)	20697.133	60591.817
Installation labor & equipment (ILC)	9640.633	527556.667

As can be seen in Table 5, the overall cost for the purchase of the electrochemical modules that make up the BESS is exclusively related to the energy of the system, while the cost of the inverter, used for the conversion of power from direct current to alternating current and vice versa, it is entirely related to the power of BESS. [43] [44]

The abbreviation BOS stands for Balance of System and it includes all the components of a photovoltaic system except for the photovoltaic panels. This includes wiring, switches, a mounting system, one or many solar inverters, a battery bank and battery charger. For structural BOS and electrical BOS, we mean all the costs for the purchase of the devices for the construction of both the structural and electrical storage system different from those needed for the purchase of the modules and the inverter. These, like the costs attributed to the installation work and the equipment used are also function of both the capacity and the power of the BESS and therefore, as can be seen, are characterized by a relative value for both components. In this study, the costs related to the purchase of the land for the construction of the plant have been neglected.

Therefore, starting from the relative values obtained, it is possible to evaluate the overall costs of any plant taken into consideration, characterized by specific values of power P_b [MW] and of accumulable energy E_b [MWh], first evaluating the total costs for each item:

$$BC = 209000 E_b + 0 P_b \quad (29)$$

$$IC = 0 E_b + 70000 P_b \quad (30)$$

$$SC = 10897.333 E_b + 8429.533 P_b \quad (31)$$

$$EC = 20697.133 E_b + 60591.817 P_b \quad (32)$$

$$ILC = 9640.633 E_b + 527556.667 P_b \quad (33)$$

From the total cost for each item evaluated, the overall cost for the realization of the BESS was evaluated as:

$$bessC = C + IC + SC + EC + ILC + 10000 P_{pv} \quad (34)$$

where the last term represents the developer costs, that is the costs attributed to the preliminary development of the project until the release of the single authorization for the start of the works. This cost item includes, for example, the expenses for the preliminary scouting of the land, for obtaining the authorizations and for the complete drafting of the project. As can be seen, this cost was assumed to be proportional to the peak power of the PV park, therefore constant within this study since no variation in the size of the PV was considered.

In Figure 39, the costs obtained by varying the sizes taken into consideration are represented. In the figure there is one curve for each considered size of the BESS (1 hour, 2 hours, 3 hours and 4 hours).

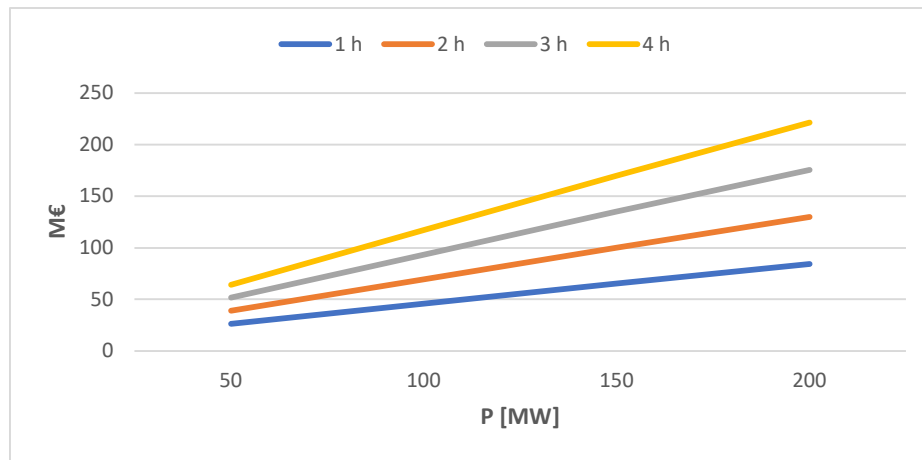


Figure 39 Initial BESS Cost in relation to the considered size.

It can be observed that when the power size increases, the price increase is not linear, therefore, in relative terms the smaller size systems are less convenient. As example, an initial cost of 38.96 M€, or 0.39 M€/MWh, is associated with a 50 MW 100 MWh BESS, while for a system of 4 times larger size, 200 MW and 400 MWh, the resulting initial cost is equal to 129,88 M€, or 0.32 M€/MWh. The effect of the increase in prices relative to the decrease of the size in power can be observed in detail in Figure 40 where the same initial costs are reported but expressed in terms relating to the capacity of the BESS. Finally, as regards the initial cost attributed to the

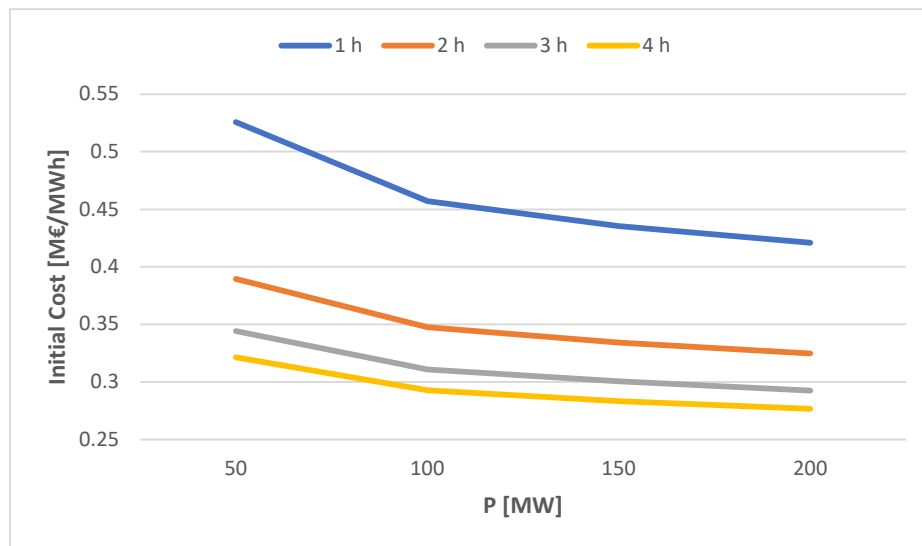


Figure 40 Variation of the relative initial cost of the BESS according to the size considered.

photovoltaic system, since the accurate determination of the economic aspects concerning the PV is not the purpose of this thesis, a relative cost of 600 €/kW_p has been assumed in a simplified way and therefore an initial total cost of 231 M€. [45]

In the next paragraphs it will be explained the different simulations that have been done in the software Matlab.

It has been considered a scenario where the BESS Initial Investment cost could decrease of 30 % of the actual 2020 cost. So, different simulations have been done also considering this possible cost decrease. The results of the simulations will be discussed in the next paragraphs.

6.6.2 Energy Prices

Regarding the purchase and sale prices of energy [€/MWh], which characterize the power exchanges with the grid, the Chilean Real Marginal Cost (*Costo Marginal Real*) of the Substation Carrera Pinto referred to the year 2020 was initially considered, which values are were taken from the databases of the *Coordinador Electrico Nacional* (CEN). [46]

The data of the Substation Carrera Pinto have been considered since it is the Substation where the PV Park Campos del Sol is connected to feed the produced power into the grid.

The data series obtained, with a price value for each hour, were subsequently processed in MATLAB in order to obtain a price value for each production data (four values for each hour) considering that the price remains constant within each hour considered.

Figure 41 shows some price profiles thus obtained, referring to different days of the year. In general, it can be observed that the price has the typical "double hump" shape and that the values can change even significantly considering different periods of the year.

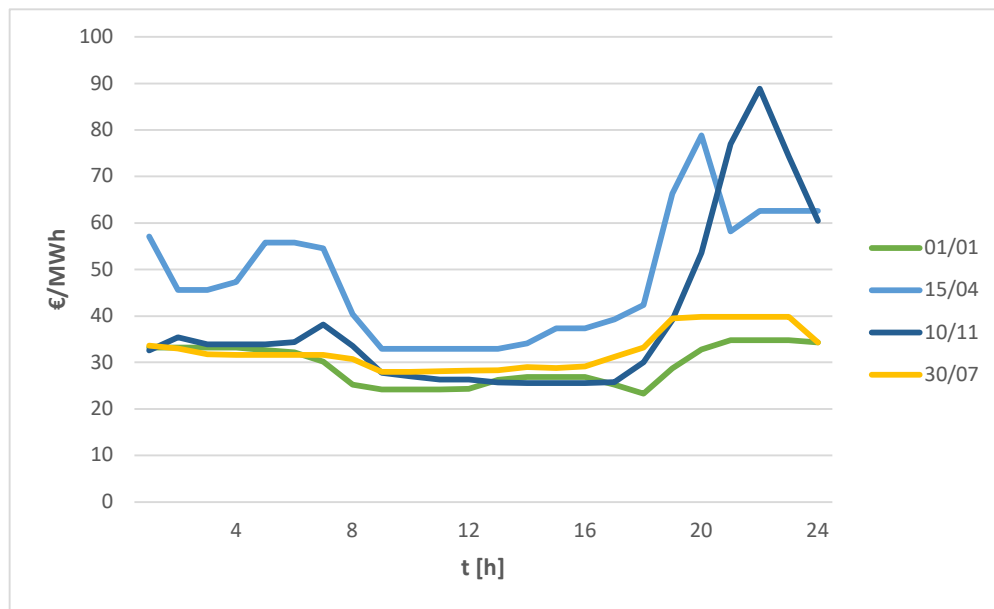


Figure 41 Carrera Pinto Substation Energy Prices for different days of year 2020

Subsequently, in order to produce further price scenarios to differentiate the simulations conducted, price profiles were generated strictly correlated to the instant-by-instant production of the photovoltaic park in order to increase the price spread between the production hours and the hours of non-production and therefore to make the use of a storage system for energy shifting more profitable. These scenarios want to consider the predictable change in prices resulting from the increase in the power produced by renewable energy plants. In this way, when the renewable energy power plant (in this case the PV park) is generating a lot of energy, the prices would decrease since there is a lot of generation; while when there is no renewable generation the prices would increase and so the BESS would deliver the power to the grid at a higher energy price.

For the creation of the price scenarios, multiplicative coefficients were defined. These coefficients change linearly according to the value of the power (P_{PV}) produced by the PV instant by instant represented in Figure 42. Subsequently, the hourly price values that make up the annual profiles of the different scenarios were calculated by multiplying the Chilean price of 2020 by the corresponding multiplicative coefficient.

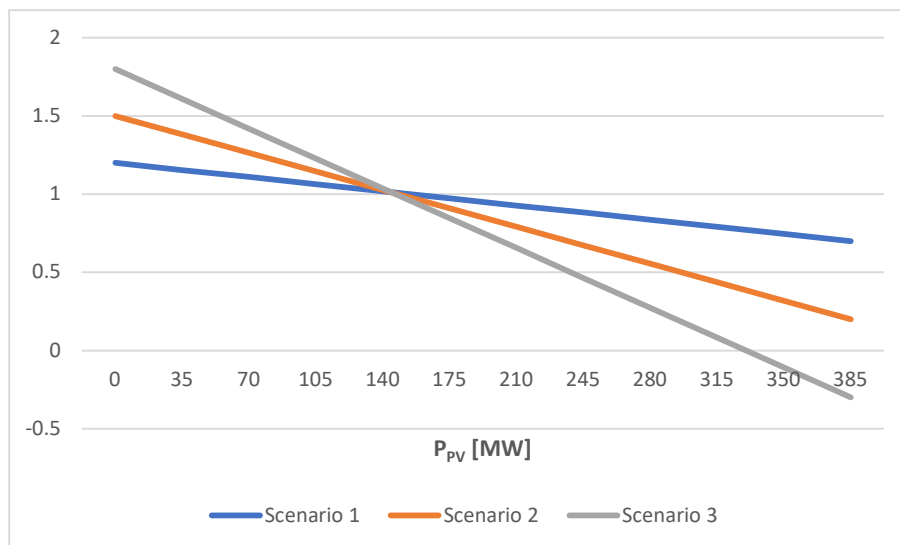


Figure 42 Considered Price Scenario

Figure 43 shows the price trend of the three different scenarios as a function of the power produced in the first three days of January, where it is possible to appreciate that the variation made to the original profile is strictly linked to the production of the PV Park.

Specifically, as can be observed, in each scenario considered, in the hours when the PV production is low the price increases, vice versa, in the hours when the PV power is massive the price is reduced.

In detail, in scenario 1, that is the least pushed in terms of spread increase, the multiplicative coefficient is equal to 1.2 when the power produced is zero, while it is equal to 0.7 when the power produced is equal to the peak power. In scenario 2, the intermediate scenario, the value of the coefficient varies between 1.5 and 0.2. Finally, in scenario 3, the one where the spread is increased the most, the coefficient assumes values between 1.8 and -0.3. Therefore, in the latter case, it is expected that the energy price may also become negative if there is a power produced close to the peak power, precisely when the average hourly production exceeds 330 MW.

This hypothesis, until a few years ago, was purely theoretical in the electricity market, however, the massive and rapid penetration of intermittent renewable sources has radically changed the landscape, making it an

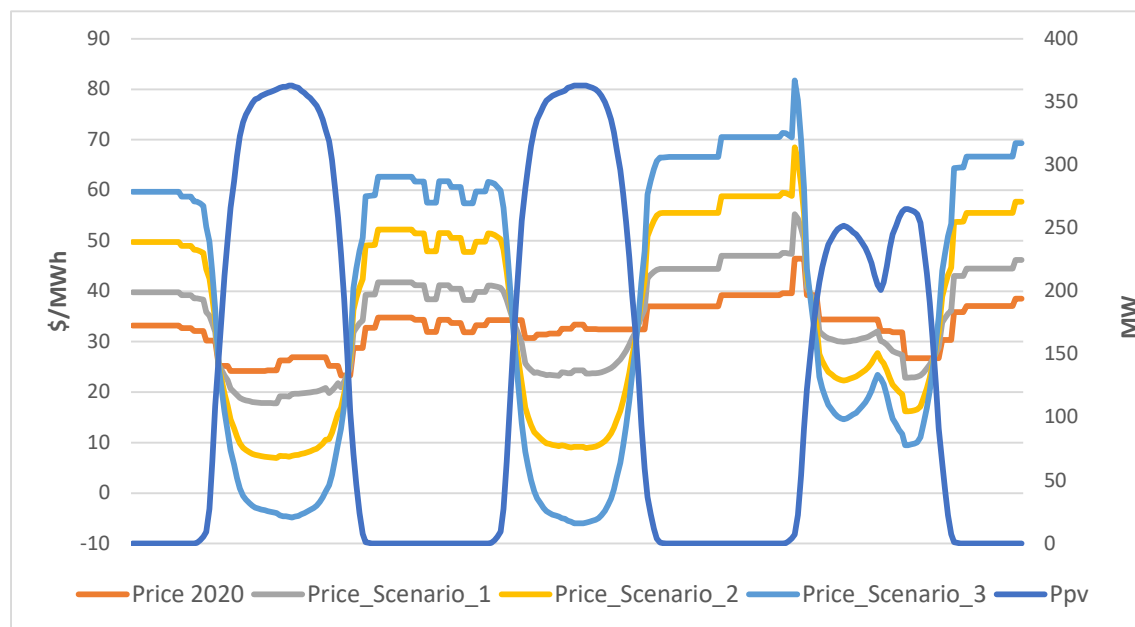


Figure 43 Prices Profile Scenarios for the first three days of January.

increasingly concrete reality. In general, for the price of energy to become negative, low energy demand must occur simultaneously with an excess of supply due to an inflexible generation park, just like wind park and photovoltaic park. [47]

Therefore, considering that the share of power produced by renewable plants continues to grow, it is realistic to assume that in the near future the price may also assume negative values, thus making it even more interesting to use an accumulation system that allows to store at least part of the energy produced in the time slots in which feeding the grid would involve a cost.

It has been considered also two more Energy Price Scenarios, that consider a constant variation of the 2020 Energy Price equal to $\pm 10\%$.

In total 7 different scenarios were considered:

- Carrera Pinto 2020 Energy Price
- Scenario 1
- Scenario 2
- Scenario 3
- Initial BESS Cost = 70% Actual Cost
- Energy Price = 90% Actual Price
- Energy Price = 110% Actual Price

6.6.3 Evaluation of effective revenues and economic parameters

For the economic evaluations, used to understand if it is convenient to associate a BESS to a PV system and, in the positive case, which size of the system has to be considered in order to have the largest revenue. It has been studied the net revenues correlated to the energy shifting and also the economic parameters Internal Rate of Return (IRR), that has been computed with the specific function IRR in the software Excel.

In details, the daily revenues attributed specifically to the BESS $R(d)$, in each day considered, are computed by diminishing the revenues linked to the power flux that is given from the BESS to the grid during the charging phase:

$$R(d) = \left(\sum_{i=1}^N P_{bg}(i) Price(i) \eta_{bg} \Delta t \right) - gbC_d - pvbC_d - omC_d \quad (35)$$

Specifically, the terms of the equation are the following:

- gbC_d represents the daily expense to absorb energy from the grid to charge the battery. This term is function of the power P_{gb} absorbed by the BESS and it is evaluated as:

$$gbC_d = \sum_{i=1}^N P_{gb_i} Price_i \Delta t \quad (36)$$

- $pvbC_d$ considers the lost revenues, that are linked to the absorption of the energy from the PV system in order to charge the BESS. This term of cost is proportional to the power from the PV system to the BESS and it is computed as:

$$pvbC_d = \sum_{i=1}^N P_{pvb_i} Price_i \eta_{pvb} \Delta t \quad (37)$$

- The last term, called omC_d , considers the daily operative costs and the costs for the maintenance (O&M) of the BESS. These costs are computed by dividing the annual costs (supposed that are equal to 1.5% of the initial investment of the BESS) by the number of days of the year as expressed in the following equation.

In this way, it is considered that the O&M costs are equally distributed in each day of the year.

$$omC_d = \frac{0.015}{365} batC \quad (38)$$

Starting from the daily revenues, evaluated in every day of the BESS lifetime, it is possible to obtain the Net Present Value, also called NPV , by discounting the deferred revenues in time and keeping in consideration the initial battery energy storage system's expense $batC$:

$$NPV = \left[\sum_{y=1}^Y \left(\sum_{d=1}^{365} R(d) \right) \frac{1}{(1+r)^y} \right] - batC \quad (39)$$

where Y represents the lifetime of the BESS in years and r the discount rate. The discount rate used is 6.5% as an average value of the actual Chilean discount rate for energy projects [48].

Only if NPV is positive then the obtained revenues during the BESS, thanks to the energy shifting, allow to recover the initial expenses so generating earnings for the owner of the system.

Vice versa, if the values of $totR$ is negative, it means that the revenues are not able to recover all the costs and so it would be not advantageous the realization of the BESS linked to the PV system.

Starting from the evaluation of the annual revenues, it is possible to rebuild the cash flow.

In this way, it has been introduced the operative costs and the yearly maintenance costs for the BESS, supposed equal to 1.5% of the initial investment.

From the analysis of the cash flows, it is possible to evaluate the internal rate of return IRR thanks to the dedicated function (function IRR) in Excel.

When the BESS reach the end of its lifetime it has been considered a replacement, considering the cost of the replacement 70% of the initial cost of the BESS.

It is then computed the NPV, Cash Flow and IRR for the two investments, in order to understand the economic feasibility of the BESS during the lifetime of the PV park.

Chapter 7: Results

In this chapter the results of the simulations will be discussed.

These simulations exploit the potential of the tool created and have the purpose of comparing the use of storage systems from an economic point of view, with different sizes, to enslave a photovoltaic system of 385 MW_p. In each simulation conducted, the power flows exchanged between the systems (BESS, PV Park and Grid) derive from the resolution of the previously described optimization problem which aims at maximizing daily revenues.

The results of the simulations will be discussed in the next paragraphs, describing the results of the different considered scenarios for the sensitivity analysis:

- Scenario 1
- Scenario 2
- Scenario 3
- Initial BESS Cost = 70% Actual Initial BESS Cost
- Energy Price = 90% Actual Price
- Energy Price = 110% Actual Price

Scenario 1, 2, 3 have the energy prices that change with a multiplicative factor, as it has been explained in Chapter 6.

The search for the optimal size (capacity and power) of the BESS that maximize the revenues of the system over its entire life, was conducted without imposing any minimum and maximum limits on the SOC level, which can therefore vary between 0% and 100%, and setting the end of life of the BESS when the accumulated energy reaches 75% of the initial value. In this way it was taken into consideration that BESS characterized by lower C-rates are able to perform more cycles and therefore, under the same operating conditions, have a longer life and may be able to produce higher overall revenues.

In order to differentiate the results and also consider the predictable developments of the electricity market, the simulations were conducted with all the price scenarios implemented, accurately described in the previous paragraphs.

Therefore, for each size considered, a simulation was conducted with each price profile.

The economic assessments were then conducted by taking into consideration the same period of time for each size under analysis equal to 24/25 years, that is the lifetime of the photovoltaic system.

For each analysis, the NPV and the IRR were calculated in order to compare the results with each other.

It is possible to discriminate whether the PV + BESS coupling is advantageous or not from an economic point of view and, if so, which of the sizes analyzed is more advantageous.

7.1 Chosen Configurations

In order to understand the feasibility of a battery system, 16 different Li-Ion battery systems have been analyzed.

Table 6 shows the different BESS configurations that have been considered for all the simulations.

Table 6 BESS considered configurations

Power [MW]	Capacity [MWh]
50	50
50	100
50	150
50	200
100	100
100	200
100	300
100	400
150	150
150	300
150	450
150	600
200	200
200	400
200	600
200	800

The power of the BESS taken in consideration are 50MW, 100MW, 150MW, 200MW and for each power a capacity of 1, 2, 3, 4 hours has been studied.

During the analysis, some considerations and hypothesis, upon which the evaluation has been based on, have been made, that will be explained in the “methods” chapter.

7.2 2020 Chilean Energy Price

The first simulations have been done with the actual Chilean Energy price. As previously discussed, the Energy Price of the year 2020 of the Substation Carrera Pinto has been used.

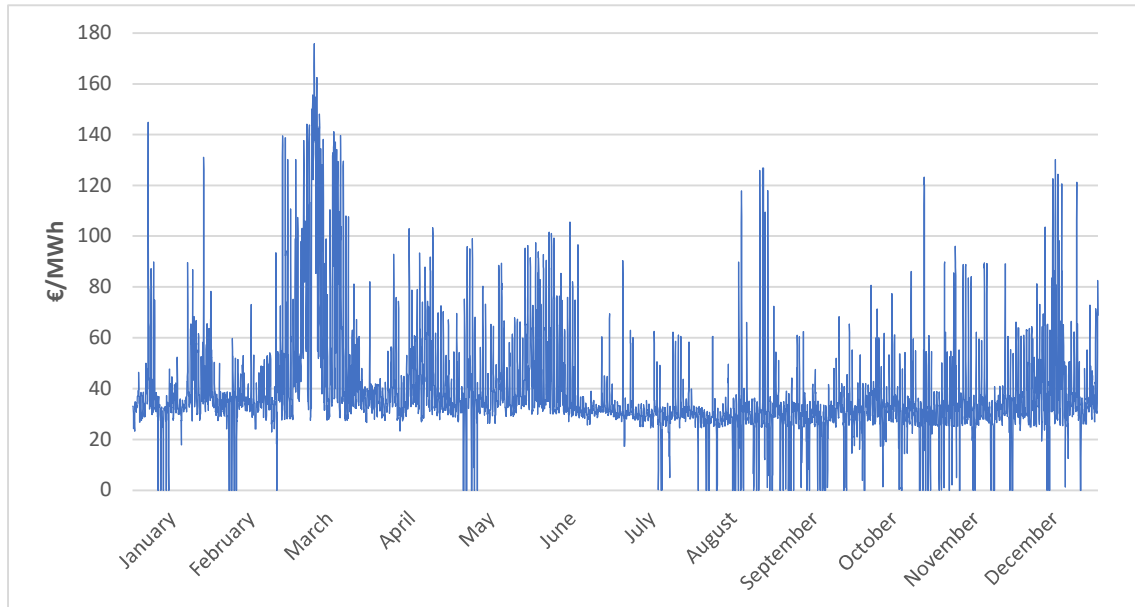


Figure 44 Carrera Pinto 2020 Energy Price. From CEN Website.

In the Figure 44 it is possible to see the hourly energy price considered.

The Carrera Pinto substation prices are quite variable, the hourly average price is around 40 €/MWh with peak around 180 €/MWh and minimum of 0 €/MWh.

These real energy prices have been used for the first simulations, in order to understand if the actual energy prices the BESS could be economically feasible.

The results with the actual prices can be seen in the Table 7.

It is possible to see in the Table 7 that with the actual prices (for the initial investment and energy prices) the BESS is not economically feasible.

This is mainly related to the fact that the initial investment in this moment is still too high, as computed in the software Matlab.

In fact, all the NPV are negatives, meaning that the BESS is not profitable, while the values of the parameter IRR (Internal Rate of Return) are all negatives too.

Table 7 NPV and IRR with the actual Carrera Pinto Substation Energy Prices

MW	MWh	NPV BESS	IRR BESS
50	50	-26,681,082 €	-11.83%
50	100	-29,371,072 €	-7.76%
50	150	-40,081,903 €	-9.11%
50	200	-50,082,358 €	-10.02%
100	100	-39,626,739 €	-9.45%
100	200	-44,363,803 €	-6.68%
100	300	-61,081,210 €	-7.32%
100	400	-78,368,668 €	-8.19%
150	150	-53,011,912 €	-8.65%
150	300	-58,962,501 €	-6.06%
150	450	-87,463,434 €	-7.88%
150	600	-107,832,516 €	-7.64%
200	200	-64,898,440 €	-7.98%
200	400	-71,993,678 €	-5.65%
200	600	-108,551,189 €	-7.43%
200	800	-171,752,213 €	-11.28%

The “best” NPV results is for the BESS with 50 MW 50 MWh, simply for the fact that it is the configuration with the lowest initial investment. In Figure 45 it is possible to see that the initial investment is around 25 M€ and after 12 years there is the replacement of the BESS.

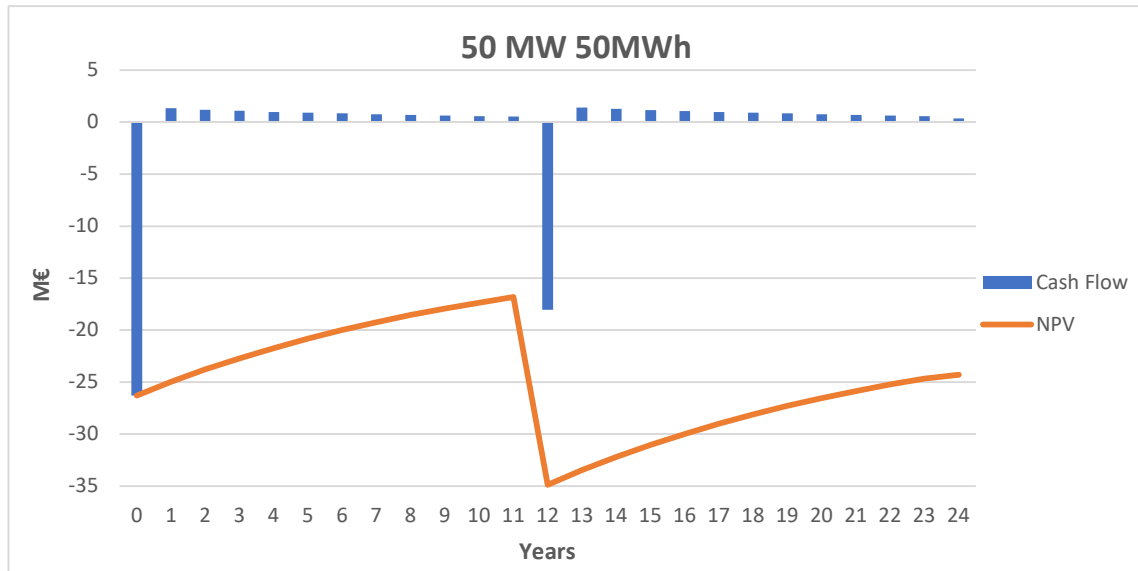


Figure 45 NPV and Cash Flow for the BESS 50 MW 50 MWh

At the end of the PV park lifetime (after 24/25 years), the NPV of the BESS is -26.681.082 €, it means that the configuration is very far from being economically feasible.

This fact is mainly due to the fact that the BESS initial investment is nowadays too high to make its installation economically feasible.

7.3 Initial BESS Cost = 70 % Actual Initial BESS Cost

The simulations have been run also considering a decrease of 30% of the initial BESS Cost.

As previously described, this assumption has been done considering that the BESS cost are decreasing year by year, and it is expected to decrease by 30% in the next 5 years [49].

Table 8 NPV and IRR considering a 30% decrease in the initial BESS investment

MW	MWh	NPV BESS	IRR BESS
50	50	-12,556,994 €	-6.83%
50	100	-8,437,248 €	-2.75%
50	150	-12,506,188 €	-3.37%
50	200	-15,851,918 €	-3.66%
100	100	-15,071,214 €	-4.44%
100	200	-7,130,220 €	-1.31%
100	300	-11,254,202 €	-1.61%
100	400	-16,040,955 €	-1.94%
150	150	-17,931,355 €	-3.62%
150	300	-5,269,963 €	-0.66%
150	450	-15,524,725 €	-1.63%
150	600	-17,300,004 €	-1.42%
200	200	-19,648,790 €	-2.98%
200	400	-2,401,022 €	-0.23%
200	600	-15,091,727 €	-1.20%
200	800	-54,396,860 €	-3.95%

It can be seen in Table 8 that in this case the results are still not economically feasible (the NPV are still negative), but the results are certainly more interesting.

In fact, there are systems that have the NPV closer to zero than the previous scenario, meaning that the initial investment has almost been recovered.

The configurations that have the “best” results are 150 MW 300 MWh and 200 MW 400 MWh.

Figure 46 shows that the initial investment for the 150 MW 300 MWh configuration is around 70 M€ and before the replacement done in year 14, the NPV already reaches a value around -10 M€. The yearly revenues of each

configuration are the same that have been computed with the actual costs and prices (since the energy prices have not been changed), but the fact that the BESS initial cost decrease, makes the application more interesting.

It is still not enough to make this configuration economically profitable since the final value of NPV is still negative (-5,269,963 €).

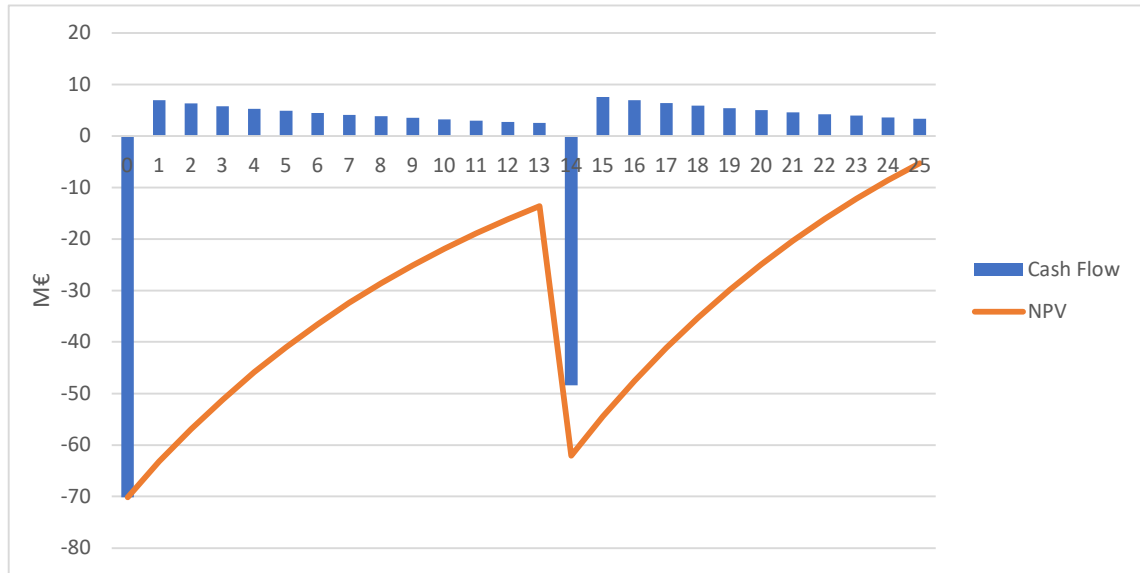


Figure 46 NPV and Cash Flow for the BESS 150 MW 300 MWh

Figure 47 shows the cash flows for the 200 MW 400 MWh configuration, that is the configuration with the “best” results for the scenario taken in consideration in this paragraph.

The initial investment (decreased by 30 %) is around 90 M€ and the final value of the NPV is -2,401,022 €.

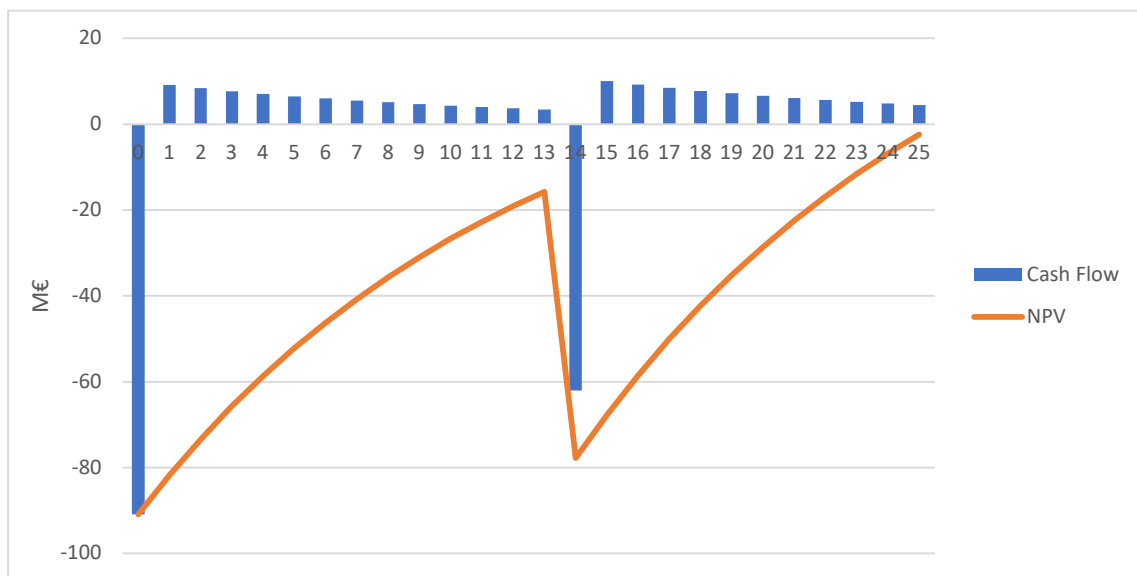


Figure 47 NPV and Cash Flow for the BESS 200 MW 400 MWh

These results show that the initial investment is really affecting the economic feasibility for the BESS, and an important decrease in the BESS cost would really change the economic discussion.

7.4 Energy Prices Scenarios

During the sensitivity analysis it has been then considered the possible variations in the energy prices, since it is the second factor that could change after the BESS cost.

In this case it has been kept the real initial investment (computed as described in the previous chapter) and the values that are changing regard only the energy price.

The new scenarios created considering possible variations in the energy prices are the following:

- Energy Price = 90% Actual Price
- Energy Price = 110% Actual Price
- Scenario 1
- Scenario 2
- Scenario 3

7.4.1 Energy Price = 90% Actual Energy Price

The first scenario considers a decrease of 10% of the values of the energy prices during the whole year.

It can be seen that in this case that values are always included between 0 €/MWh and 160 €/MWh.

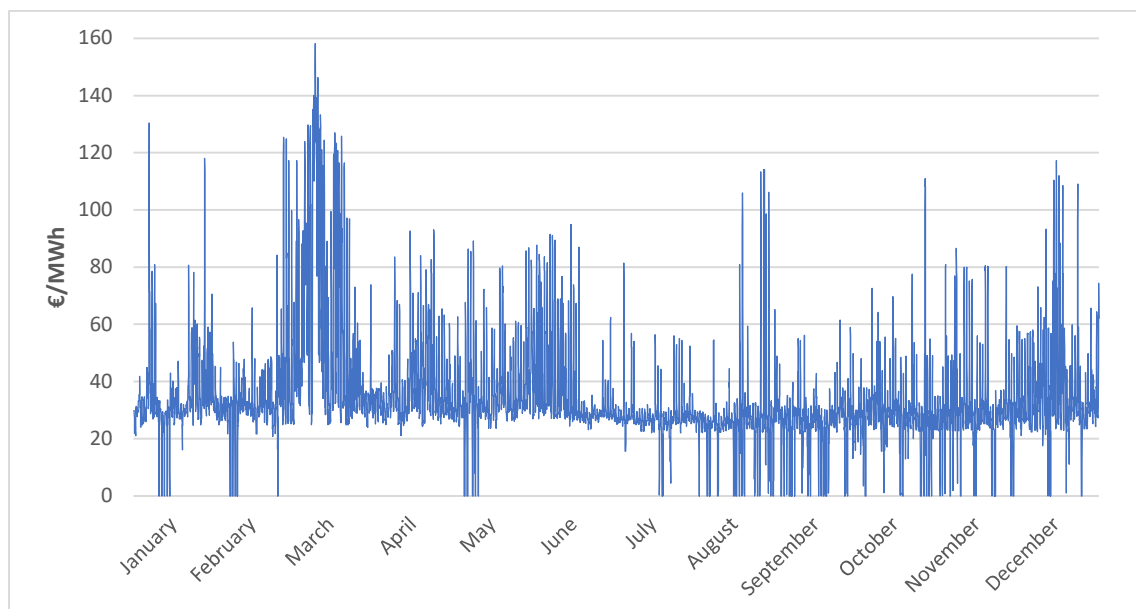


Figure 48 Energy Prices decreased by 10%.

The results in this case are worse than the real value (Carrera Pinto Substation Energy Prices 2020).

In Table 9 it is possible to see that all the NPV and IRR values are worse than the values in the real case, except for the 200 MW 800 MWh where the results are almost the same.

Table 9 NPV and IRR considering a general decrease of 10% of the Energy Price

MW	MWh	NPV BESS	IRR BESS
50	50	-29,038,638 €	-13.38%
50	100	-33,935,417 €	-9.34%
50	150	-46,099,503 €	-11.01%
50	200	-57,554,275 €	-12.17%
100	100	-44,395,740 €	-10.99%
100	200	-53,326,108 €	-8.38%
100	300	-73,106,866 €	-9.22%
100	400	-93,288,893 €	-10.33%
150	150	-60,137,468 €	-10.17%
150	300	-72,382,674 €	-7.76%
150	450	-104,991,067 €	-10.01%
150	600	-130,094,912 €	-9.77%
200	200	-74,536,939 €	-9.53%
200	400	-89,794,871 €	-7.35%
200	600	-131,750,858 €	-9.54%
200	800	-171,427,289 €	-11.28%

The final values of the NPV are negative in the order of tens of millions of euros, and the configurations with the “best” NPV is the 50 MW 50 MWh configuration, simply for the fact that it is the configuration with the lowest initial investment. The initial investment is around 26 M€ and after 24 years of operation of the PV park, the final NPV value for the battery energy storage system is -29,038,638 €.

Figure 49 shows that the configuration is not economically feasible.

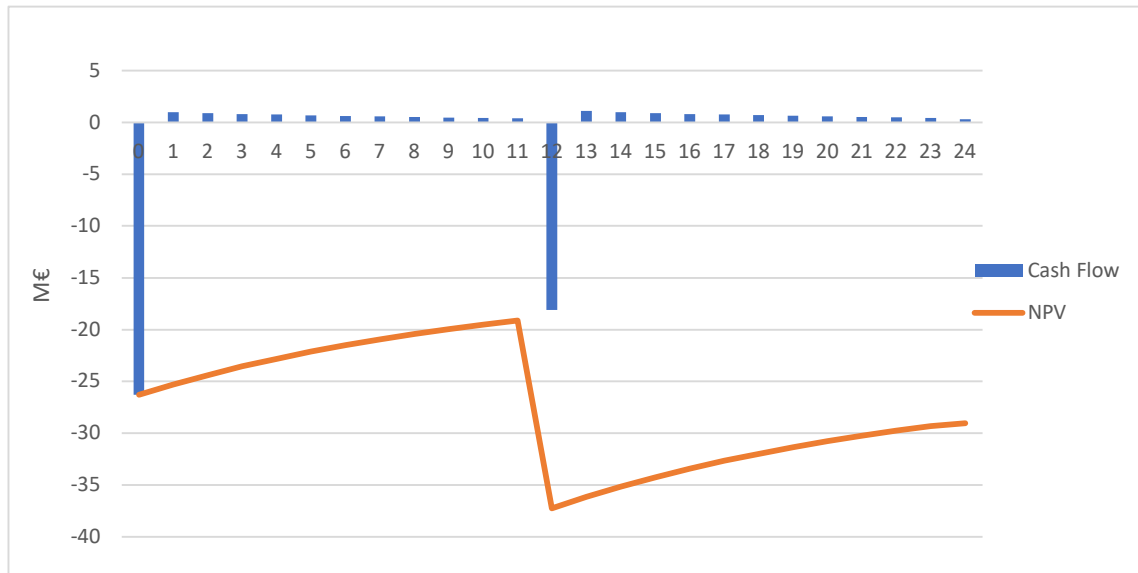


Figure 49 NPV and Cash Flow for the BESS 50 MW 50 MWh

7.4.2 Energy Price = 110% Actual Energy Price

The second scenario considers an increase of 10% of the values of the energy prices during the whole year.

It can be seen that in this case that the values are always included between 0 €/MWh and 200 €/MWh.

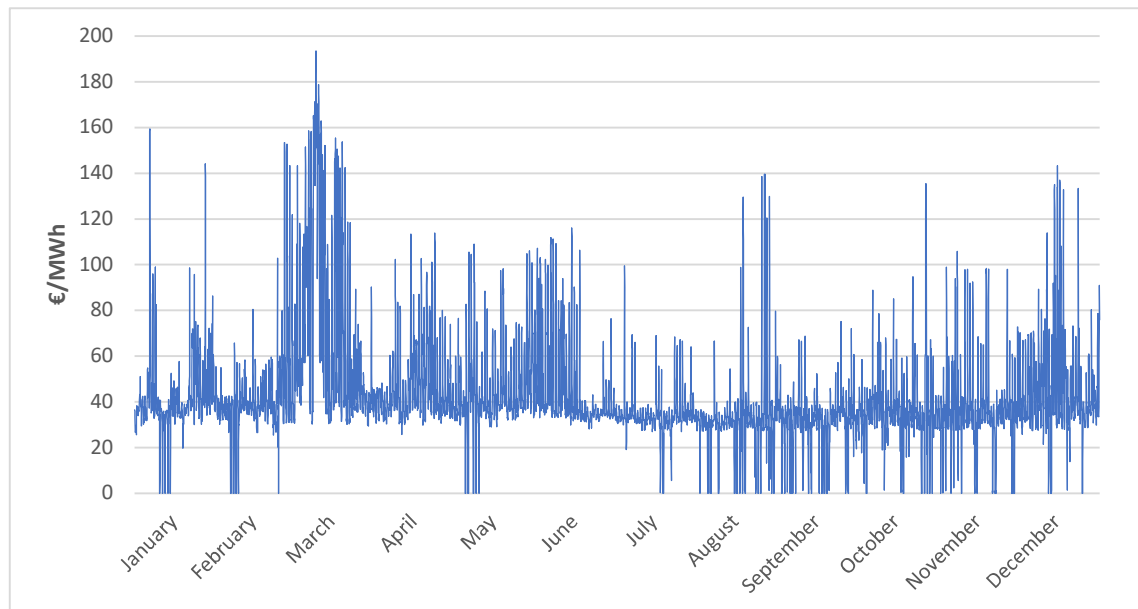


Figure 50 Energy Prices increased by 10%.

A general increase in the Chilean energy prices raises the price differences between the hours of the day, making the use of a BESS more feasible. The values in Figure 50 have a mean value of 42 €/MWh while for the real values of energy prices the mean value is around 38 €/MWh.

The results with this scenario are all better than the results with the real energy prices, but the NPV are still all negatives.

The 200 MW 800 MWh is the configuration with the biggest savings considering the real prices, since with this new price scenario it is gaining around 60 M€.

The best configuration is once again the 50 MW 50 MWh configuration, always for the fact that it is the configuration with the smallest initial investment.

Table 10 NPV and IRR considering a general increase of 10% of the Energy Price

MW	MWh	NPV BESS	IRR BESS
50	50	-24,300,216 €	-10.42%
50	100	-24,753,540 €	-6.31%
50	150	-34,056,930 €	-7.40%
50	200	-42,740,020 €	-8.12%
100	100	-34,821,480 €	-8.05%
100	200	-35,316,536 €	-5.12%
100	300	-49,087,975 €	-5.63%
100	400	-63,705,117 €	-6.32%
150	150	-45,850,355 €	-7.26%
150	300	-45,618,260 €	-4.52%
150	450	-69,990,516 €	-5.99%
150	600	-85,906,841 €	-5.77%
200	200	-55,060,570 €	-6.54%
200	400	-53,955,110 €	-4.07%
200	600	-85,598,858 €	-5.57%
200	800	-114,599,882 €	-6.63%

The 50 MW 50 MWh configuration has an initial investment around 26 M€ and after the 24 years of lifetime of the PV park the NPV of the BESS is -24,300,216 €, as it is possible to see in Figure 51.

The change in the energy prices of $\pm 10\%$ does not make the installation of a BESS from the economic point of view.

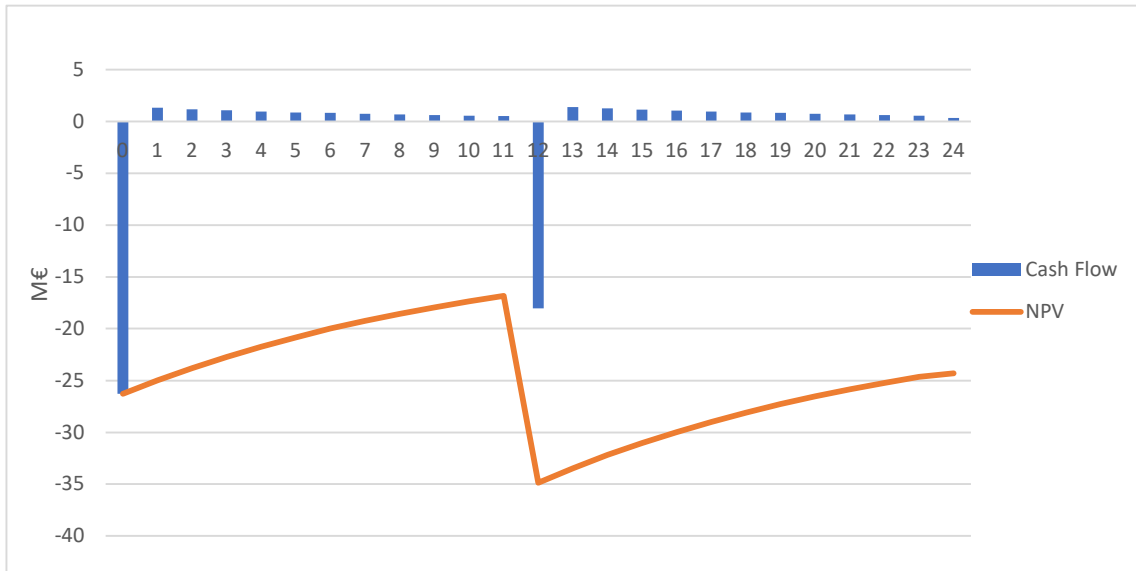


Figure 51 NPV and Cash Flow for the BESS 50 MW 50 MWh

For this reason, as explained in the previous chapter, different scenarios (scenario 1, 2, 3) have been created in order to analyze possible results with the energy prices that change in relation to the renewable (photovoltaic) energy production.

7.4.3 Scenario 1, Scenario 2

As already described in the previous chapter, the scenarios 1, 2, 3 have been created in order to simulate the fact that in the near future, with more and more renewable energy installation, the energy prices would be affected from the renewable energy production.

In this case, it means that during the day when the PV production is high the energy prices would decrease while in the hours with no PV production the energy prices would decrease, making more profitable selling energy from the BESS to the grid.

Table 11 shows the results obtained considering the energy prices with the scenario 1 and scenario 2, these are the two scenarios with less extreme characteristics than scenario 3.

Table 11 NPV and IRR considering Price Scenario 1, Scenario 2.

MW	MWh	SCENARIO 1		SCENARIO 2	
		NPV BESS	IRR BESS	NPV BESS	IRR BESS
50	50	- 22,476,569 €	-9.11%	- 16,245,025 €	-6.11%
50	100	- 23,343,550 €	-6.19%	- 11,990,513 €	-2.93%
50	150	- 32,266,535 €	-7.54%	- 17,050,843 €	-3.56%
50	200	- 38,473,980 €	-7.11%	- 22,032,778 €	-3.13%
100	100	- 31,216,208 €	-6.88%	- 18,412,567 €	-3.77%
100	200	- 30,193,417 €	-4.28%	- 6,996,149 €	-0.92%
100	300	- 45,094,303 €	-5.52%	- 14,292,969 €	-1.56%
100	400	- 54,539,632 €	-5.25%	- 21,466,022 €	-2.04%
150	150	- 40,475,955 €	-6.14%	- 21,059,124 €	-2.97%
150	300	- 37,457,338 €	-3.62%	- 2,401,190 €	-0.21%
150	450	- 58,385,732 €	-4.83%	- 11,810,420 €	-0.88%
150	600	- 71,223,164 €	-4.64%	- 21,297,732 €	-1.37%
200	200	- 48,120,398 €	-5.58%	- 22,022,453 €	-2.37%
200	400	- 42,895,594 €	-3.16%	- 2,021,341 €	-0.15%
200	600	- 68,983,032 €	-4.33%	- 6,738,023 €	-0.38%
200	800	- 84,918,673 €	-4.20%	- 17,934,671 €	-0.87%

It can be seen that these two scenarios have results much better from the real energy prices.

In fact the NPV and the IRR for all the configurations are better than the results with the real Chilean energy prices. It is due to the fact that these scenarios make the BESS installation more profitable since the energy is delivered from the battery to the grid in the hours when the energy is more expensive.

Scenario 1 have better results than the actual energy prices, but still the results are not economically feasible. In fact, as for the other scenarios, the configuration with the best NPV remains the 50 MW 50 MWh configuration, for the fact that the initial investment is the lowest between all the configurations.

With the Scenario 2, the results become interesting and the NPV for different configurations almost reach the zero value.

In detail, we can see that the configuration with 100 MW 200 MWh, 150 MW 300 MWh, 200 MW 400 MWh, 200 MW 600 MWh, have the NPV almost equal to zero, and considering the initial investment for these configurations it is an interesting result.

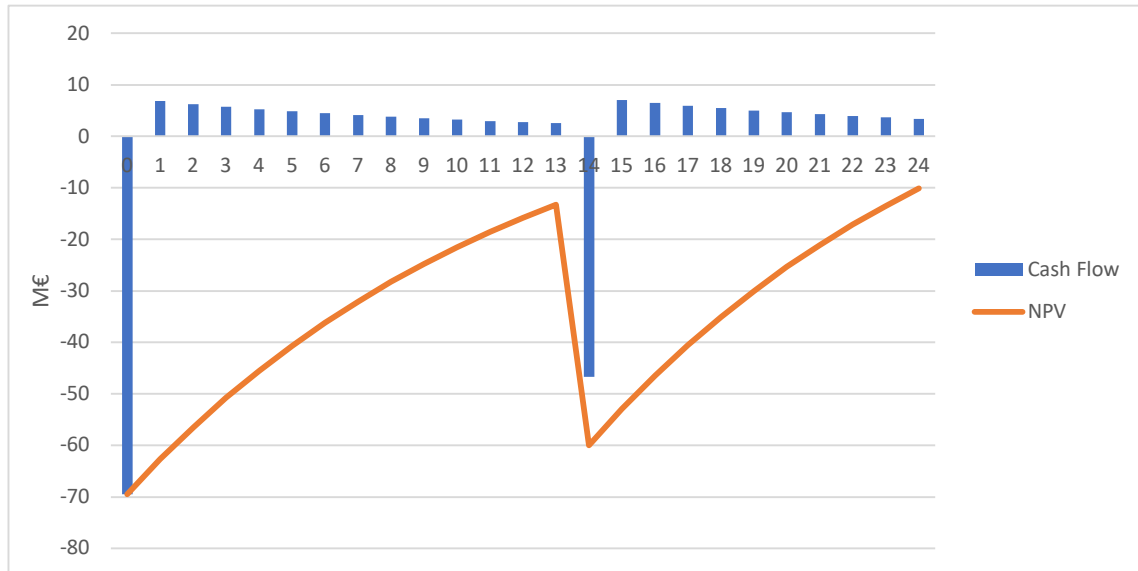


Figure 53 NPV and Cash Flow for the BESS 100 MW 200 MWh considering Price Scenario 2.

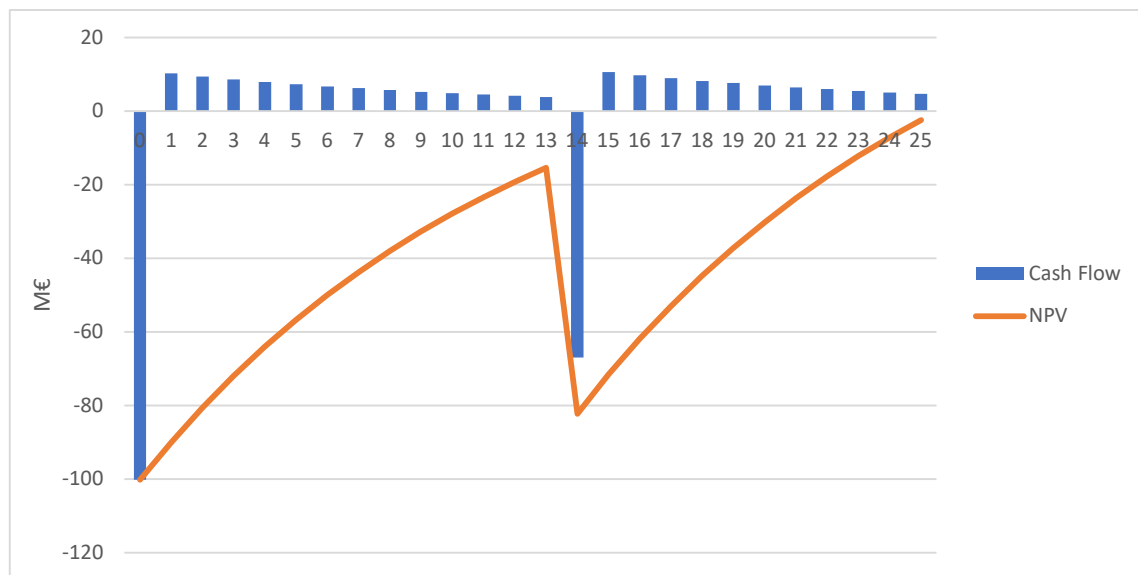


Figure 52 NPV and Cash Flow for the BESS 150 MW 300 MWh considering Price Scenario 2.

The Figure 54 shows the cash flows of the four best configuration with the energy price scenario 2.

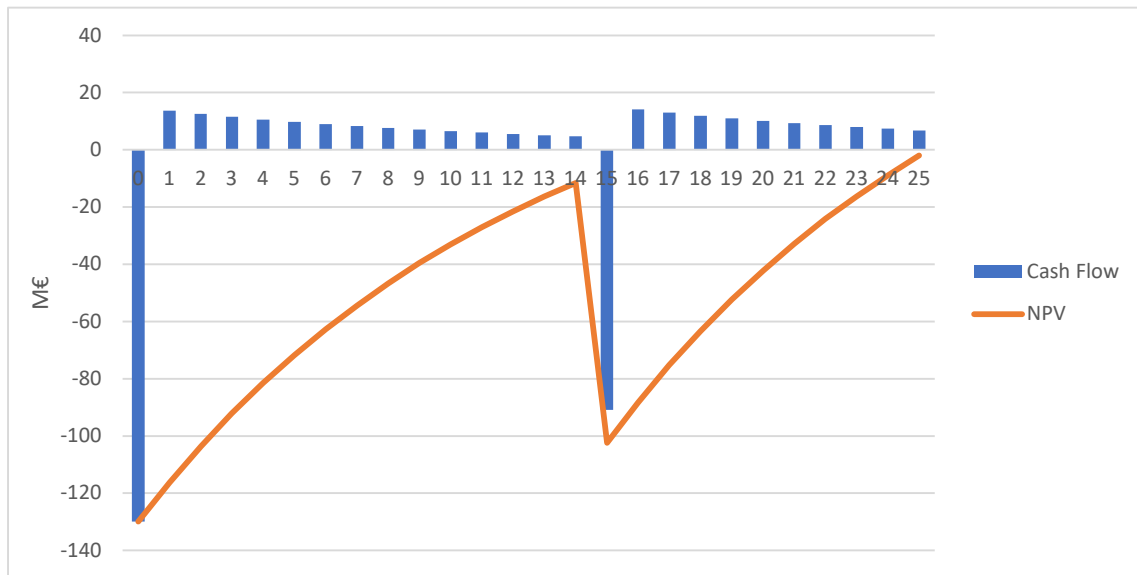


Figure 54 NPV and Cash Flow for the BESS 200 MW 400 MWh considering Price Scenario 2

The best NPV is reached by the configuration 200 MW 400 MWh that start with an initial investment of 130 M€ and at the end of the PV park lifetime reaches an NPV value of -2,021,341 €.

This configuration could be considered economically feasible just if we would consider one year more for the PV park lifetime, an assumption that could be acceptable, since 25 years is an average for the PV module lifetime.

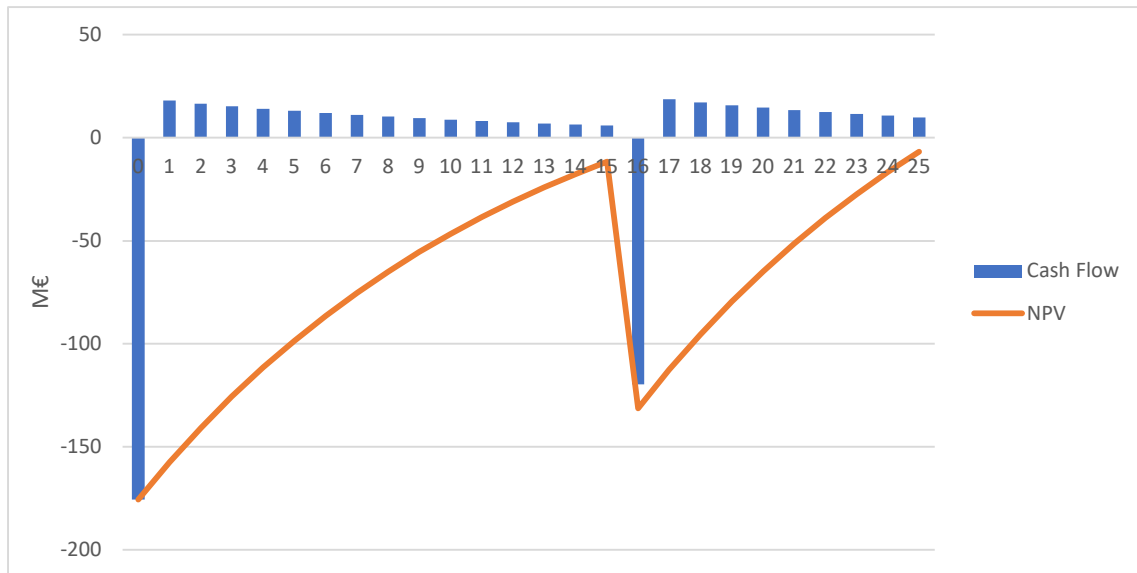


Figure 55 NPV and Cash Flow for the BESS 200 MW 600 MWh considering Price Scenario 2.

7.4.4 Scenario 3

The results with the price Scenario 3 are certainly the most promising results, in fact there are 9 different configurations that at the end of the PV park lifetime have a positive NPV.

Table 12 shows the results considering the Scenario 3 for the energy prices.

Table 12 NPV and IRR considering Price Scenario 3.

MW	MWh	NPV BESS	IRR BESS
50	50	- 12,104,780 €	-4.50%
50	100	- 1,763,445 €	-0.41%
50	150	- 2,567,185 €	-0.49%
50	200	- 3,508,691 €	-0.58%
100	100	- 10,006,210 €	-2.02%
100	200	13,660,289 €	1.70%
100	300	14,872,298 €	1.51%
100	400	15,704,471 €	1.36%
150	150	- 8,029,104 €	-1.11%
150	300	28,891,117 €	2.45%
150	450	32,085,451 €	2.20%
150	600	34,555,215 €	2.02%
200	200	- 4,100,279 €	-0.43%
200	400	51,554,183 €	3.24%
200	600	52,151,417 €	2.72%
200	800	56,938,215 €	2.52%

These results are particularly favorable for the fact that this scenario have the highest multiplicative coefficients and so the application of the BESS results economically feasible.

There are nine different configurations that reach positive NPV after the 25 years lifetime of the PV park.

Finally, it is possible to say that with this last considered scenario the BESS results economically feasible.

The two configurations that reaches the highest NPV are the 200 MW 600 MWh, 200 MW 800 MWh for the fact that can deliver the biggest quantity of energy during the late hours when the energy prices are the highest, and when the multiplicative coefficient is 1.8 as explained in the previous chapter.

The 200 MW 600 MWh configuration reaches positive NPV already before the battery replacement after 15 years and reaches after 25 years a Net Present Value of 52,151,417 €.

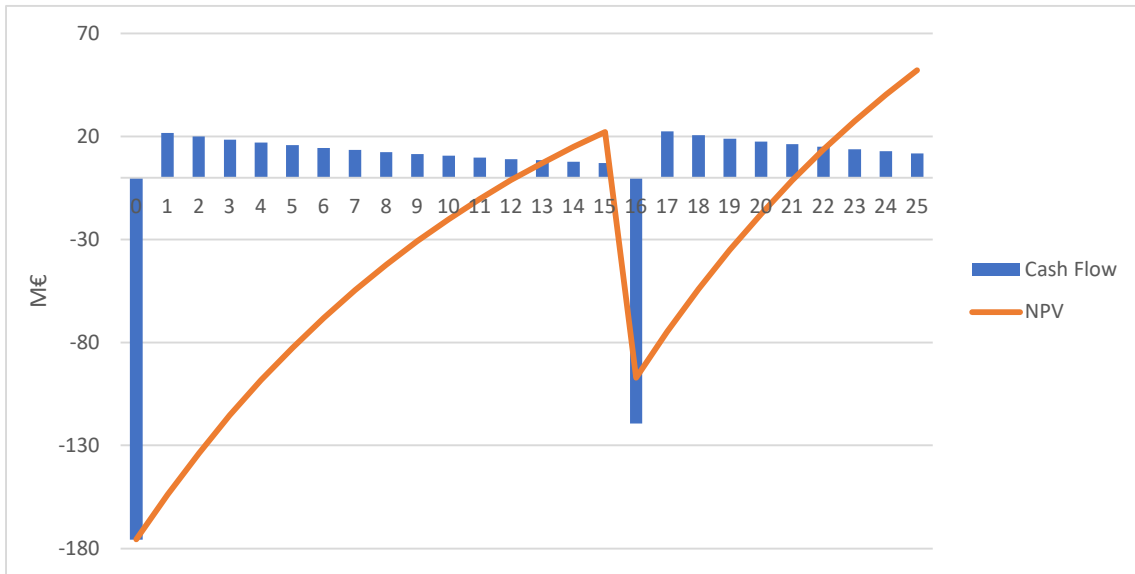


Figure 56 NPV and Cash Flow for the BESS 200 MW 600 MWh considering Price Scenario 3.

It is interesting to see such a big profit, considering that the initial investment for this type of configuration is of the order of 180 M€ at year 0.

The results for the 200 MW 800 MWh are really similar, but in this case the NPV is even bigger and reach a final value of 56,938,215 € as we can see in Figure 57.

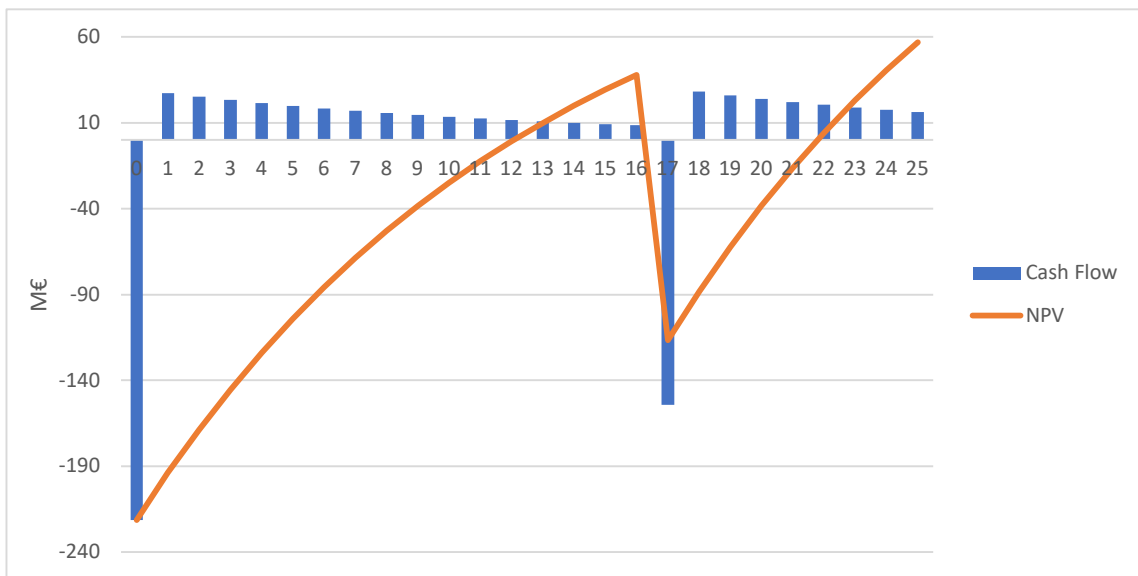


Figure 57 NPV and Cash Flow for the BESS 200 MW 800 MWh considering Price Scenario 3.

These configurations with this price scenario make the BESS favorable for the energy shifting and so the overall system PV+BESS would be economically interesting.

Chapter 8: Conclusions

In this thesis the feasibility of battery energy storage system for a 385 MWp photovoltaic power plant has been studied.

At this moment, considering real data (energy price from year 2020 and current battery costs) the investment of the battery energy system is not recovered during the PV park lifetime, so it is not economically feasible. This unfeasibility is due to the fact that in this moment the battery cost is still too high, and the initial investment for such big BESS (from the smallest configuration of 50 MW 50 MWh to the biggest configuration of 200 MW 800 MWh) will not be recovered. During the thesis different scenarios have been analyzed and the results have been particularly interesting in Energy Price Scenario 3, that is the scenario with the “biggest” multiplicative coefficient. This scenario reflects the fact that in a near future, with more and more renewable energy power plant, the energy prices will be influenced more and more from the photovoltaic energy production (in this specific case of the Campos del Sol project) and so, as explained in Chapter 6, during the maximum PV production hours the energy prices would be really low, and so it would be favorable to store the energy in a BESS. The possibility to combine a PV power plant with a BESS is a possibility to increase more and more the renewable energy production. The considered energy price scenario shows that the BESS could be really interesting in a near future, since in Chile there are building more and more photovoltaic power plant in the Atacama Desert.

Another aspect that has to be kept in mind is that the battery costs are decreasing year by year, and in a near future the BESS costs could become really interesting. In this thesis work it has been considered one scenario where the BESS initial investment is decreasing of 30% of the actual cost, the initial cost is still too high to make the system economically feasible, however it could be possible that in the future a new type of battery or new material will be found, cheaper than the current one, further decreasing the initial investment.

The renewable energies are more and more important, and the future of the energy production is clearly related to the renewable energy production, so the development of the energy storage system is fundamental, in order to control the variability and unpredictability of the renewable energy sources.

It could be interesting to study different storage system combined with the photovoltaic power plant, considering that the technologies and the costs are rapidly changing in the last years.

Future studies on this field will show for sure more interesting results, also considering the fact that in Chile the photovoltaic power plants are increasing year by year and so the proposed energy price scenarios could become more and more realistic.

It would be interesting to scale the analysis also to smaller system, considering residential solution and not only utility-scale photovoltaic power plant and showing if the BESS is an interesting solution for residential application, both from the technical and economic point of view.

References

- [1] J. Gustavsson, "Energy Storage Technology Comparison", 2016.
- [2] Theopold, P. F., Klaus, & Richard Langley et al. "Batteries and Fuel Cells", 2020.
- [3] P. Kurzweil, K. Brandt, "Secondary batteries – lithium rechargeable systems | Overview", Elsevier, 2009.
- [4] Antonio N. Negri et al., "L'accumulo di energia elettrica.", IL MELOGRANO Editore srl, 2011.
- [5] D. Linden, T.B. Reddy., "Handbook of Batteries, Lithium-ion Batteries", McGraw-Hill, pp. 304, 2001
- [6] LG CHEM, Energy Solutions Company, ESS Battery Division, December 6th, 2018
- [7] Energy Storage Classes Material, Instituto Superior Tecnico, 2020
- [8] Isidor Buchmann, "Batteries in a Portable World - A Handbook on Rechargeable Batteries for Non-Engineers", Cadex Electronics Inc., 2016
- [9] H. Beltran, P. Ayuso and E. Pérez, "Lifetime Expectancy of Li-Ion Batteries used for Residential Solar Storage", *Energies*, 2020, vol. 13, pp.568
- [10] Hoda Akbari, Maria C. Browne, Anita Ortega, Ming Jun Huang, Neil J. Hewitt, Brian Norton, Sarah J. McCormack, "Efficient energy storage technologies for photovoltaic systems", *Solar Energy*, 2019, vol. 192, pp. 144-168
- [11] Meysam Qadrdan, Nick Jenkins and Jianzhong Wu, "Smart Grid and Energy Storage", Soteris A. Kalogirou, McEvoy's Handbook of photovoltaics, Academic press, 2018, pp. 915-928
- [12] "Le batterie al litio", ENEA Agenzia Nazionale per le Nuove Tecnologie, l'Energia e lo Sviluppo Economico Sostenibile
- [13] Madeleine Ecker, Nerea Nieto, Stefan Käbitz, Johannes Schmalstieg, Holger Blanke, Alexander Warnecke, Dirk Uwe Sauer, "Calendar and cycle life study of Li(NiMnCo)O₂-based 18650 lithiumion batteries", *Journal of power sources*, 2013, vol. 248, pp.839-851
- [14] M. Assembayeva, N. Zhakiyev, Y. Akhmetbekov, "Impact of storage technologies on renewable energy integration in Kazakhstan", *Materials today: Proceedings*, 2017, vol. 4, no. 3, Part A, pp. 4512-4523
- [15] Crabtree G., Misewich J et al., "Integrating Renewable Electricity on the Grid, A Report", American Physical Society, 2011
- [16] International Energy Agency, "Harnessing variable renewables: A guide to the balancing challenge.", OECD Publishing, Paris, 2011
- [17] Mills, A., Ahlstrom, M., Brower, M., Ellis, A., George, R., Hoff, T., ... & Wan, Y. H., "Understanding variability and uncertainty of photovoltaics for integration with the electric power system" Ernest Orlando Lawrence Berkeley National Laboratory, Berkeley, CA (US), 2009
- [18] Martinez Romero S. and Hughes W., "Bringing Variable Renewable Energy Up to Scale: Options for Grid Integration Using Natural Gas and Energy Storage", ESMAP Technical Report. The World Bank Group, Washington, 2015
- [19] Guodong Xu, Ce Shang, Songli Fan, Xiaohu Zhang, Haozhong Cheng, "Sizing battery energy storage systems for industrial customers with photovoltaic power", *Energy Procedia*, 2018, vol. 158, pp. 4953-4958.
- [20] Antonio Colmenar-Santos, Mario Monteagudo-Mencucci, Enrique Rosales-Asensio, Miguel de Simón-Martín, Clara Pérez-Molina, "Optimized design method for storage systems in photovoltaic plants with delivery limitation", *Solar Energy*, 2019, vol. 180, pp. 468-488
- [21] Reinhold Elsen et al., "Ancillary Services: Unbundling Electricity Products – an Emerging Market", Union of the Electricity Industry – EURELECTRIC, 2003

- [22] Zabudskij, E.I. & Baladina G.I., "Automatic control system for power grid voltage stabilization", *Procedia Computer Science*, 2017, vol. 103, pp. 511-516
- [23] Weber, A. Z., Mench, M. M., Meyers, J. P., Ross, P. N., Gostick, J. T., & Liu, Q., "Redox flow batteries: a review", *Journal of Applied Electrochemistry*, 2011, vol. 41(10), pp. 1137-1164
- [24] Sauer, Dirk & Fuchs, Georg & Lunz, Benedikt & Leuthold, Matthias, "Technology overview on electricity storage – overview on the potential and on the deployment perspectives of electricity storage technologies", ISEA and SEFEP, 2012
- [25] Besseghini et al., "I sistemi di accumulo elettrochimico: prospettive ed opportunità", *RSE & ANIE energia*, 2017.
- [26] Vazquez, S., Lukic, S. M., Galvan, E., Franquelo, L. G., & Carrasco, J. M. "Energy storage systems for transport and grid applications", *IEEE Transactions on Industrial Electronics*, 2010, vol. 57(12), pp. 3881-3895.
- [27] Vargas, Luis & Jimenez-Estevez, Guillermo, "Practical Experiences as part of Engineering Education for Sustainable Development: The Ollagüe Smart Microgrid Energy Project", *Engineering Education for Sustainable Development Conference EESD13*, Cambridge, UK, 2013
- [28] Moreira-Muñoz A., "Plant Geography of Chile", Springer, 2011
- [29] M. Osses, C. Ibarra, B. Silva, M. Roth, "Solar Energy in Chile SXX-SXXI" IEA SHC International Conference on Solar Heating and Cooling for Buildings and Industry, 2019
- [30] SolarGIS: Solar Irradiance Data, Solargis s.r.o., Bratislava, Slovakia
- [31] Cereceda P, Larrain H, Osses P, Fariás M, Egaña I. "The climate of the coast and fog zone in the Tarapacá region, Atacama Desert, Chile", *Atmospheric Research*, 2008, vol. 87, pp.301–11
- [32] Garreaud R, Molina A, Farias M. "Andean uplift, ocean cooling and Atacama hyperaridity: a climate modeling perspective", *Earth Planetary Science Letter*, 2010, vol.292, pp.39–50
- [33] Houston J., "Variability of precipitation in the Atacama Desert: its causes and hydrological impact", *International Journal of Climatology*, 2006, vol.26, pp.2181–98
- [34] A. Zurita, A. Castillejo-Cuberos, M. Garcia, C. Mata-Torres, Y. Simsek, R. Garcia, F. Antonanzas-Torres, R. A. Escobar, "State of the art and future prospects for solar PV development in Chile", *Renewable and Sustainable Energy Reviews*, 2018, vol. 92, pp. 701-727
- [35] Escobar RA, Cortés C, Pino A, Salgado M, Pereira EB, Martins FR, et al., "Estimating the potential for solar energy utilization in Chile by satellite-derived data and ground station measurements", *Solar Energy*, 2015, vol. 121, pp.139–51
- [36] Del Sol F. & Sauma E., "Economic impacts of installing solar power plants in northern Chile", *Renewable and Sustainable Energy Reviews*, 2013, vol.19, pp.489–98
- [37] Parrado C, Girard A, Simon F, Fuentealba E. "2050 LCOE (Levelized Cost of Energy) projection for a hybrid PV (photovoltaic)-CSP (concentrated solar power) plant in the Atacama Desert, Chile", *Energy*, 2016, vol.94, pp.422–30
- [38] Ferrada, Pablo & Rabanal Arabach, Jorge & Marzo, Aitor & Cabrera, Enrique & Schneider, Andreas & Kopecek, Radovan, "AtaMo: PV meets the high potential of the Atacama Desert", *PV Tech Power*, 2015, vol. 5, pp.55
- [39] <https://sam.nrel.gov/weather-data> (visited on 05/2021)
- [40] Makibar, Aitor & Narvarte, L. "Characterisation and efficiency test of a li-ion energy storage system for PV systems", *European Photovoltaic Solar Energy Conference and Exhibition, EU PVSEC, Hamburg*, 2015
- [41] Xu, B., Oudalov, A., Ulbig, A., et al., "Modeling of Lithium-Ion Battery Degradation for Cell Life Assessment", *IEEE Transactions on Smart Grid*, 2018, vol.9, pp.1131-1140

- [42] Makinejad, K. et al. "A Lumped Electro-Thermal Model for Li-Ion Cells in Electric Vehicle" World Electric Vehicle Journal, 2015, vol. 7, pp. 1-13
- [43] Fu, R. & Remo, T. & Margolis, R., "2018 U.S. Utility-Scale Photovoltaics- Plus-Energy Storage System Costs Benchmark", National Renewable Energy Laboratory, 2018
- [44] "Lazard's Levelized Cost of Storage Analysis – Version 6.0", Lazard and Roland Berger, 2020
- [45] Jaeger-Waldau, A., "PV Status Report 2019", EUR 29938 EN, Publications Office of the European Union, Luxembourg, 2019
- [46] <https://www.coordinador.cl/operacion/graficos/operacion-real/costo-marginal-real/> (visited on 05/2021)
- [47] Aust, B. & Horsch, A., "Negative market prices on power exchanges: Evidence and policy implications from Germany", The Electricity Journal, 2020, vol.33, issue 3
- [48] "Chile Investment in the Energy Sector", Chile 2020 Green Hydrogen Summit, Ministerio de Energia, Gobierno de Chile, 2020
- [49] Mongird, K. & Viswanathan, V. & Balducci, P.J. & Alam, Md J.E. & Fotedar, V. & Koritarov, V S. & Hadjerioua, B., "Energy Storage Technology and Cost Characterization Report", Pacific Northwest National Lab. (PNNL), Richland, WA (USA), 2019